Dissertation

submitted to the

Combined Faculties for the Natural Sciences and for Mathematics

of the Ruperto-Carola University of Heidelberg, Germany

for the degree of

Doctor of Natural Sciences

presented by

Master of Medicine (Huazhong University of Science and Technology) Qi Li

born in Hubei, P.R. China

Oral-examination: 26.07.2012

Title:

“Functional roles of bone morphogenetic protein-9 in liver pathology”

Referees:

Prof. Dr. Stefan Wölfl, University of Heidelberg, Germany

PD. Dr. Katja Breitkopf-Heinlein, University of Heidelberg, Germany

Statement

I hereby declare that I have written the submitted dissertation myself on the basis of the acquired data from the experiments I have performed and have used no other sources and materials than those expressly indicated.

I hereby declare that I have applied to be examined at the Faculty of Biosciences rather than any other institution and I have not used the dissertation in this or any other form at any other institution as an examination paper, nor submitted it to any other faculty as a dissertation.

Signature

Acknowledgments

I would like to sincerely thank Prof. Dr. Stefan Wölfl for the scientific support during my PhD studies, Prof. Dr. Steven Dooley for giving me the chance to pursue this project, PD. Dr. Katja Breitkopf-Heinlein for encouragement, supervision and critical discussions, Shahrouz Ghafoory and Dr. Li Li for an excellent cooperation. I appreciate the help from all colleagues working at the Institute of Molecular Hepatology - Alcohol Associated Diseases, II. Medical Clinic, Medical Faculty Mannheim at Heidelberg University with a nice working atmosphere.

I would like to thank all my friends for always encouraging me with great patience and also specially thank my family for endless love and support.

Summary

Bone morphogenetic protein (BMP)-9 belongs to the transforming growth factor (TGF)-β superfamily and has been suggested to play a role in bone formation, hematopoiesis, glucose homeostasis, iron homeostasis, angiogenesis and cancer development. Using the acute carbon tetrachloride (CCl_4) mouse model for liver injury we found that BMP-9 expression increased rapidly, reaching a maximum at day 3 after injection of CCl_4. At this time-point, positive BMP-9 staining was mainly localized to the pericentral area, where hepatocytes were seriously damaged. Phosphorylation of Smad1, one of the main BMP's transducing signaling molecules, was increased mainly in hepatocytes already at 3 h after CCl_4 application, although some positive staining for pSmad1 was also observed in sinusoidal cells. At day 3, positivity was additionally detected in infiltrating cells, representing most likely proliferating, activated hepatic stellate cells (HSCs). Immunostainings for α-smooth muscle actin (SMA), desmin and cleaved caspase3 showed that at day 3, in pericentral areas the extent of hepatocyte apoptosis reached its peak and HSCs significantly proliferated and activated. Even though *in vitro* BMP-9 did not cause apoptosis directly, it enhanced TGF-β1-induced hepatocyte apoptosis. I*n vitro* experiments demonstrated that BMP-9/Smad1 signaling was involved in the transdifferentiation of HSCs. In human hepatocellular carcinoma (HCC) samples, mildly positive (1+) BMP-9 immunostaining was observed in 25/41 (61%), and moderately to strongly positive staining (2+) was observed in 16/41 (39%) patients. In 27/41 (65.85%) patients, BMP-9 protein expression levels were consistent with the mRNA expression level as measured by *in situ* hybridization. In those patients with 2+ protein levels, nuclear pSmad1 expression in cancer cells was also significantly increased. BMP-9 expression was positively correlated to nuclear Snail expression and reversely correlated to cell surface E-cadherin expression, although this trend did not reach statistical significance. Expression levels of BMP-9 were significantly correlated with the T stages of the tumors, which is a measure for the degree of tumor invasion. *In vitro* in HCC cells, similar to the findings with human samples, BMP-9 treatment caused a reduction of E-cadherin and an induction of Vimentin and Snail expression, which are characteristics of epithelial-mesenchymal transition (EMT). Furthermore, BMP-9 enhanced cell migration.

In conclusion, these results imply that BMP-9 is involved in HSC activation and hepatocyte apoptosis during liver damage and regeneration, and that it acts as a tumor promoter via inducing EMT in HCC.

Zusammenfassung

Bone Morphogenetic Protein (BMP)-9 gehört zur Familie der *Transforming Growth Factor* (TGF)-β Zytokine welche als Modulatoren zentraler, zellulärer Prozesse, wie Osteogenese, Hämatopoese, Glukosehomeostase, Eisenhaushalt, Angiogenese sowie Tumorgenese beschrieben wurden. In der vorliegenden Arbeit wurden die Expressionslevel von BMP-9 in Mäuselebern nach akuter Schädigung der Leber durch einmalige CCl_4 Injektion untersucht. Es zeigte sich insbesondere in perivenösen Arealen der Leber eine schnelle Induktion der BMP-9 Expression, welche an Tag 3 ihr Maximum erreichte. Bereits 3 h nach CCl_4 Applikation konnte mittels Western blot und Immunfärbungen gegen phosphoryliertes Smad1 eine starke Aktivierung des BMP-9 Signalweges gezeigt werden, die bis mindestens Tag 3 erhöht blieb. Außer in Hepatozyten fand sich diese Smad1 Aktivierung auch in sinusoidalen Zelltypen. An Tag 3 waren auch Zellen positiv gefärbt, bei welchen es sich vermutlich um aktivierte hepatische Sternzellen (HSC) handelt. Immunfärbungen gegen α-smooth muscle actin (SMA), Desmin und aktivierte Caspase-3 deuten stark darauf hin, dass an Tag 3 nach CCl_4 Injektion HSC im perivenösen Bereich aktiviert sind und proliferieren sowie dass Hepatozyten (HC) dann vermehrt in Apoptose gehen. In Zellkulturexperimenten konnte gezeigt werden, dass BMP-9 bei der Aktivierung primärer Maus-HSC eine Rolle spielt und dass es die TGF-β vermittelte Apoptose in primären Maus-HC verstärkt. In Gewebeschnitten von Patienten mit hepatozellulärem Karzinom (HCC) fand sich in 25/41 (61%) Patienten eine leicht positive Immunfärbung für BMP-9 ("1+"), und in 16/41 (39%) eine stark positive Färbung ("2+"). In 27/41 (65.85%) konnte darüber hinaus mittels in situ Hybridisierung eine Korrelation zwischen BMP-9 Protein- und mRNA-Ebene nachgewiesen werden. Des Weiteren korrelierte eine positive phospho-Smad1 Färbung mit erhöhter BMP-9 Expression ("2+" Proteinebene). Tendenziell ging die BMP-9 Expression mit erhöhter Expression von Snail und verminderter Expression von E-Cadherin einher, diese Korrelation erreichte jedoch keine Signifikanz. Schließlich konnte eine signifikante Korrelation der BMP-9 Expression mit der Invasivität der Tumoren nachgewiesen werden. BMP-9 Stimulation von HCC Zellen in vitro induzierte die Expressionen von Vimentin und Snail und reduzierte die von E-Cadherin, ein Expressionsmuster, das charakteristisch für eine epitheliale-mesenchymale Transition (EMT) ist. In Korrelation zu diesen Befunden verstärkte BMP-9 auch die in vitro Migration von HCC Zellen.

Insgesamt konnte gezeigt werden, dass BMP-9 nach Leberschädigung eine wichtige Rolle bei der Aktivierung von HSC und der TGF-β vermittelten Apoptose von Hepatozyten spielt und daß es über Induktion von EMT pro-tumorigene Effekte beim HCC ausübt.

Table of contents

1. Introduction

1.1. The liver

The liver is a fundamental organ for humans and most animals. It is the largest visceral organ and gland in the body. It has been identified to play a role in more than 500 separate functions. The major functions include synthesis of various amino acids, converting ammonia into urea, synthesis and degradation of proteins, taking part in carbohydrate metabolism, lipid metabolism, production of albumin, production of coagulation factors (I, II, V, VII, IX, X, XI, protein C, protein S and anti-thrombin), excretion of bile, detoxification and drug metabolism, breakdown of insulin and other hormones, storage of necessary nutrients for body health such as glucose, Vitamin A, Vitamin D, iron and others, and production of immune factors.

1.2. Hepatocytes and hepatic stellate cells

Hepatocytes are the dominant parenchymal cell type of the liver. They account for almost 90% of the liver mass and provide about 60% of the total number of liver cells (Michalopoulos and DeFrances, 1997). They execute the major functions of the liver, which have been mentioned above. Even though hepatocytes do not proliferate in culture, they have very strong proliferative potential *in vivo*. Owing to this potential, liver function and size can be restored in several days after partial hepatectomy. Hepatocytes are arranged into liver plates, which are separated by sinusoids. The plates are only as thick as one cell in mammals and sinusoids are lined with fenestrated and discontinuous endothelial cells. Between the hepatocyte plate and the endothelial cell lining there is the space of Disse, where lymph is drained into the portal tract lymphatics. When live injuries like drugs, chemical toxins (e.g., carbon tetrachloride), liver resection or acute viral infections occur, normally non-dividing mature hepatocytes start to re-enter the cell cycle and undergo mitosis to regenerate the liver. However, if the injury is more severe, or chronic or the mature hepatocytes have no more capacity because of cell senescence or arrest for liver regeneration, another type of quiescent cell, progenitor cells which are thought to reside in the canals of Hering will be activated. These cells can differentiate into either hepatocytes or cholangiocytes. Therefore liver regeneration can still be achieved (Riehle et al., 2011).

In normal liver, hepatic stellate cells (HSCs) situated in the space of Disse account for 5 - 8% of the whole liver cell number. In a quiescent state, HSCs are the principle cell type for storage of retinoids, but it is difficult to visualize them by light microscopy (Geerts, 2001). The function of quiescent HSCs is largely unknown so far except several studies showing that HSCs act as antigen-presenting cells and stimulate NKT cell proliferation (Winau et al., 2007). When the liver is injured, quiescent HSCs are firstly activated, followed by evolving into myofibroblast-like cells, which is a key step to develop liver fibrosis (Friedman, 2004). In the normal liver, there is low density of "basement membrane-like" extracellular matrix (ECM) in the Disse space as cellular support. Activated HSCs (aHSC) represent a smooth muscle myofibroflast-like cell type and α-SMA is a typical histological marker for these cells. The aHSC secretes large amounts of type I and III collagens, other extracellular matrix (ECM) and tissue inhibitor of metalloproteinase (TIMP)-1 that inhibits matrix-metalloproteinase-induced matrix degradation (Benyon and Arthur, 2001). ECM deposits in the sinusoids and deteriorates the liver function (Friedman, 2003). When liver injury is slight and normal structure and functions are preserved, deposited ECM will be dissolved within a certain period of time and aHSCs will most likely go to apoptosis. However, when the injury is too severe, HSC activation and proliferation exist constantly, which finally leads to liver fibrosis or even liver cirrhosis (Lafdil et al., 2006).

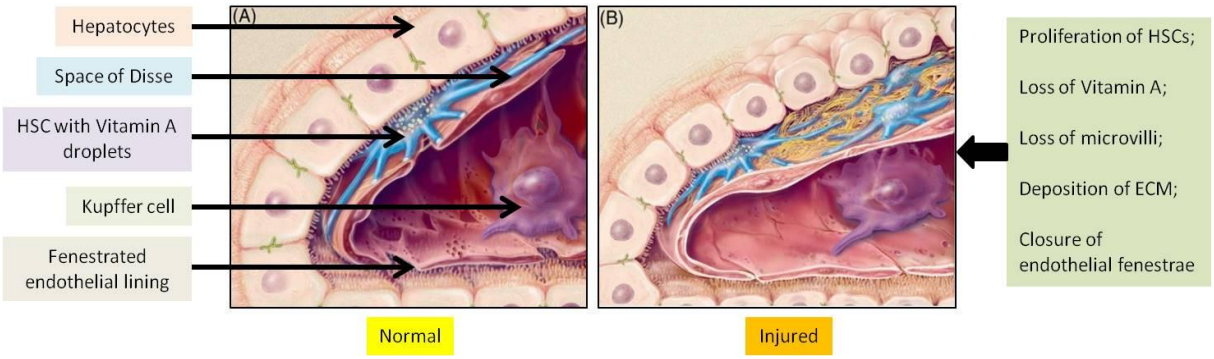

(modified from (Friedman, 2003))

Fig.1. Sub-endothelial changes in response to liver injury. **A,** Normal liver: HSCs are quiescent and store Vitamin A droplets and there is low density of matrix in the space of Disse. Fenestrated endothelial lining supports the normal liver architecture. **B,** Injured liver: HSCs are activated and increase their proliferation, ECM accumulates, endothelial fenestrae close. Hepatocyte polarity and functions get lost.

1.3. TGF-β

The TGF-β family includes TGF-β isoforms, BMPs, growth and differentiation factors, inhibins, Muellerian inhibiting substance and activins (Piek et al., 1999). TGF-β is a 25 kDa cytokine which is secreted by nearly all cell types in the body in physiological as well as pathological conditions (Massague, 1990). There are 3 isoforms, TGF-β1, TGF-β2 and TGF-β3 in mammals. Among them, TGF-β1 is most widely distributed and most intensively studied. TGF-β mediates multiple cellular responses including cell proliferation, differentiation, apoptosis, migration, invasion, ECM deposition and angiogenesis (Rahimi and Leof, 2007). As far as liver is concerned, TGF-β1 has been reported to play crucial roles in liver repair since it has inhibitory effects on proliferation of hepatocytes and exerts fibrogenic functions on HSCs (Bedossa and Paradis, 1995).

1.4. BMP-9

Bone morphogenetic proteins (BMPs) are a subgroup belonging to the TGF-β superfamily. Until now, more than 15 kinds of BMP-related proteins have been discovered (Miyazono et al., 2005). They were divided into 4 subgroups according to the similarity of their amino acid sequences and functions. The BMP-2/4 subgroup includes BMP-2, BMP-4 and the Drosophila dpp, functioning in embryonic development. The BMP-7 subgroup is composed of BMP-5, 6, 7, 8 and the Drosophila gbb. The third is the GDF-5 subgroup, including GDF-5, 6 and 7. These three subgroups are important for keeping up normal tissue functions. BMP-9 and BMP-10 are the two members of a fourth subgroup, whose functions are now being discovered (David et al., 2009). Current studies have implicated that some BMPs function in cancer progression and may be potential therapeutic targets for cancer treatment (Li, 2008).

BMP-9, also termed growth differentiation factor-2 (GDF-2), was firstly cloned from a fetal mouse liver cDNA library (Celeste, 1994). The precursor human BMP-9 is constituted of 429 amino acids with a rough molecular weight of 47 kDa. Following post-transcriptional modification, the immature precursor is divided into a pro-region and a mature region (13 kDa). However, both dimers of mature regions and BMP-9 pro-region complexes have the same biological functions after secretion (Brown et al., 2005). In physiological conditions BMP-9 circulates in serum and plasma at a concentration of about 5 ng/ml (Herrera and Inman, 2009). Emerging evidences indicate that BMP-9 participates in various physiologic processes such as bone formation, hematopoiesis, glucose homeostasis, iron homeostasis and angiogenesis (Bessa et al., 2009; Chen et al., 2003; Suzuki et al., 2010; Truksa et al., 2006).

Like other BMPs, BMP-9 has also been suggested to be involved in cancer development in a small number of studies. But its effects on different cancer cells are controversial. This might be due to tissue differences and cellular environments where BMP-9 is expressed. Blanca Herrera et al reported that about 25% of epithelial ovarian cancers express BMP-9, but normal human ovarian surface epithelial specimen do not. Furthermore, some ovarian cancer cell lines can acquire autocrine BMP-9 signaling to facilitate cancer cell proliferation (Herrera et al., 2009). On the contrary, in prostate cancer, BMP-9 suppresses cancer cell growth via inducing cell apoptosis (Ye et al., 2008). In breast cancer cells it inhibits growth, migration and invasion (Wang et al., 2011). Song et al reported that BMP-9 induces cell proliferation in a HCC cell line, HepG2 and sub-confluent rat primary hepatocytes (Song et al., 1995), however, possible roles for BMP-9 in liver diseases have been largely unknown so far.

1.5. Signal transduction pathways initiated by TGF-β or BMPs

TGF-β superfamily members signal via two canonical pathways, the Smad pathways and via non-canonical pathways, the non-Smad pathways. By now, also receptor tyrosine kinases, cytokine receptors and G-protein-coupled receptors have been described to mediate TGF-β signaling (Derynck and Zhang, 2003).

1.5.1. Smad signaling

Signal transduction induced by TGF-β isoforms is initiated by the binding of a ligand to its corresponding type II receptor, which triggers association and complex formation with a type I receptor which gets transphosphorylated by the type II receptor. There are 5 type II receptors and 7 type I receptors which have special affinities to certain ligands. Both types of receptors possess serine/threonine kinase activity and can phosphorylate and thereby activate the down-stream molecules termed Smads (ten Dijke and Hill, 2004).

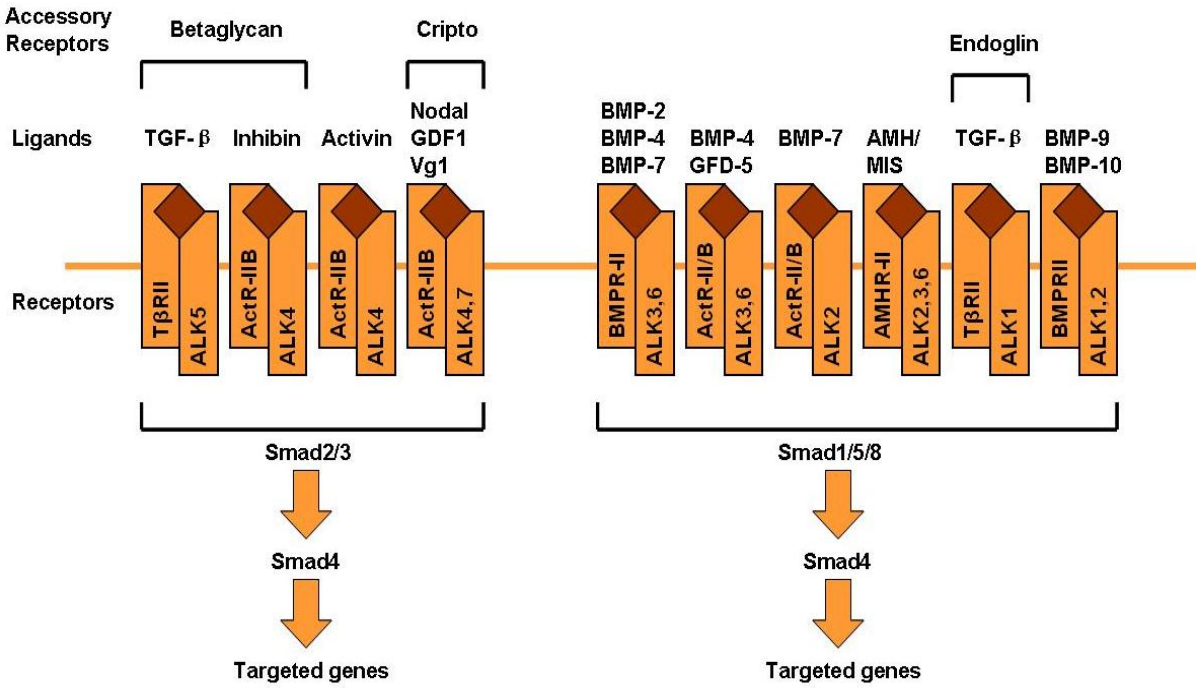

(modified from (Shi and Massague, 2003))

Fig.2. TGF-β superfamily ligands signal through specific type I and II receptors and activate Smad1/5/8 or Smad2/3 pathways, resulting in the regulation of expression of target genes. In vertebrates some accessory receptors further modify the signaling of TGF-β superfamily members.
GDF-growth and differentiation factor (Vg1 in Xenopus), MIS- Mülerian inhibiting substance (also known as AMH- anti-Mülerian hormone).

Smads are intracellular transcription factors in mammalian cells, and in Drosophila and C. elegans they are named as MAD and Sma, respectively (Derynck, 1998). Until now 8 Smad family members have been identified and according to their function they have been divided into three subfamilies: Smad1, Smad2, Smad3, Smad5 and Smad8 are defined as receptor-activated Smads (R-Smads) which become phosphorylated by a type I receptor, the common mediator Smad (Co-Smad) Smad4 which forms complexes with the activated R-Smads and inhibitory Smads (I-Smads: Smad6 and Smad7), which antagonize the signaling of TGF-β family members (Park, 2005). There are two conserved domains: the N-terminal Mad Homology 1 (MH1) domain and the C-terminal MH2 domain in both R-Smads and Smad4 (ten Dijke and Hill, 2004). But I-Smads do not share the conserved MH1 domain with R-Smads and Smad4, which is the reason that I-Smads can not bind DNA. The MH2 domain is highly conserved in all three types of Smads and is responsible for receptor interactions (Shi and Massague, 2003). The type I receptor phosphorylates the R-Smads on a C-terminal SSXS (Ser-Ser-X-Ser sequence) motif (ten Dijke and Hill, 2004).

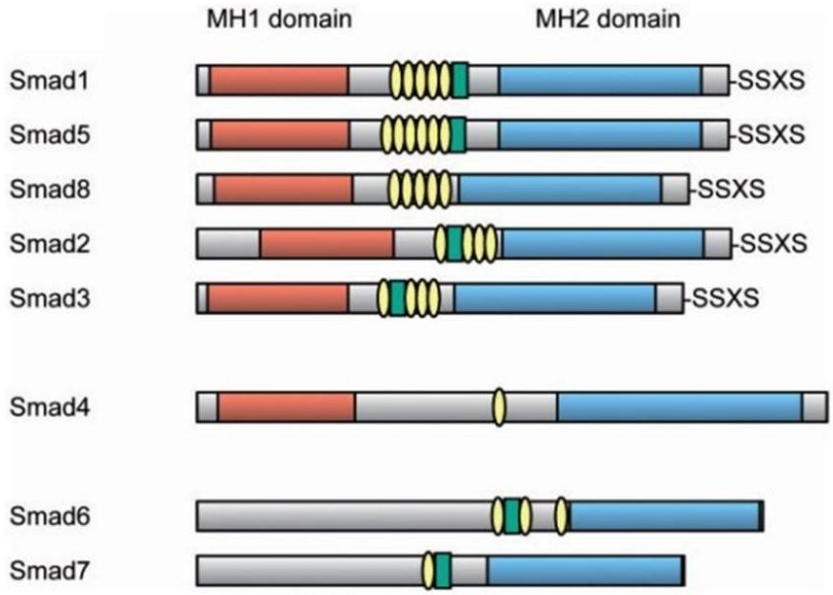

(From (Miyazono et al., 2010))

Fig.3. Schematic structure of R-Smads, co-Smad and I-Smads. In the linker region green squares represent the phosphorylation site of R-Smads and I-Smads, and yellow circles represent the PXS/TP (or S/TP) motif which is potentially phosphorylated by MAP kinases. MH1 domains are shown in red and MH2 domains in blue.
SSXS: C-terminal phosphorylation site of R-Smads.

There have been two Smad signaling cascades identified: the classical TGF-β branch including phosphorylation of Smads 2 and 3 which is activated by TGF-β, nodal, activin and myostatin, and the BMP branch involving phosphorylation of Smads 1, 5 and 8 which is initiated by BMPs and GDFs (Moustakas and Heldin, 2003). TβR-II and ALK5 are the main receptors involved in the TGF-β branch. TGF-β and activin possess higher affinity to TβR-II and can not bind to the type I receptor alone. In contrast to this, some BMPs including BMP-9 display higher affinity for their type I receptors, than for their type II receptors. The BMP-type I receptor group contains BMP receptor type IA (BMPR-IA/ALK3), type IB (BMPR-IB/ALK6), activin receptor-like kinase-1 (ALK-1) and ALK2. The typeII receptors are composed of BMP receptor type II (BMPR-II), activin A receptor type IIA (ActRII) and activin A receptor type IIB (ActRIIB). After its binding to BMPs, the type II receptors phosphorylate the type I receptors, BMPs are known to activate only the Smad 1/5/8 pathway but do not lead to activation of Smads 2/3. The combination of R-Smads with Smad4 facilitates the translocation of the complex into the nucleus, which then mediates the transcription of BMP-target genes. This pathway is regarded as the canonical BMP/Smad pathway (Miyazono et al., 2010). Which Smad-pathway is being activated under a given situation is determined by the type I receptor being bound by the ligand (Lopez-Coviella et al., 2006).

Activin receptor-like kinase-1 (ALK1) is a type I receptor with serine/threonine kinase activity on the cell surface, which participates in the Smad1/5/8 singnaling pathway (David et al., 2007). Several studies have demonstrated that ALK1 is mainly expressed in vascular endothelial cells and is involved in blood vessel formation during embryogenesis and wound healing (Roelen et al., 1997) as well as tumor angiogenesis (Lamouille et al., 2002). A mutation in the ALK1 gene causes hereditary hemorrhagic telangiectasia (HHT), a disease characterized by autosomal dominant vascular dysplasia (Johnson et al., 1996). Genetic deletion of ALK1 in mice results in embryonic lethality attributed to defects in angiogenesis (Urness et al., 2000). Endothelial-targeted ALK1 gene disruption leads to dilated vessels in the yolk sac without capillary beds which normally connect arteries and veins, which is similar to the characteristics of HHT (Park et al., 2008). Besides TGF-β1 and TGF-β3 which may activate ALK1 in some cell types (Lux et al., 1999), BMP-9 and BMP-10 have been identified as highly specific ligands for ALK1 (David et al., 2007).

Smad1 was the first cloned mammalian Smad gene (Itoh et al., 2000). Smad1-knockout mice experience normal gastrolation, but die in midgestation because of defective allantois development and chorioallantoic placenta formation (Huang et al., 2000). Smad1-deletion can also result in defects of yolk sac angiogenesis (Chang et al., 2002). Smad1 transgenic mice show early postnatal death and impaired cell cycle of the embryonic fibroblasts (Queva et al., 1999).

1.5.2. non-Smad pathway

A large amount of in vitro cell experiments implicate that the small GTPase Ras and mitogen-activated protein kinases (MAPKs) including ERKs, p38 and c-Jun N-terminal kinases (JNKs), phosphatidylinositol-3'-kinase and Src kinase are involved in non-Smad pathways of TGF-β family members (Moustakas and Heldin, 2005). There are three general mechanisms for non-Smad signaling to mediate the responses to TGF-β family members: (1) Non-Smad signaling directly interacts with the Smads, like phosphorylation, and modulates their activity. (2) The receptor complex directly modifies non-Smad proteins which induces signaling in parallel with the Smad pathways. (3) Smads directly influence the activity of non-Smad proteins. Ras and MEK have been revealed to be partially required for Smad1 phosphorylation initiated by TGF-β1 as well as BMPs (Yue and Mulder, 2000). The

epidermal growth factor and hepatocyte growth factor phosphorylate Smad1 via ERK signaling, which inhibits BMP-induced nuclear accumulation and transcription of Smad1 (Kretzschmar et al., 1997a). Smad1 phophorylation by JNK, ERK or p38 MAPK is necessary for the phosphorylation of GSK3β. GSK3β in turn phosphorylates the linker region of Smad1, which enhances the recruitment of Smurf1, an ubiquitin ligase, facilitating suppression of the transcriptional activity of Smad1, resulting in proteasomal degradation of activated Smad1. Fibroblast growth factor can activate MAPKs, thereby reducing BMP/Smad1 signaling. Wnt inhibits GSK3β which promotes BMP/Smad signaling (Fuentealba et al., 2007). Through these mechanisms, non-Smad signalings participate in cell apoptosis, EMT and migration, cell proliferation and matrix regulation in parallel to Smad signalings triggered by TGF-β family members (Moustakas and Heldin, 2005).

1.6. Liver injury by carbon tetrachloride (CCl_4) intoxication

Liver injury in rodents induced by CCl_4 intraperitoneally represents a most widely accepted canonical animal model to investigate the response of acute and chronic liver injury since the elementary lesions caused by this hepatotoxin replicate those seen in most cases of human liver diseases (Taniguchi et al., 2004). In mature hepatocytes, cytochrome P-450 IIE1 (Cyp2E1) bioactivates CCl_4 to $\cdot CCl_3$ free radical, which is then converted to a peroxy radical, $CCl_3O\cdot_2$ (Slater, 1987). Reaction of these free radicals with polyunsaturated fatty acids triggers a reaction cascade which results in peroxidation of cellular lipids, proteins and DNA as well as injury by reactive oxygen species (ROS) (Johansson and Ingelman-Sundberg, 1985). Secondary liver injury comes from inflammatory reactions mediated by Kupffer cells which are largely activated and release important cytokines such as tumor necrosis factor (TNF)-α (Schumann and Tiegs, 1999). Those cytokines recruit and activate neutrophils, the latter releases ROS and further enhances liver injury (Louis et al., 1998). Liver damage is accompanied by liver repair, during which hepatocytes surrounding the necrotic area proliferate and the synthesis of ECM accelerates transiently.

1.6.1. Acute liver injury

Normally, the CCl_4-induced acute liver injury model is generated with a single injection of 1 ml/kg, which functions as a strong regenerative stimulus. This acute model is characterized by inflammatory responses caused by CCl_4 aiming at clearance of the tissue from the damaged

tissue debris, followed by the regenerative processes leading to a final restoration of the original liver structure and function. This acute model involves generation of oxidative stress and recruitment of inflammatory cells, which is reported to induce liver architectural and functional damage. Upon acute CCl_4 hepatotoxicity, the opposing biological responses, tissue injury and repair are simultaneously happening (Rao et al., 1997). CCl_4 causes pericentral liver damage (Lindroos et al., 1991) and it has been reported that centrilobular necrosis occurs one day after CCl_4 administration in rats and mice (Louis et al., 1998; Sigala et al., 2006). Except hepatocyte necrosis, another type of cell death, apoptosis also occurs in the ballooned and damaged hepatocytes within the centrilobular area. Jialan Shi et al have found that large numbers of hepatocytes undergo apoptosis. The amount of apoptotic hepatocytes is increased at 3 h and peaks at 6 h after CCl_4 intoxication in rat. Furthermore, the percentage of apoptotic ballooned cells is increased until day 3 (Shi et al., 1998).

Genes representing liver functions like catalase, albumin, aldolase B are significantly reduced at 24 h and return to normal at 48 h after CCl_4 injection (Taniguchi et al., 2004). Furthermore, liver regeneration is obviously increased, which is reflected by the mitotic activity of hepatocytes, with a peak between 48 and 72 hours after CCl_4 intoxication (Theocharis et al., 2000). Preceding the recovery of liver function, expression of pivotal factors such as HGF, NF-κB and AP-1 responsible for liver regeneration are significantly increased (Taniguchi et al., 2004). TGF-β1 has been regarded as a crucial player in liver repair (Bedossa and Paradis, 1995). During liver regeneration after CCl_4 induced liver injury, TGF-β1 mRNA is increased, reaching a peak on day 3. TGF-β1 is secreted by both hepatocytes and non-parenchymal cells like HSCs (Tsuchiya et al., 2007). It reduces the transcription of genes responsible for DNA synthesis and inhibits growth of hepatocytes (Bissell et al., 1995). Furthermore, it causes hepatocyte apoptosis via an oxidative stress process during which reactive oxygen species are produced, resulting in loss of mitochondrial-transmembrane potential, the release of cytochrome c and activation of caspases (Carmona-Cuenca et al., 2008).

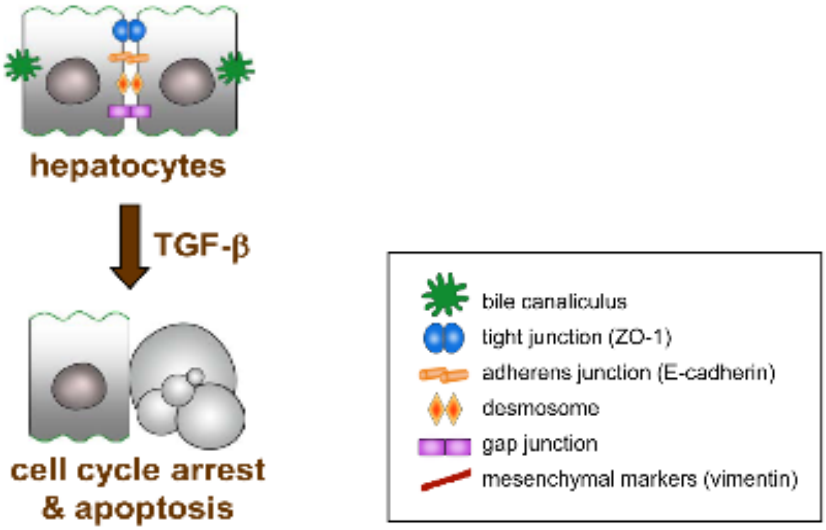

(modified from (van Zijl et al., 2009))

Fig.4. TGF-β induces cell cycle arrest and apoptosis in hepatocytes.

At sites of damaged liver, aHSCs produce a transient scar to prevent the liver tissue from further damage. At the same time, aHSCs have pro-inflammatory and hepatomitogenic functions via secreting cytokines such as HGF and IL-6 so that the infection and cellular debris can be cleaned together with hepatocyte regeneration. During acute injury such aHSC induced wound-healing responses are rapidly resolved again due to the apoptosis of aHSCs (Elsharkawy et al., 2005). Whether some percentage of aHSCs might also disappear by some kind of "deactivation" resulting in regain of their quiescent phenotype is still under investigation.

1.6.2. Chronic liver injury by CCl_4

With chronic CCl_4 exposure, the regenerative capacity of mature hepatocytes is exhausted and liver progenitor cells will participate in liver regeneration. Since the liver is consecutively injured by CCl_4, the wound-healing initiated by aHSCs will not be reversed, but progresses until liver fibrosis and even liver cirrhosis will happen (Mann and Mann, 2009). Ample evidences point to a critical role of TGF-β in the activation and transdifferentiation of HSCs, leading to CCl_4-induced liver fibrogenesis (De Bleser et al., 1997; Doh et al., 2008; Jeong et al., 2006). Treatment strategies aiming at neutralization of TGF-β or inhibition of its pathway have been proven to reduce and/or prevent experimental fibrogenesis (Mizuno and Nakamura, 2007; Weng et al., 2007). However, with chronic damage the liver architecture can not be reversed back into the normal status any more (Weber et al., 2003), although with cessation of

the damaging stimulus reversion of fibrosis is until a certain point still possible whereas cirrhosis is considered as irreversible.

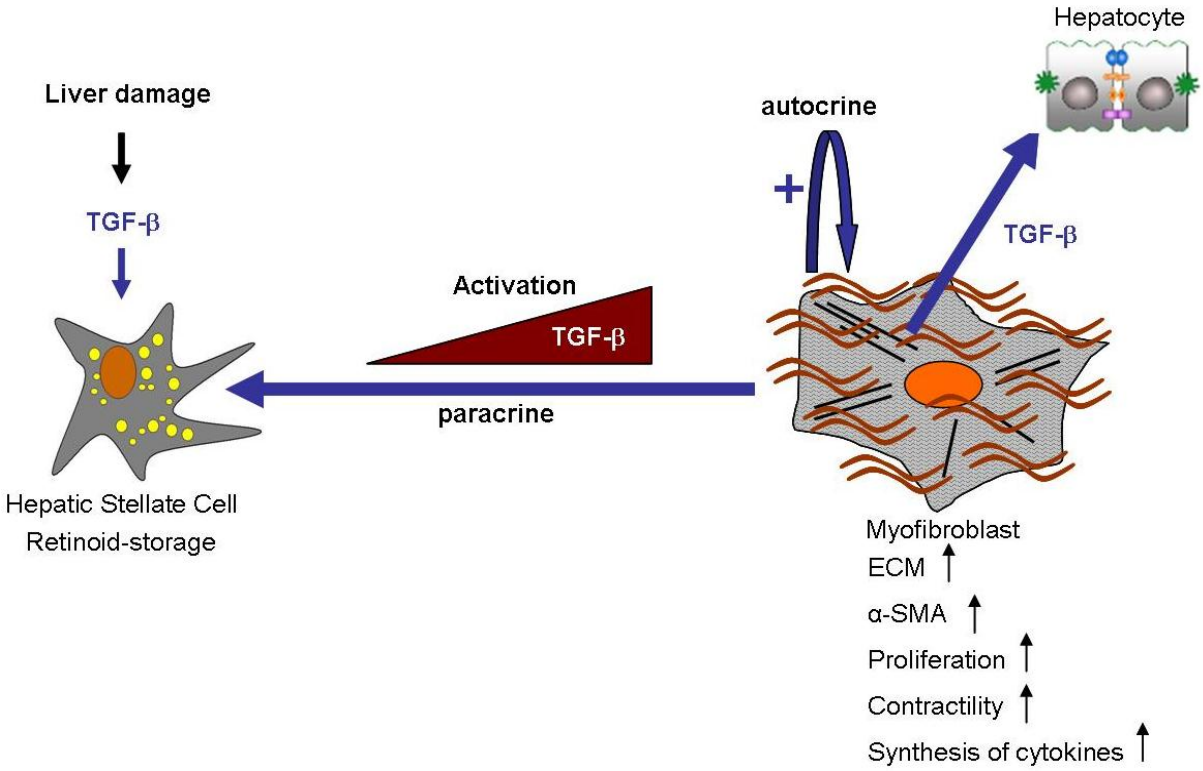

(modified from (Dooley et al., 2008) and (Hamzavi et al., 2008))

Fig.5. TGF-β plays a key role in HSC activation and transdifferentiation. Liver injury induces HSC activation. HSCs are the main source of TGF-β in injured liver which functions in paracrine and autocrine ways to mediate HSC activation and synthesis of ECM. Finally released TGF-β also affects other liver cells, like hepatocytes.

1.7. Hepatocellular carcinoma (HCC)

Liver cirrhosis is considered as pre-stage for the development of liver cancer although in a small percentage of cases liver cancer also develops without pre-existing cirrhosis. 80 - 90% of primary liver cancer cases originate from hepatocellular carcinoma (HCC), which has been regarded as the fifth most common cancer and the third most fatal reason responsible for cancer-related death in the world (Yang and Roberts, 2010). The majority of HCC is related to cirrhosis, which is the end stage of various liver diseases (Calle et al., 2005; Lau and Lai, 2008). Current therapeutic options including surgical resection, liver transplantation and chemoembolization can be only eligible for early stages of HCC. However, cancer recurrence will happen in around 50% of the patients (Josephs and Ross, 2010; Whittaker et al., 2010). Therefore the prognosis of HCC is nowadays still poor and HCC is inclined to tumor

invasiveness as well as intra- and extra-hepatic metastases formation. The main risk factors responsible for HCC include hepatitis B or hepatitis C infection, alcoholic liver cirrhosis, aflatoxin B and non-alcoholic steatohepatitis.

It is accepted that both genetic and epigenetic factors initiate and promote the development of HCC. HCC originates from the malignant change of hepatocytes and/or hepatic stem cells (Sell, 2002). In healthy liver, mature hepatocytes are highly differentiated and perform the normal liver functions such as detoxification, drug metabolism and glucose metabolism. Mature hepatocytes and/or liver stem cells undergo proliferation, apoptosis, dysplasia and neoplasia as result from external stimuli and/or liver damages (Farazi and DePinho, 2006; Villanueva et al., 2007). Before neoplasia forms, activated signaling pathways may facilitate cell growth and at the same time, dysplastic cell clones may be selected and induced. Once genomic alterations like point mutations or abnormal methylation of critical gene promoters occurs, these dysplastic cell clones may convert into a malignant phenotype (Minguez et al., 2009). In the progression of HCC, the cell proliferation is abnormal and hepatocytes become dedifferentiated. Until now, several molecular mechanisms have been reported as significant events in HCC including activation of Ras/mitogen activated protein kinase (MAPK) signaling, transforming growth factor (TGF)-β signaling, TGF-α/Epidermal growth factor, and Wnt/β-catenin signaling, unregulated expression of tumor suppressors like p53, Rb, and others (Breuhahn et al., 2006). TGF-β may provide tumor promoting effects towards hepatocytes via Smad and non-Smad signaling pathways (Dooley et al., 2009). BMP-4, 6, 7, 8, 9, 10, 11, 13 and 15 are reported to be up-regulated in HCC cell lines and their enhanced expression levels suggest enhanced migratory and invasive activity of HCC cells dominantly via Smad signaling (Maegdefrau and Bosserhoff, 2012). BMP-2 induces angiogenesis in HCC xenografted nude mice (Qiu et al., 2010) and BMP-4 promotes HCC progression and may be a novel prognostic marker in HCC (Guo et al., 2012; Maegdefrau et al., 2009).

1.8. Epithelial-mesenchymal transition (EMT)

EMT is characterized by loss of epithelial cells' differentiated traits including cell-cell contact, cell polarity as well as acquisition of mesenchymal appearances such as higher motility, invasiveness and resistance to apoptosis (Polyak and Weinberg, 2009). Properties characteristic for EMT consist of down-regulation of epithelial markers like E-cadherin and ZO-1, nuclear translocation of β-catenin and up-regulation of mesenchymal markers like

Vimentin and N-cadherin (Thiery, 2002; Yang and Weinberg, 2008). The zinc-finger transcription factors Snail and Slug, the basic helix-loop-helix transcription factors Twist, E47 and E2-2, the ZEB family factors ZEB1 and ZEB2, and the inhibitors of differentiation/DNA-binding (Ids) have been described to drive EMT (Bolos et al., 2003; Peinado et al., 2007; Yang et al., 2004). The EMT program has been demonstrated to play a central role in pathophysiological conditions including normal embryogenesis and wound healing, but also carcinogenesis. EMT first occurs during gastrulation of the embryonic development, in which the epithelial cells are converted into mesenchymal cells and the three-layered embryo forms (Thiery and Sleeman, 2006). Furthermore, EMT takes significant parts in the process of organogenesis when the heart, craniofacial structures, the cardiac valves and the secondary palate form (Polyak and Weinberg, 2009). EMT is further implicated in wound healing. In the epidermis, the adhesiveness of the epithelial cells is reduced as a consequence of injury with increasing migratory potential to remold the intact epithelial layer (Bissell and Radisky, 2001). This is an example for regenerative repair ascribed to EMT. EMT has also been mentioned in fibroproliferative wound healing, for instance, in the liver, which is specially dominated as liver fibrosis. One previous study in our group has addressed EMT of hepatocytes and participation of such cells in liver fibrosis. Adult primary mouse hepatocytes can lose their epithelial characteristics with TGF-β stimulation, showing loss of E-cadherin and up-regulation of Snail, a key transcriptional factor repressing E-cadherin (Dooley et al., 2008), and this process seems to participate in liver fibrogensis. In addition, hepatocytes isolated from cirrhotic livers acquire a fibroblastoid phenotype with expression of Vimentin and Collagen, whereas hepatocytes from normal healthy livers are different, having completely epithelial traits (Nitta et al., 2008). In carcinogenesis, EMT has been recognized as a paramount player contributing to cancer invasion, metastasis, intratumoural heterogeneity and resistance capacity to therapy, which leads to poor clinical prognosis in various malignancies (Sabbah et al., 2008). EMT can be initiated by various mediators such as signaling pathways (TGF-β signaling, Wnt signaling, Notch signaling and others), tumor-stromal interaction, hypoxia, microRNA and epigenetic regulators (Polyak and Weinberg, 2009).

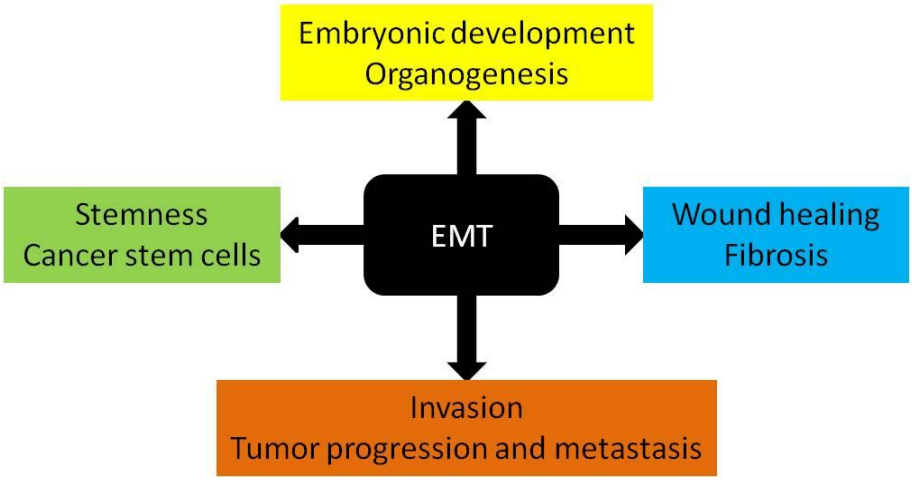

(modified from (van Zijl et al., 2009))

Fig.6. The involvement of EMT in physiological and pathophysiological events.

As for HCC, growing evidences indicate a central role of EMT in tumorigenesis. TGF-β signaling has a dual role in hepatic carcinogenesis. In healthy liver and at the early stage of HCC, TGF-β performs cell cycle arrest and apoptosis, whereas at later stages, it causes cell dedifferentiation and EMT (Gotzmann et al., 2002). TGF-β1 activates diverse factors and signaling pathways such as cyclooxygenase-2, platelet derived growth factor (PDGF), PI3K/Akt pathway, which facilitate the induction of EMT (Ogunwobi et al., 2012). Histone deacetylase 1 might be necessary for TGF-β induced EMT in HCC (Lei et al., 2010). Except the universal mediators for EMT, some liver specific factors contribute to EMT too. EMT in HCC is coupled with reduction of HNF-4 (hepatocyte nuclear factor), a transcription factor specific for hepatocyte differentiation and HNF-4α1 facilitates the reversion of the epithelial phenotype from a progressive one in rapidly growing HCC cells (Lazarevich et al., 2004). HCC cell experiments indicate that HCV core proteins strengthen tumor-promoting functions of TGF-β signaling by inducing EMT in human HCC cells, leading to strong reduction of E-cadherin. Furthermore, HBV-encoded protein HBX facilitates EMT through up-regulation of STAT5b (Battaglia et al., 2009; Lee et al., 2006). Hepatocyte growth factor (HGF) has also been reported to induce EMT in HCC via c-met signaling, Akt and COX-2 pathways (Ogunwobi and Liu, 2011; You et al., 2011).

1.9. Cell apoptosis

Apoptosis is a type of programmed cell death characterized by nuclear fragmentation, chromatin condensation, shrinkage of the cell and membrane blebbing (Danial and Korsmeyer,

2004). It plays crucial roles in developmental processes, deprivation of altered cells such as cancer cells and tissue remodeling during wound healing which is executed by the activation of caspases (a cystein-dependent aspartate specific protease). Caspases are highly conserved proteases that perform the cleavage between a cystein and an aspartic residue on their substrates. Until now 14 caspases have been discovered and most of them play a role in apoptosis. There are 2 subgroups of caspases: initiator caspases (caspase2, 8, 9 and 10) and effector caspases (caspase3, 6 and 7). Both the so called extrinsic and the intrinsic pathways can activate caspases. The extrinsic one is regulated by death receptors, primarily members of the tumor necrosis factor receptor (TNFR) family, like Fas-FasL on the cell surface, resulting in activation of caspase8. The intrinsic pathway is initiated by cytotoxic injury or developmental cues like stress, ionizing radiation, viral infection or DNA damage, and is strictly controlled by Bcl-2 family members, leading to the release of cytochrome c from the mitochondria, formation of the apoptosome composed of caspase 9 and apoptotic protease-activator factor-1 (APAF1) (Youle and Strasser, 2008). Activation of caspases8 or 9 triggers the activation of caspases3, 6 and 7 causing the typical features of cell apoptosis (Thornberry and Lazebnik, 1998).

The Bcl-2 family of proteins is crucial for the intrinsic pathway and includes 2 classes: anti-apoptotic members like Bcl-2, Bcl-xL and Mcl-1, and pro-apoptotic members like Bax, Bcl-x_S, Bad, Bim, Bak, Bmf, Bok, Noxa and Bid. They are composed of several structural domains: the hydrophobic domains in the BH1, BH2 and BH3 regions, and the amphipathic alpha-helix domain in the BH3 region (Burlacu, 2003; van Delft and Huang, 2006). The pro-apoptotic members can be divided into 2 subgroups: one containing 3 domains like Bax, Bak and Bok, and another with only the BH3 domain such as Bid, Bad, Bim, Mbf, Bik and Nova.

The pro-apoptotic members Bax and Bak interact with Bcl-2 and Bcl-xL in the cytoplasm. It was reported that BH3-only proteins directly bind and inhibit Bcl-2 and other anti-apoptotic members, thus de-repress Bax and Bak. And it is also postulated that BH3-only members directly activate Bax and Bak (Galonek and Hardwick, 2006). When there is stimulation of cell apoptosis, Bax, normally located in the cytosol, binds to the mitochondrial membrane, leading to the formation of pores termed mitochondrial voltage-dependent anion channel which facilitate the loss of selective ion permeability and release of cytochrome c and AIFs (apoptosis-inducing factors) into the cytosol (Shimizu et al., 2000). BH3-only proteins are controlled by transcriptional and post-transcriptional mechanisms. For instance, NOXA is

induced by p53 upon DNA damage. Growth factor deprivation induces the class O forkhead box transcription factor-3A (FOXO3A), leading to the activation of Bim (Cory and Adams, 2002).

In some conditions, the intrinsic and extrinsic pathways have a crosstalk via Bid. For example, in hepatocytes, caspase8, activated by the extrinsic stimuli can cleave Bid, whose cleaved fragments translocate into the mitochondrial outer membrane, which causes the execution of the intrinsic apoptosis pathway (Li et al., 1998).

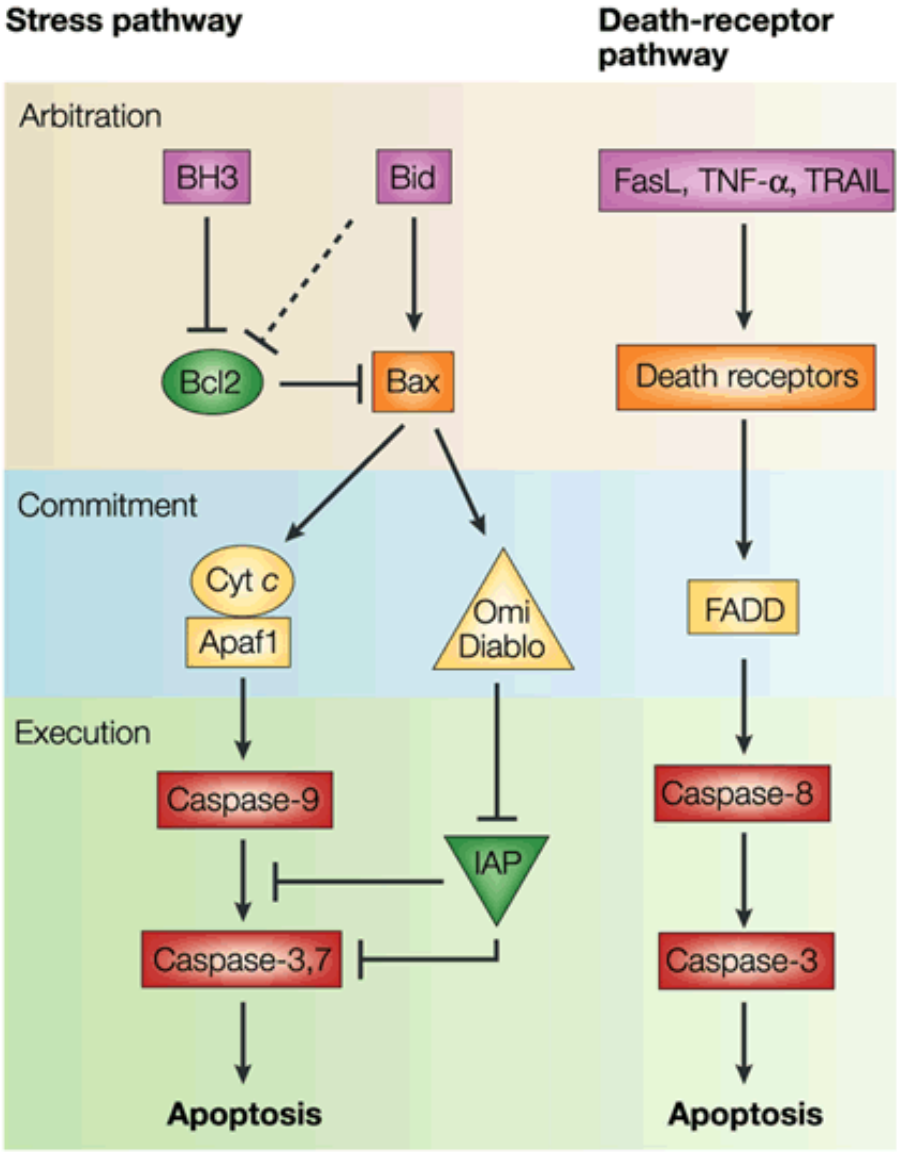

(From (Cory and Adams, 2002))

Fig.7. Stress (intrinsic) or death-receptor (extrinsic) pathways activate apoptosis cascades. The arbitration is determined by the Bcl family members for the stress pathway and by death receptors for the extrinsic pathway which drives a cell into apoptosis. Commitment to apoptosis is achieved by the release of cytochrome-c from the

mitochondria and by the release of Diablo as well as recruitment of FADD to the death receptor complex. Execution is demonstrated by the consecutive activation of initiator caspases (caspase9 and 8) and executer caspases (caspase3 and 7).

2. Aims of the study

In order to explore the potential functions of BMP-9 in the liver, we investigated expression and target gene regulation of BMP-9 in two settings of liver damage:
A) a single injection of CCl_4 in mice (a classic model for acute liver damage);
B) hepatocellular carcinoma (HCC; using human patient material and HCC cell lines).

The addressed questions included:
A) Is BMP-9 up-regulated under conditions of damage?
B) What are the BMP-9 target genes in hepatocytes?
C) Does BMP-9 play a role in hepatocyte apoptosis?
D) Is the BMP/Smad1 pathway involved in hepatic stellate cell (HSC) activation and their subsequent fibrogenic transdifferentiation to myofibroblasts?
E) Is BMP-9 potentially pro- or anti-carcinogenic in HCC?

The role of BMP-9/Smad1 signaling was assessed by *in vivo* experiments using the acute CCl_4-induced model of liver injury in mice and with *in vitro* experiments using primary cultures of hepatocytes or HSCs. To acquire a comprehensive view on BMP-9 effects in hepatocytes, a microarray analysis was performed to identify specific genes regulated by BMP-9 in proliferation/differentiation, apoptosis, iron homeostasis, sugar metabolism and others. Since epithelial-mesenchymal transition (EMT) is known to be critically involved in carcinogenesis, the influence of BMP-9 and its correlation with expression of EMT markers and invasiveness was analyzed in HCC cells and in human samples.

In conclusion, the study may have significant implications for delineating the roles of BMP-9 in the physiology and pathology of the liver and may aid to develop new therapeutic strategies for the treatment of liver diseases and/or liver cancer.

3. Materials and Methods

3.1. Media, buffers and reagents

3.1.1. Cell culture reagents

DMEM, Dulbecco's Modified Eagle's Medium with 25 mM Hepes and 4.5 g glucose per 500 ml (Lonza, Basel, Switzerland).
Williams' medium E, with sodium bicarbonate, without L-glutamine and phenol red (Sigma-Aldrich, Munich, Germany).
Trypsin, 10x (2.5% in PBS w/o Calcium and Magnesium) (PAA Laboratories, Darmstadt, Germany).
HBSS, Hank's buffered salt solution without Calcium and Magnesium (PAA Laboratories, Darmstadt, Germany).
Penicillin/Streptomycine, stock solution 10000 U/ml and working solution 100 U/ml (Biochrom KG, Berlin, Germany).
L-Glutamine, stock solution 200 mM and working solution 4 mM (Lonza, Basel, Switzerland).
FCS, fetal calf serum (Invitrogen, Karlsruhe, Germany).
Dexamethasone, working solution 100 nM (Sigma-Aldrich, Munich, Germany).
Trypan blue solution, stock solution 0.4% (Sigma-Aldrich, Munich, Germany).

3.1.2. Cytokines

BMP-9, recombinant human Bone Morphogenetic Protein-9 (rhBMP-9; R&D Systems, Wiesbaden-Nordenstadt, Germany).
TGF-β1, recombinant human Transforming Growth Factor-β1 (rhTGF-β1; R&D Systems, Wiesbaden-Nordenstadt, Germany).
PDGF-BB, recombinant human Platelet-derived Growth Factor-BB (rhPDGF-BB; PeproTech GmbH, Hambourg, Germany).
BMP-2, recombinant human Bone Morphogenetic Protein-2 (rhBMP-2; R&D Systems, Wiesbaden-Nordenstadt, Germany).
BMP-6, recombinant human Bone Morphogenetic Protein-6 (rhBMP-6; R&D Systems, Wiesbaden-Nordenstadt, Germany).

3.1.3. Inhibitors

Dorsomorphin, BMP/Smad1 signaling inhibitor (Miltenyi Biotec, Bergisch Gladbach, Germany).

3.1.4. Buffers and reagents for Western blot

RIPA buffer, 50 mM Tris-Cl (pH 7.5), 150 mM NaCl, 1% Nonidet P-40 (NP-40), 0.5% sodium deoxycholate, 0.1% SDS.
Complete proteases inhibitor cocktail, (Roche, Mannheim, Germany).
Phosphatases inhibitor cocktail II, (Sigma-Aldrich, Munich, Germany).
NuPAGE MOPS SDS running buffer, (20x) (Invitrogen, Karlsruhe, Germany).
NuPAGE transfer buffer, (20 x) , for 1 L 1x buffer dilute 50 ml 20x buffer in 750 ml distilled water and 200 ml methanol (Invitrogen, Karlsruhe, Germany).
10x TBS, Tris-buffered-saline: dissolve 12.10 g Tris-base and 87.66 g NaCl (both: Merck, Darmstadt, Germany) in 800 ml distilled water, adjust pH to 7.6 and add water to 1000 ml.
TBST, dilute 100 ml 10x TBS in 895 ml distilled water and add 5 ml 20% Tween20 solution (Bio-Rad Laboratories, Hercules, CA).
Ponceau S solution, (Sigma-Aldrich, Munich, Germany).
Stripping buffer, (Thermo scientific, Dreieich, Germany).
Blocking solution, 5 g non-fat milk power dissolved in 100 ml 1x TBS.
1M DTT, 0.154 g Dithiothreitol (Sigma-Aldrich, Munich, Germany) dissolved in 1 ml distilled water, store aliquots at -20°C.
NuPage LDS sample buffer, (4x) (Invitrogen, Karlsruhe, Germany).
Super Signal west dura luminol/enhancer solution, (Thermo scientific, Dreieich, Germany).
PageRulerPlus Prestained Protein Ladder, (Fermentas, St. Leon-Rot, Germany).
Protein standard, Bovine albumin, Fraction V (Sigma-Aldrich, Munich, Germany) diluted in RIPA buffer at concentrations of 1, 2, 4, 6 and 8 µg/µl was used as a standard to determine the protein concentration of samples.

3.1.5. Buffers and reagents for immunohistochemistry staining

Xylene, (Sigma-Aldrich, Munich, Germany).

Ethanol absolute, (Sigma-Aldrich, Munich, Germany).

Dual endogenous enzyme block, (DakoCytomation, Hamburg, Germany).

1mM EDTA, dilute 0.372 g EDTA (Ethylenediaminetetraacetic acid, Calbiochem, Darmstadt, Germany) in 1 L dH_2O and adjust pH to 8.0.

PBS, Phosphate buffered saline: dilute 9.55 g Instamed 9,55 g/l, PBS Dulbecco, w/o Ca2+, Mg2+ (Biochrom, Berlin, Germany) in 1 L dH_2O.

DAB, 3,3'-diaminobenzidine tetrahydrochloride (Sigma-Aldrich, Munich, Germany).

0.05 M Tris, (hydroxymethyl) aminomethane pH 7.6, 6.057 g of hydroxymethyl aminomethane (Serva, Dossenheim, Germany) was diluted in 1000 ml distilled water and adjusted to pH 7.6.

H_2O_2, (Merck, Darmstadt, Germany).

Malinol, (Waldeck GmbH, Muenster, Germany).

Hematoxylin, Hematoxylin-Solution, modified according to Gill III, (Merck, Darmstadt, Germany).

Phosphate buffered Formaldehyde 4%, (Sigma-Aldrich, Munich, Germany).

EnVision+ System-HRP (DAB) for rabbit, (DakoCytomation, Hamburg, Germany).

3.1.6. Buffers and reagents for immunofluorescent staining of monolayer cell cultures

Fixative solution, dissolve 20 g paraformaldehyde (Sigma-Aldrich, Munich, Germany), 50 µl 1 M $CaCl_2$ (Sigma-Aldrich, Munich, Germany) and 50 µl 1 M $MgCl_2$ (Sigma-Aldrich, Munich, Germany) in 500 ml heated PBS (to 80°C) and adjust pH to 7.4. Final concentration: 4%. Aliquots were stored at -80°C.

Permeabilization solution, dilute 150 µl Triton-X-100 (Sigma-Aldrich, Munich, Germany) in 50 ml HBSS.

Blocking solution, 1% (w/v) BSA in HBSS: 1 g Bovine albumin, Fraction V, (Sigma-Aldrich, Munich, Germany) diluted in 100 ml HBSS.

0.1% Tween20 solution, dilute 250 µl 20% Tween20 solution (Bio-Rad Laboratories, Hercules, CA) in 50 ml HBSS.

AlexaFluor 488 (green) 555 (red) 633 (far red) secondary antibodies, (Invitrogen, Karlsruhe, Germany).

DRAQ5, fluorescent nuclear staining (NEB, Canada).

DAKO Cytomation Fluorescent Mounting Medium, (DakoCytomation, Hamburg, Germany).

3.1.7. Buffers and reagents for *in situ* hybridization

SP6 or T7 RNA polymerase, 20 U/µl, (Fermentas, St. Leon-Rot, Germany).

NucleoSpin® TriPrep purification system, (Macherey-Nagel, Düren, Germany).

Hexamer primers, (Fermentas St. Leon-Rot, Germany).

AMV reverse transcriptase, (Promega, Madison, USA).

DreamTaq, 5 u/µl, (Fermentas St. Leon-Rot, Germany).

DNA extraction kit, NucleoSpin® Extract II, (Macherey-Nagel, Düren, Germany).

DIG 10x nucleotide mix, (Roche, Mannheim, Germany).

Fat pen, (Vector Laboratories, Loerrach, Germnay).

Alkaline phosphatase-coupled anti-digoxigenin antibody, at a dilution of 1:1000 in B-Block (Roche/Boehringer, Mannheim, Germany).

Alkaline phosphatase-coupled anti-fluorescein antibody, at a dilution of 1:1000 in B-Block (Roche/Boehringer, Mannheim, Germany).

0.2% Glycin, dissolve 0.5 g Glycin (DakoCytomation, Hamburg, Germany) in 250 ml 1x PBS.

Proteinase K, (Stock: 10mg/ml, DakoCytomation, Hamburg, Germany) diluted in 1x PBS.

4% PFA, heat 150 ml water to 60°C. Add 8 g PFA (Paraformaldehyde; Sigma-Aldrich, Munich, Germany), 1 ml 2 N NaOH and 20 ml 10x PBS. Wait till the solution is clear, and adjust the pH to 7.4 with 1 N HCl (ca. 1400 µl). Fill up to 200 ml with water and let it cool down.

4% PFA + 0.2% Glutaraldehyde, dilute1.6 ml Glutaraldehyde (Sigma-Aldrich, Munich, Germany) in 200 ml 4% PFA in 1x PBS.

1x PBS+Tween, add 10 ml 10% Tween20 (Bio-Rad Laboratories, Hercules, CA) to 1 ml 1x PBS.

B-Block, dissolve 1 g Boehringer Block (Roche/Boehringer, Mannheim, Germany) in 45 ml 1x PBS +Tween in a water bath at 65°C. After cooling add 5 ml sheep/goat serum. Aliquots are stored at -20°C.

NTM pH9.5, mix 25 ml 1 M Tris-HCl pH 9.5, 5 ml 5 M NaCl with 12.5 ml 1 M $MgCl_2$ and add Milipore-water (Milipore, Schwalbach, Germany) to 250 ml.

20x SSC, 175.3 g of NaCl and 88.2 g of sodium citrate were dissolved in 800 ml distilled water. The pH was adjusted to 4.5 and the end volume was adjusted to 1000 ml followed by autoclaving to be sterile.

2x SSC, dilute 50 ml 20x SSC pH 4.5 in 450 ml Milipore-water.

50% Formamid/2x SSC, mix 50 ml 20x SSC pH 4.5 with 250 ml 100% Formamide, then add Milipore-water to 500 ml.

10x PBS, dissolve 1.37 M NaCl 80.1 g, 0.027 M KCl 2.0 g, 0.015 M KH_2PO_4 2.0 g, 0.065 M Na_2HPO_4 x $2H_2O$ 11.6 g and Na_2HPO_4 x$12H_2O$ 23.3 g in 800 ml distilled water, adjust pH to 7.2-7.4 and add water to 1000 ml.

HYBmix, mix 5 ml Formamide, 2.5 ml 20x SSC pH 4.5, 100 mg Boehringer Block and 2 ml Milipore-water in a water bath at 65°C, add 100 µl 0.5 M EDTA pH 8.0, 100 µl Tween20 (10%), 100 µl 10% CHAPS, 4 µl Heparin (50 mg/ml) and 200 µl tRNA (50 mg/ml) (denature at 95°C for 5 min immediately before adding to the HYBmix).

Aquatex, mounting medium (Merck, Darmstadt, Germany).

NBT/BCIP, 20 µl/ml, (Roche/Boehringer, Mannheim, Germany).

INT/BCIP, 7.5 µl/ml, (Roche/Boehringer, Mannheim, Germany).

3.1.8. Buffers and reagents for RT-PCR

High Pure RNA isolation kit, (Roche, Mannheim, Germany).

50x TAE buffer, dissolve 121 g Tris base in 250 ml dH_2O, add 28.6 ml acetic acid and 50 ml 0.5 M EDTA pH 8.0, finally add dH_2O to 500 ml.

1x TAE buffer, dilute 20 ml 50x TAE buffer in 980 ml dH_2O.

Agarose gel, dissolve Universal agarose 1.5 g (Axon, Urbach, Germany) in 100 ml 1x TAE buffer in the microwave for 2 min, add 3 µl Ethidium Bromide solution 10 mg/ml (Sigma-Aldrich, Munich, Germany).

Reverse transcription kit, (Roche, Mannheim, Germany).

Trizol reagent, (GIBCO BRL, Eggenstein, Germany).

Chloroform, (Carl Roth GmbH, Karlsruhe, Germany).

Isopropanol, (VWR International GmbH, Darmstadt, Germany).

3.1.9. Reagents for animal experiments

CCl_4, carbon tetrachloride (Sigma-Aldrich, Munich, Germany).

Fluitest GOT AST kit, (Analyticon, Lichtenfels, Germany).
Fluitest GPT ALT kit, (Analyticon, Lichtenfels, Germany).
Fluitest LDH kit, (Analyticon, Lichtenfels, Germany).

3.1.10. Reagents for Caspase3 assay

Cell lysis buffer, 50 ml of 100 mM HEPES, 13.3 ml of 750 mM NaCl, 0.1 g of CHAPS, 0.1 ml of 100 mM EDTA and 0.1 ml of 1 M DTT are mixed and adjusted to 100 ml with pH7.4.
Assay buffer, 50 ml of 100 mM HEPES, 13.3 ml of 750 mM NaCl, 0.1g of CHAPS, 0.1 ml of 100 mM EDTA, 1 ml 1M DTT and 10 ml Glycerol are mixed and adjusted to 100 ml with distilled water.
AC-DEVD-AFC (substrate), 5 mg Caspase3 substrate AC-DEVD-AFC is dissolved in 5 ml DMSO and aliquots are stored in -20°C (Biomol, Hamburg, Germany). 1:20 dilution of the stock solution is prepared in assay buffer for the experiments.

3.2. Cells and cell culture

3.2.1. Isolation of primary hepatocytes and their culture

Mouse hepatocytes were isolated from male C57/BL6 mice (8 - 13 weeks old) using collagenase perfusion. Hepatocyte isolation from mice was approved by the animal experimental committees and all animals received humane care in compliance with the German Animal Protection Act. They were housed in the standard animal house at the University-Hospital Mannheim. Mice were anesthetized with intraperitoneal injection of ketamine hydrochloride 10% (115.34 mg/ml; Essex Tierarznei, Munich, Germany; 5 mg/100 mg body weight) and xylazine hydrochloride 2% (23.32 mg/ml; Bayer Leverkusen; 1 mg/100 mg body weight). BASAL HANKS solution was prepared with 8 g NaCl, 0.4 g KCl, 3.57 g Hepes, 0.06 g Na_2HPO_4 x 2 H_2O, 0.06 g KH_2PO_4 in 1 L distilled H_2O, which was adjusted to pH 7.4 and sterilized. HANKS solution I was comprised of BASAL HANKS solution with 2.5 mM EGTA, 0.1% glucose and penicillin/streptomycin diluted at 1:100. HANKS solution II was obtained by supplementing BASAL HANKS solution with 0.3 mg/ml collagenase CLSII and 5 mM $CaCl_2$. HANKS solution I and HANKS solution II were pre-warmed in a water bath at 42°C. Collagenase was supplemented right before liver perfusion. The abdominal cavity was exposed under sterile conditions and the portal vein was punctured with

a 24 G catheter which was connected with a silicon tube (2.4 mm diameter). The mouse liver was perfused with HANKS solution I via a peristaltic pump at a perfusion rate of 8 ml/min. The vena cava and right hear ventricle were incised for fluent outflow. Perfusion of HANKS solution I lasted 2 min and HANKS solution II 5 to 7 min. After successful perfusion the whole liver was transferred to a sterile Petri dish and the gall bladder was removed. In the sterile bench, the liver capsules were removed with a pincette without damage to the live tissue. The perfused liver was divided into a suspension of single cells, cell clumps and debris with gentle shaking. The suspension was transferred to a 100 μm cell strainer and filtered. Then the filtrate was transferred to a 50 ml Falcon tube and washed with Williams E medium twice, followed by centrifugation at room temperature at 37.5 × g for 2 minutes. The cells were re-suspended with Williams E medium. The percentage of viable cells was determined by counting with trypan blue.

For primary hepatocyte culture, 3 kinds of medium were prepared. Medium 1 was Williams' medium E supplemented with 10% FCS, 2 mM L-glutamine, 1% penicillin/streptomycin and 100 nM dexamethasone. Medium 2 was medium 1 without 10% FCS. Medium 3 was Williams' medium E supplemented only with 2 mM L-glutamine and 1% penicillin/streptomycin.

Isolated fresh hepatocytes were plated on collagen-coated 6-well plates at a density of 4×10^5 cells/well in Medium 1 and incubated in 5% CO_2 at 37° C. After 4 hours, Medium 1 was replaced with Medium 2. On the second day, Medium 2 was changed to Medium 3. Cells were stimulated with recombinant TGF-β1 (5 ng/ml) or BMP-9 (5 - 50 ng/ml) for the indicated time points.

3.2.2. Isolation of primary hepatic stellate cells and their culture

Hepatic stellate cells were isolated from female Balb/c mice by the pronase/collagenase method followed by single-step density gradient centrifugation with Nycodenz (Nyegaard Co. AS, Oslo, Norway) as previously described (Dooley et al., 2000). Balb/c mice (weight around 20 g) were anesthetized and the abdominal cavity was opened under sterile conditions. The liver was perfused via the *vena portae* with HBSS buffer w/o Ca^{2+} and Mg^{2+}. After enough perfusion, the liver was transferred to a funnel and perfused with pronase for 10 min, followed by being perfused with collagenase for 30 min. Then the liver was disintegrated and cell

suspension was obtained which was centrifuged with Nycodenz in gradient and washed several times. The cells were re-suspended with DMEM + 10% FCS. The percentage of viable cell number was determined by counting with trypan blue. The mean purity was higher than 95%. The cells were cultured in DMEM medium, supplemented with 4 mmol/L L-Glutamine, 10% FCS and penicillin (100 IU/ml)/Streptomycin (100 µg/ml). The first change of medium was performed 24 h after seeding. The cells were maintained at 37°C, 5% CO_2 in a humidified atmosphere. FCS was reduced to 0.5% for starvation overnight followed by stimulation with the indicated factors.

3.2.3. Cell lines and their culture

Hepatocellular carcinoma cell lines HepG2 and HLE cells were cultured in DMEM supplemented with 10% FCS, L-glutamine and penicillin/streptomycin.

HEK293A, human embryonic kidney cells were transformed by sheared human Ad5 DNA and were used for adenovirus amplification. Low-passaged cells were cultured in DMEM supplemented with 10% FCS, L-glutamine and penicillin/streptomycin.

LX-2 is a human hepatic stellate cell line (Xu et al., 2005). Cells were cultured in DMEM supplemented with 2% FCS, L-glutamine and penicillin/streptomycin.

3.3 Animal experiments

CCl_4 injection in mice is a widely accepted model to study liver fibrosis and/or liver regeneration *in vivo*. All animal protocols completely complied with the guidelines for animal care. All mice were fed at libitum and received humane care in compliance with Heidelberg's guidelines for the care and use of laboratory animals in research.

30 male Balb/c mice weighing 20 - 25 g 8 weeks after birth were used in this study. Acute liver injury was induced by intraperitoneal injection with 1 ml/kg body weight of CCl_4 (CCl_4 was prepared in a mixture with mineral oil with a ratio of 1:8), and mice were sacrificed at 3 h, 6 h, day 1, day 2, day 3, and day 6 post injection. Mice without CCl_4 injection sacrificed at 0 h served as normal control. Blood was taken for serum parameters and livers were used for preparation of protein lysates (Western blot), immunohistochemistry and total RNA.

Aspartate aminotransferase (AST), alanine aminotransferase (ALT) and lactate dehydrogenase (LDH) activities in serum from the treated mice were determined by assay kits. A portion of liver samples were fixed in 4% buffered paraformaldehyde for histological examination and immunostaining. The left were snap frozen in liquid nitrogen. 4 - 6 mice were used for every time point.

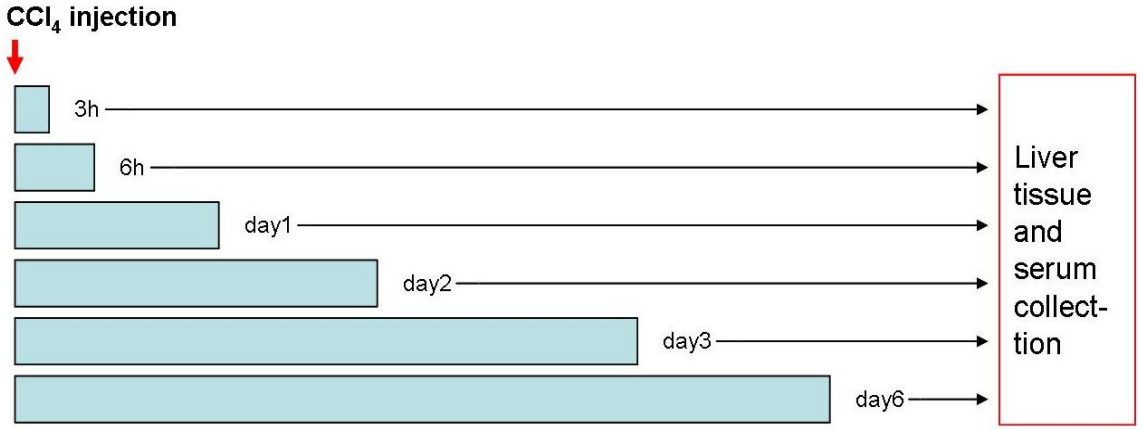

Fig.8. Time schedule of acute CCl_4 treatment and sample collection. Mice were introperitoneally injected with CCl_4. Blood and liver tissue samples were taken at the indicated time points (3 h, 6 h, d 1, d 2, d 3 and d 6 after a single CCl_4 injection and 0 h without CCl_4 injection).

3.4. Adenoviruses

3.4.1. Virus amplification

Human recombinant E1-deleted adenoviral vectors which carry a DNA construct of interest were amplified in HEK293A cells. The amplifications were performed with low-passaged HEK293A cells. HEK293A cells were cultured in DMEM plus 10% FCS till 80% confluence. Medium was changed. Cells were infected with viruses of moi 10 (infectious units) in DMEM with 10% FCS. After 48 to 96 hours, the complete cytopathic effect can be observed. Both cells and medium were harvested. The virus ‘soup’ can be obtained after freezing (-80°C) and thawing (room temperature) 3 times followed by centrifugation with 2,500 g for 15 min at 4°C.

3.4.2. Constructs

No.	Name	Description	Source
1	AdLacZ	Adenovirus expressing bacterial β-galactosidase under the control of a CMV promoter (constitutively active promoter comprising a cytomegalovirus enhancer)	Biosciences Clontech, Palo Alto, CA
2	AddnALK1/2	dominant negative mutant of ALK1 and ALK2 under the control of CMV-promoter; HA-tag	kindly provided by Dr. Peter ten Dijke, Leiden, Netherland
3	AdcaALK1	mutant, constitutively active BMP-, Activin- or TGF-β receptor type I under the control of the CMV-promoter; HA-tag induced mutation: Q200D	kindly provided by Dr. Carl-Henrik Heldin, Uppsala, Sweden
4	AdcaALK2	mutant, constitutively active BMP-, Activin- or TGF-β receptor type I under the control of the CMV-promoter; HA-tag induced mutation: Q207D	kindly provided by Dr. Carl-Henrik Heldin, Uppsala, Sweden
5	AdSmad1	Smad cDNA under the control of CMV-promoter	kindly provided by Dr. Carl-Henrik Heldin, Uppsala, Sweden

Tab.1. List of adenoviral constructs used in this study.

3.4.3. Infection of cell cultures

Cells were plated in the morning in DMEM with 10% FCS. In the late afternoon, medium was changed and viruses of different moi (1, 5, 10, 15, 25, 50) were added. 24 h later, medium was changed. In the morning of the third day, serum starvation was performed. 4 h later, cells were stimulated with BMP-9.

3.4.4. Measurement of virus titer

Determination of virus titer was achieved using the "Adeno-X^{TM} Rapid Titer Kit" (BD Bioscience, Heidelberg, Germany). 0.5 ml HEK293A cells were plated in a 24-well plate with a density of 2.5×10^5 cells/well in standard growth medium (DMEM + L-glutamine + Penicillin/Streptomycin + 10 % FCS). Descending dilutions of viral samples were prepared (10^{-2}, 10^{-3}, 10^{-4}, 10^{-5}, 10^{-6}). 50 µl viral dilution was added to each well (each dilution was assayed in duplicate). After 48 h incubation at 37°C with 5% CO_2, medium was removed and

cells were fixed with methanol at -20° for 10 min, then incubated with the primary antibody against viral hexon protein at 37°C for 1 hour. Cells were washed with PBS 3 times and incubated with the secondary antibody at 37°C for 1 hour. Positive staining (brown color) was visualized with DAB. Positive cells were counted under the microscope (×10) and infectious units (ifu/ml) were calculated according to the following formula:
[(infected cells / field) × (fields / well)] / [(volume of virus [ml]) × (dilution factor)] = [(infected cells / field) × 247] / [0.05 ml × (dilution factor)] = [ifu / ml]
The typical yield ranged between 0.5 - 2 × 10^9 ifu/ml.

3.4.5. Determination of virus function

HCC cells were infected with 0.5, 1.0, 1.5, 2.0 × 10^7 ifu per 10^5 cells followed by 24 h culturing. Cell lysates were tested in Western Blot (using specific antibody, e.g. anti-HA when the cells were infected with AddnALK1/2). For further experiments the smallest amount of virus still causing strong expression of the transgene was used.

3.5. Western blot

Western blotting was used for the analysis of protein expression.

3.5.1. Preparation of protein lysates from liver tissue

50 - 100 mg liver tissue was mixed with 500 µl RIPA (containing complete protease inhibitor + phosphatase inhibitor cocktail II), homogenized using an Ultraturax. The homogenate was centrifuged at 10,000 rpm for 10 min at 4°C. The supernatant was transferred to a fresh tube and the pellet containing tissue debris was disposed. Protein lysates were stored at -20°C.

3.5.2. Preparation of protein lysates from cultured cell

Cells were washed twice with HBSS. 50 to 100 µl RIPA (depending on the cell number and protein content in the cells) added to the wells. Cells were scraped off with a cell scraper on ice, then the cell debris and RIPA buffer were transferred to fresh 1.5 ml Eppendorf tubes which were centrifuged with 10,000 rpm for 10 min at 4°C. The supernatant was transferred to a fresh tube and the pellet was disposed. Protein lysates were stored at -20°C.

3.5.3. Measurement of protein concentration

Protein concentrations were measured with the DC Protein Assay (Bio-Rad Laboratories, Munich, Germany). Each sample was prepared in duplicate into a 96-well plate and measured. The absorbance was read at 690 nm using a spectrophotometer (Wallac 1420 Victor, Wallac, Turku, Finland). Protein concentrations were calculated as an average value of double counts and related to the protein standard curve and blank value of RIPA.

3.5.4. Sample preparation for denaturing NuPAGE® Gel electrophoresis

The volumes of protein, dH_2O and the mixture of DTT and LDS sample buffer were calculated. The NuPage LDS sample buffer (4x) was re-warmed to 37 °C. Certain amount of dH_2O, mixture of DTT and LDS sample buffer and protein samples were added into a 1.5 ml eppendorf tube. The mixture was vortexed and centrifuged shortly, followed by being heated to 95° C in a heating block for 5 min with shaking. After brief centrifugation the samples were loaded on a pre-cast NuPAGE® 4 - 12% Bis-Tris Gel. 1.5 µl of PageRulerPlus Prestained Protein Ladder was used as a protein marker.

3.5.5. SDS gel electrophoresis

The proteins were separated on the pre-cast NuPAGE® 4 - 12% Bis-Tris Gel in the XCell SureLock™ Novex Mini-Cell (Invitrogen) at 145 V for 105 min.

3.5.6. Western blot

XCell II blotting apparatus and XCell II Blot Module (Invitrogen) were used. The gel-membrane sandwich was composed of chromatography paper (Whatmann 3MM, Maidstone, England) and nitrocellulose membrane. The proteins were transferred from a gel onto the nitrocellulose membrane (Pierce, Woburn, MA, USA) via blotting at 300 V and 250 mA for 2 h (cell lysates) or 3 h (tissue lysates).

Ponceau S solution was used to view whether the proteins were successfully transferred to the membrane.

3.5.7. Antibodies for Western blot

First antibodies					
Cat. No	**Clonality**	**Supplied by**	**Antibody, epitope, location**	**Species***	**Dilution**
610181	Mouse- mono	BD Biosciences	E-cadherin	h, m, r	1:1000
sc-25778	Rabbit- poly	Santa cruz biotechnology	GAPDH	h,m,r	1:1000
No.A2547	Mouse-mono	Sigma	α-SMA, N-terminal peptide	h, m, r	1:1000
A-5441	Mouse-mono	Sigma	β-actin, N-terminal peptide	h, m, r	1:1000
#1649-1	Rabbit- mono	Epitomics	Smad1	h,m	1:1000
H6908	Rabbit	Sigma	HA	h, m, r	1:1000
Ab20346	Mouse- mono	Abcam	Vimentin	h,m,r,chicken, dog,pig	1:1000
1880-1	Rabbit- mono	Epitomics/Biomol	pSmad3 (pS423/425)	h,m	1:1000
9664	Rabbit- mono	Cell signaling	cleaved Caspase3	h, m, r, monkey, dog	1:500
25280	Mouse-mono	Santa cruz	PCNA	h, m, ra	1:1000
GTX108417	Rabbit-poly	Genetex	BMP-9	h, m, r	1:500
ab12221	Rabbit-poly	Abcam	N-cadherin	h, m, Ra, Chicken, Cow, Zebrafish	1:1000
2870	Rabbit-mono	Cell signaling	Bcl-2	h, m, r	1:1000

Tab.2. First antibodies used for Western blot.

*h, human; m, mouse; r, rabbit; ra, rat.

Secondary antibodies	**Company**	**dilution**
Goat anti-mouse HRP	Santa Cruz Biotechnology, California, USA	1:5000
Goat anti- rabbit HRP	Santa Cruz Biotechnology, California, USA	1:5000

Tab.3. Horseradish peroxidase (HRP)-conjugated antibodies used for immunostaining. Dilutions of the antibodies were used according to instructions provided by the companies.

3.5.8. Immunodetection of proteins

The blotting membrane was blocked with the blocking solution for 1 h at room temperature, followed by wash with TBST for 5 min 3 times. The membrane was incubated with the first

antibody at 4 ° C overnight. Afterwards, it was washed with TBST for 5 min 3 times. Then it was incubated with the certain secondary antibody for 1 h at room temperature. After being washed with TBST for 5 min 3 times, the membrane was incubated with ECL solution for 2 min. Then the chemiluminescence was detected with a Fujifilms LAS 1000 image detection system.

3.6. Immunohistochemistry (IHC)

3.6.1. Deparaffinization

Formalin fixed and paraffin embedded tissue sections were incubated at 60° C for 60 min. They were dewaxed with xylene for 5 min 3 times.

3.6.2. Dehydration

Sections were incubated through descending ethanol: 100% ethanol for 5 min twice and 95% ethanol for 5 min once.

3.6.3. Rehydration

Sections were incubated in distilled water 1 × 5 min, followed by being rinsed in PBS 1 × 5 min.

3.6.4. Antigen demasking

Sections were heated up to 95° C (2 - 3 min 200 W) in 10 mM EDTA pH 8, then 50 sec-off-10 sec-on of the microwave were performed for 10 min. Then sections were cooled for 35 - 40 min to reach a temperature of 37° C and washed with PBS 3 × 5min.

3.6.5. Blocking of endogenous peroxidase

Tissues were covered with some drops of “Dual Endogenous Enzyme Block” in a humid atmosphere for 15 min. For some antibodies, additional blocking with 3% H_2O_2 was performed.

3.6.6. Antibody incubation

After sections were washed with PBS 3 × 5min, they were incubated with the diluted first antibodies at 4° C overnight. Afterwards, they were re-warmed at room temperature for 1 hour. The corresponding secondary antibodies were added after washing the sections with PBS 3 × 5 min.

First antibodies					
Cat. No	**Clonality**	**Supplied by**	**Antibody, epitope,lacation**	**Species***	**Dilution**
1406-1460	Rabbit-mono	AbD serotec	BMP-9	h	1:400
#9511	Rabbit- poly	Cell signaling	pSmad1 (Ser463/465)/Smad5 (Ser463/465)/Smad8 (Ser426/428)	h,m,r	1:100
M0851	Mouse-mono	DAKO	α-SMA	h, m, r	1:500
3195	Rabbit-mono	Cell signaling	E-cadherin	h, m, dog	1:400
ab15200	Rabbit- poly	Abcam	desmin	h, m, rat	1:100
ab17732	Rabbit-poly	Abcam	Snail	h, m	1:1000
2870	Rabbit-mono	Cell signaling	Bcl-2	h, m, r	1:100
9664	Rabbit-mono	Cell signaling	cleaved caspase3	h, m, r, monkey, dog	1:100

Tab.4. First antibodies used for IHC staining.

Second antibodies	**Company**	**dilution**
Goat anti-mouse	DAKO, Glostrup, Denmark A/S	1:200
Swine anti-rabbit	DAKO, Glostrup, Denmark A/S	1:200

Tab.5. Secondary antibodies used for IHC staining.

3.6.7. Preparation and application of peroxidase substrate DAB

1 tablet of DAB was dissolved in 15 ml 0.05 M Tris (hydroxymethyl) aminomethane, pH 7.6 (keep in dark) which was filtered with filter paper. 12 µl H_2O_2 was added to the filtrate. Sections were washed with PBS 3 × 5 min and covered with 200 µl of the substrate. The color development was observed under the microscope (maximally incubation time: 10 min) and the reaction was stopped by immersing the sections in distilled water for 5 min.

3.6.8. Counterstaining, clearing and mounting

Sections were immersed in Mayers Hämalaun solution for several seconds and then rinsed with water for 10 min, followed by being dehydrated through ascending ethanol: 95% ethanol 2 × 10 sec and 100% ethanol 2 × 10 sec. Clearing was performed in xylene 2 × 10 sec. Finally sections were mounted with malin oil and covered with glass.

3.6.9. Semi-quantitative analysis for IHC staining

Staining scores were calculated according to the following method: positive cell number was graded as 0 - 4 (0, no positive cells; 1, less than 25% positive cells; 2, 25% - 50% positive cells; 3, 50% - 75% positive cells; 4, more than 75% positive cells). The intensity of positivity was graded as 1 - 3 (1, weak yellow staining; 2, strong and brown staining; 3, very strong and deep brown staining). The score was calculated according to this formula: grade of number × grade of intensity. According to the calculated score, the staining level was divided into 3 levels: 0, no positive staining; 1+, score of 1 to 5; 2+, score of no less than 5.

3.7. Immunofluorescence (IF)

3.7.1. Preparation of cover slips and plating of the cells

One cover slip per well was placed in a 12-well plate, which was exposed to UV light under the sterile hood for 1 h. Wells were washed once with HBSS before cell plating. Cell treatment was done at the indicated time point.

3.7.2. Fixation and permeabilization of cells

Cell medium was removed and cells were washed twice with HBSS. Cells were incubated with 300 µl 4% PFA solution for 5 min. 4% PFA was discarded and cells were permeabilized with 300 µl permeabilization buffer for 5 min. After discarding the permeabilization buffer, cells were fixed with 2% PFA for 5 min. 2% PFA was removed and cells were washed once briefly with HBSS. Then the slides were dried.

3.7.3. Incubation with primary antibody

Cells were washed with HBSS 2 × 5 min, followed by 0.1% Tween20 solution 1 × 1 min. Then cells were blocked with the blocking solution for 1 h at room temperature. Cells were washed with 0.1% Tween20 solution 1 × 1 min. The cover slips were placed in the lid, which was then put in a humid chamber. The primary antibody solution was added onto the cover slips. Cells were incubated with the primary antibody at 4°C overnight.

First antibodies					
Cat. No	**Clonality**	**Supplied by**	**Antibody**	**Species***	**Dilution**
610181	Mouse- mono	BD Biosciences	E-cadherin	h, m, r	1:200
Ab20346	Mouse- mono	Abcam	Vimentin	h, m, r, chicken, dog, pig	1:200

Tab.6. First antibodies used for IF staining.

3.7.4. Incubation with secondary antibody

The primary antibody solution was discarded. Cells were washed with HBSS 3 × 5 min and 0.1% Tween20 solution 1 × 1 min. The secondary antibody diluted in blocking buffer was added onto the cover slips. Cells were incubated with it for 45 min at room temperature.

Second antibodies	**Company**	**dilution**
Goat anti-mouse Alexa488	Invitrogen	1:200
Goat anti-rabbit Alexa488	Invitrogen	1:200

Tab.7. Secondary antibodies used for IF staining.

3.7.5. Nuclear staining

The secondary antibody solution was discarded. Cells were washed with HBSS 3 × 5 min and with 0.1% Tween20 solution 1 × 1 min. DRAQ5 diluted in HBSS (1:5000) was added onto the cover slips. Cells were incubated for 5 min at room temperature.

3.7.6. Mounting

The cover slips were removed from the lid without washing steps. A drop of mounting medium was put on a clean slide and a cover slip was placed up-side-down into the mounting medium. The slides can be stored in the dark at -80°C for at least 2 weeks.

3.8. Detection of mRNA expression

3.8.1. Isolation of total RNA from monolayer cells

RNA isolation was performed using the High Pure RNA Isolation kit from Roche according to the company's instruction. After being washed with HBSS, cells cultured in 6-well plates were incubated with 400 µl lysis buffer for 1 min, following by 200 µl HBSS. Both the lysis buffer and HBSS were transferred into a fresh sterile eppendorf tube and vortexed vigorously for 50 sec, then they were pipetted into a spin column for adsorption. After centrifugation, followed by 3 washing steps, the RNA was eluted with elution buffer. RNA concentration and purity were determined using a spectrophotometer.

3.8.2. Isolation of total RNA from mouse liver tissue

50 - 100 mg liver tissue was homogenized in 1 ml Trizol using an UltraTurrax (IKA, Staufen, Germany). This homogenate was centrifuged with 12,000 g for 10 min at 4°C. The supernatant was transferred to a fresh sterile tube. 200 µl isopropanol was added into 1 ml Trizol. The mixture was shaken vigorously for 15 sec, incubated for 2 - 3 min at room temperature and centrifuged with 12,000 g for 15 min at 4°C. The aqueous phase was transferred into another fresh sterile tube. Then 500 µl isopropanol was added into 1 ml Trizol. The mixture was incubated for 10 min at room temperature and centrifuged with 12,000 g for 10 min at 4°C. Afterwards, the supernatant was removed and 1 ml 75% ethanol was added. This mixture was centrifuged with 10,000 g for 5 min at 4°C and the supernatant was removed. 1 ml 75% ethanol was added and the mixture was centrifuged with 7,500 g for 5 min at 4°C. The supernatant was removed and the pellet was dried for 5 - 10 min. The latter was dissolved in RNase/DNase free water, cooled on ice for 2 min. The RNA was purified with High Pure RNA Isolation kit from Roche according to the company's instruction mentioned above. RNA concentration and purity were determined using a spectrophotometer.

3.8.3. Reverse transcription (RT)

Reverse transcription reaction was performed with the Reverse Transcription Kit from Roche by following the instruction manual. 1 µg total RNA was reversely transcribed into 20 µl cDNA, diluted with 60 µl d H_2O and used for standard PCR.

3.8.4. Polymerase chain reaction (PCR)

2 µl of cDNA was used in conventional PCR amplification to detect the expression of interest. Samples were initially denatured at 95°C for 5 min and then subjected to different cycles of amplification (detail in Tab.8.). PCR products were separated on 1.5 % agarose gels.

Gene name	Forward	Reverse	Size (bp)
Snail	AATCGGAAGCCTAACTACAGCG	GTCCCAGATGAGCATTGGCA	147
Collagen 1a(2)	GGCTTCCTGGTGAGAGAGG	CCTCTCTTTCCTTCTTCACC	497
human rS6	GACTGATACTACAGTGCCTC	GTAGAAGCTCGCAGAGAGG	371
mouse rS6	GTGCCTCGTCGGTTGGGAC	GACAGCCTACGTCTCTTGGC	320
desmin	CTACTCGTCCAGCCAGCG	CGGATCTCCTCTTCATGCAC	732
ALK1	CTTCTCCTCGAGGGATGAAC	TGGTTTGCCCTGTGTACCG	283
ALK2	TTCCAGGTTTATGAGCAGGG	CGTTTCCCTGAACCATGACT	537
BMPRII	GGACGCATGGAATATTTGCT	TGGCTGCATTATCTTCCTCC	310
ACVR2A	CAAACTGGTGTTGAACCGTG	GCACCAAGGAATAGAGCAGG	307
Smad1	CCAGCCGCTATGAATGTGAC	GAGTGAGGGTAGGTGCTGC	625
Smad4	CCTCATGTGATCTATGCCCG	CTGTGGACATTGGAGAGTTG	844
Fibronectin	GGTGTGGTCTACTCTGTGG	CACACGTGCACCTCATCATG	540
BMP-9	CTGAGCTCCGACTCTATGTC	GTGCAATGATCCAGCTGTCC	581
Collagen 1a1	GTCTCACTGGCAGTCCTGG	TCTCCAGGAACACCCTGTTC	381
α-SMA	GTGCTGGACTCTGGAGATG	CCACCGATCCAGACAGAGTA	575
Id-1	CTGCTCTACGACATGAACGG	CGTCGGCTGGAACACATGC	274

Tab.8. Primer sequences used in the study.

3.8.5. Real-time quantitative PCR

Real-time quantitative PCR was done on the Sequence Detection System ABI Prism 7700 (Applied Biosystems, Foster City, CA, USA,) and TaqMan® probes abd TaqMan Universal PCR Master Mix, No AmpErase UNG (Applied Biosystems, Foster City, CA, USA, Part No. 4324018) were used according to the manufacturer's instructions. Samples in triplicate were initially denatured at 50°C for 2 min and 95°C for 10 min and then subjected to 40 cycles of 15 s at 95°C and 1 min at 60°C. PCR products were investigated with ABI Prim 7000 SDS software ® (Applied Biosystems, Foster City, CA, USA,). Expression levels of targeted genes were calculated with the comparative ΔΔCt evaluation method with PPIA as reference gene.

Gene name	Assay ID
BMP-9	Mm00807340_m1
Id-1	Mm00775963_g1
PPIA	Mm02342429_g1

Tab.9. Real-time quantitative PCR gene expression assays used in the study.

3.9. Microarray analysis of gene expression

Mouse primary hepatocytes were treated with BMP-9 (5 ng/ml) for 24 h and RNA isolated from 3 independent repetitions was collected and pooled, and was used for the microarray analysis. The gene expression was analyzed via moe430_2 microarrays (Affymetrix, Santa Clara, CA, USA). The array was scanned following the manual of the manufacturer. Raw values for fluorescence intensity were normalized via quantile normalization. Gene expression values were displayed after being converted to a $\log_2$ scale. Genes down-/up-regulated more than 1.4 fold were regarded as significantly changed.

3.10. Transwell assay

The migration of HepG2 and HLE cells was detected in a modified 24-well transwell chamber (BD Biosciences, Heidelberg, Germany). In the upper chamber, 25,000 cells in 0.25 ml of serum-free culture medium were treated with BMP-9 (50 ng/ml). Medium with 10% FCS and with or without BMP-9 (50 ng/ml) was loaded in the lower wells serving as chemotactic stimulus. After 6 (HLE cells) or 24 (HepG2 cells) hours at 37°, the cells on the upper surface of the filter and the underside were trypsinized, washed with serum-free DMEM and

transferred to a 96-well flat bottomed plate, respectively. After centrifugation at 1,000 rpm for 10 min, the supernatant was discarded and 40 ul buffer of the CellTiter-Glo® Luminescent Cell Viability Assay (Promega, Mannheim, Germany) was added to each well. Luminescence was measured by the iControl1.6 program. The percentage of migrated cells was calculated. Each experiment was conducted in triplicate, and the mean ± SD was calculated.

3.11. *In situ* hybridization (ISH) (done by Shahrouz Ghafoory)

3.11.1. RNA isolation from target tissue and cDNA synthesis

For human samples, RNA was isolated from HepG2 cells using NucleoSpin® TriPrep purification system (Macherey-Nagel, Düren, Germany). First-strand cDNA was synthesized with 3 μg total RNA, random hexamer primers and avian myeloblastosis virus (AMV) reverse transcriptase following the manufacturer's protocol.

For mouse samples, RNA was isolated from wild type male C57BL/6 mouse liver using NucleoSpin® TriPrep purification system. The following steps were the same as above described.

3.11.2. Primer design

Primers were designed to contain a short terminal 5' sequence followed by the sequence of SP6 or T7-RNA-polymerase promoter and the specific primer sequence of interested genes. The SP6 promoter was combined with the up-stream of the specific primer and the T7 promoter with the down-stream of the primer. Then anti-sense cRNA probes were synthesized using T7-RNA-polymerase, and by SP6-RNA-polymerase yielded sense cRNA probes.
The following primers were used
(H. BMP-9. SP6) 5'-
CAGTGAATTGATTTAGGTGACACTATAGAAGTGGAACAAGAGAGCGTGCTCAAG
AAGC-3' and (H. BMP-9. T7) 5'-
CAGTGAATTGTAATACGACTCACTATAGGGAGACTCCTCCACCTCTCTAACTTCC
ATC-3' (amplified fragment: 998-1820 nt of BMP-9 mRNA, GeneBank: NM_016204.1).

(M. Id1. SP6) 5’-
CAGTGAATTGATTTAGGTGACACTATAGAAGTGGTAATCGACTACATCAGGGACC
TGC-3’ and (M. Id1. T7) 5’-
CAGTGAATTGTAATACGACTCACTATAGGGAGACAGAAACACGCGGGGTTGATT
AACC-3’ (amplified fragment: 338-739 nt of Id1 mRNA, GeneBank: NM_010495.2)
(M. BMP-9. SP6) 5’-
CAGTGAATTGATTTAGGTGACACTATAGAAGTGCAGCCAAAAATGCTTACCAGGT
GGC-3’ and (M. BMP-9. T7) 5’-
CAGTGAATTGTAATACGACTCACTATAGGGAGACAGCTCTCTGCACATCACCTGT
ATC-3’ (amplified fragment: 969-1720 nt of BMP-9 mRNA, GeneBank: NM_019506.4)
(M. Albumin. SP6) 5’-
CAGTGAATTGATTTAGGTGACACTATAGAAGTGCCTGCAACACAAAGATGACAA
CCCC-3’ and (M. Albumin. T7) 5’-
CAGTGAATTGTAATACGACTCACTATAGGGAGAGGGATCCACTACAGCACTTGGT
AAC-3’ (amplified fragment: 423-1559 nt of Albumin mRNA, GeneBank: NM_009654.3)
(M. TβR-II. SP6) 5’-
CAGTGAATTGATTTAGGTGACACTATAGAAGTGCGTTCCCAAGTCGGATGTGGAA
ATGG-3’ and (M. TβR-II. T7) 5’-
CAGTGAATTGTAATACGACTCACTATAGGGAGAGAGAAGCGGCATCTTCCAGAG
TGAAG-3’ (amplified fragment: 407-756 nt of TβR-II mRNA, GeneBank: NM_009371.3)

3.11.3. Template synthesis by PCR

PCR templates were acquired as follows: 1 μg cDNA, 1 μl deoxynucleotide triphosphates (dNTPs) 10 mM, 0.5 μl of DreamTaq 5 u/μl, 0.5 μl upstream (SP6) primer and 0.5 μl downstream (T7) primer (each 100 pmol/μl) in a total volume of 50 μl were used for the first PCR reaction. Standard PCR was performed with 2 min at 95°C, preceding 30 cycles with 30 sec at 95°C, 2 min at 60°C and 1 min at 72°C.

All the products except a separate small aliquot of the reaction were run on a 1% agarose gel without ethidium bromide. And this ethidium bromide-stained lane for the small aliquot with a suitable size standard was cut from the gel and stained to visualize the PCR reaction products. The position of the PCR fragment in the ethidium bromide-stained lane was measured and a ruler was used to define the position of the corresponding non-stained gene

specific cDNA PCR fragments. They were excised from the gel and extracted with a DNA extraction kit. The remaining gel may be stained to confirm that the band was correctly excised.

The purified PCR fragments were then used for a second PCR amplification in a larger volume (e.g. 400 µl) according to the protocol described above, as well as several parallel PCR reactions of 50 µl. The resulting template PCR fragments were purified and concentrated with phenol-chloroform extraction and ethanol precipitation. The concentrated PCR fragments were purified again using agarose (1%) gel electrophoresis, the appropriate PCR fragments were excised and finally purified with a DNA extraction kit. The purified PCR fragments were utilized directly for in vitro transcription of the cRNA probes.

3.11.4. ISH riboprobe synthesis

Digoxigenin (DIG) labeled cRNA was synthesized with 1 µg of probe template DNA of interested genes, 1 µl DIG 10x nucleotide mix, 1 µl SP6 or T7 RNA polymerase (20 u/µl) in a total volume of 10 µl. SP6 RNA polymerase was used for sense labeled cRNA preparation and T7 RNA polymerase for anti-sense labeled cRNA preparation. The labeled cRNA probes were precipitated with absolute ethanol and the pellet was dissolved in 50% Formamide / 2x SSC.

3.11.5. Preparation of tissue sections

Pieces of mouse and human tissue were rapidly rinsed in PBS and fixed with 4% PFA at 4°C overnight. Fixed tissue was washed with PBS, dehydrated with 50%, 70%, 96% and 100% ethanol, immersed in xylene twice and embedded with paraffin. Sections were cut at a thickness of 4 µm and placed on poly-L-Lysine-covered slides.

Paraffin sections were deparaffinized and rehydrated in xylene 2 × 7min, xylene/ethanol 1 × 2 min, ethanol in decreasing concentration 2 × 2 min followed by PBS. Sections were then incubated with 20 µl/ml proteinase K for 8 min at 37°C, with 0.2% glycin for 6 min and post-fixed with 4% PFA supplemented with 0.2% glutaraldehyde for 20 min.

3.11.6. ISH

After ‘post-fixation’ in 4% PFA-glutaraldehyde, slides were washed twice with PBS. Liver sections were then covered with hybridization mix (5 ml Formamid, 2.5 ml 20x SSC, pH 4.5, 100 mg Boehringer Block, 2 ml Milipore-Water, 100 µl 0.5 M EDTA, pH 8.0, 100 µl Tween 20 (10%), 100 µl 10% CHAPS, 4 µl Heparin (50 mg/ml), 200 µl tRNA (50 mg/ml) and prehybridized for 1h at 69°C. The hybridization mix was denatured at 95°C for 5 min and chilled on ice immediately before it was added to tissue sections. After prehybridization, specific probes were added to 200 - 300 µl hybridization mix in order to obtain a final concentration of 2 ng/µl. The probe containing the hybridization mix was denatured at 95°C for 5 min and cooled on ice. For hybridization, the hybridization mix was added to tissue sections, which were incubated overnight at 70°C. Afterwards, tissue sections were washed with 2x SSC, incubated with 50% Formamide/ 2x SSC 30 min at 65°C, and washed with PBS containing 0.1% Tween at room temperature. Then the sections were incubated for 1 h at 37°C with 1% blocking reagent in PBS (B- Block) and 2 h at 37°C with alkaline phosphatase-coupled anti-digoxigenin antibody diluted 1:1000 in B-Block. Excess antibody was removed by washing for 2 × 8 min with PBS plus 0.1% Tween, then sections were incubated for 10 min in NTM Buffer. Color development was performed at 37°C overnight in NTM buffer with NBT/BCIP 20 µl/ml. Staining was stopped by a 10 min-wash with PBS and slides were mounted with Aquatex.

For double staining, after the washing step, the slides underwent another fixation with 4% PFA/PBS for 10 min at room temperature followed by washing 3 times with PBS plus 0.1% Tween. Afterwards, they were incubated with 1% blocking buffer for 1 h and with alkaline phosphatase-coupled anti-fluorescein antibody diluted 1:1000 in B-Block. Excess antibody was removed by washing 5 min × 3 with PBS plus 0.1% Tween, then sections were incubated for 10 min in NTM Buffer. Color development was performed at 37°C overnight in NTM buffer with INT/BCIP 7.5 µl/ml. Staining was stopped by a 10 min-wash with PBS and slides were mounted with Aquatex.

3.11.7. Semi-quantitative analysis of ISH results

For the semi-quantitative assessment of ISH staining, staining scores were calculated with the following method: positive cell number was graded as 0 - 4 (0, no positive cells; 1, less than 25% positive cells; 2, 25% - 50% positive cells; 3, 50% - 75% positive cells; 4, more than

75% positive cells). The intensity of positivity was graded as 1 - 3 (1, weak purple staining; 2, strong and purple staining; 3, very strong and deep purple staining). The score was calculated according to this formula: number × intensity. According to the calculated score, the staining level was classified into 3 levels: 0, no positive staining; 1+, score of 1 to 4; 2+, 5 and more.

3.12. Tissue specimens

A total of 41 cases diagnosed as primary HCC from the surgical files in the Eastern Hepatobiliary Surgery Hospital, Second Military Medical University, Shanghai, China were enrolled in this study. The diagnosis was determined according to the UICC TNM classification of primary liver cancer, 6th edition (Sobin, 2002). 39 of them (95.12%) were HBsAg-positive. The study protocol conformed to the ethical guideline of the Declaration of Helsinki (1975). The study was approved by the ethics committee of the Second Military Medical University, Shanghai, China. All patients provided an informed consent.

3.13. Caspase3 assay

3.13.1. Preparation of cell lysates

Cell apoptosis was induced in 12-well plates after treatment with TGF-β1 and/or BMP-9 for 72 h at 37°C. Medium was removed and cells were washed with HBSS twice, which was sucked off later. 80 μl lysis buffer was added to each well and the cells were scratched off. Cell lysates were centrifuged at 13,000 rpm for 5 min at 4°C. Then the supernatant was transferred to a fresh tube and put on ice for immediate assay. The experiments were performed in triplicates.

3.13.2. Measurement of protein concentration

The protein concentration was used to normalize the obtained data from the ELISA reading. It was done with the method described in the part of Western blot.

3.13.3. Measurement of Caspase3 activity

30 µl of the samples were transferred to each well of a 96-well plate (flat bottom white). Duplicates were performed for each sample. 70 µl of the assay buffer was added to each well. Then the plate was pre-incubated at 37°C for 10 min to allow enzyme interaction. The reaction was started when 10 µl of caspase3 substrate was added to each well and mixed gently by shaking. The plate was covered and incubated at 37°C for 60 min. The fluorescence (excitation 400 nm; emission 505 nm) was measured.

3.14. *in vitro* cell proliferation assay

1×10^4 LX-2 cells were pleated in a 6-well plate. BMP-9, TGF-β1 and PDGF were diluted in medium with a final concentration of 5 ng/ml, 5 ng/ml and 20 ng/ml, respectively. After serum starvation overnight, LX-2 cells were incubated with BMP-9, TGF-β1 or PDGF for 72 h. Fresh medium with stimulation was changed every 24 h. After 72 h stimulation, cells were trypsinized, stained with trypan blue and counted with a Neubauer improved counting chamber (Biochrom, Berlin, Germany). Every condition was performed in triplicate and the experiment was repeated three times.

3.15. Microscopy

3.15.1. Phase contrast microscopy

Phase contrast images were achieved with a Leica IPB microscope and a Leica DC500 camera (Leica Microsystems, Wetzlar, Germany). Leica IM50 software was applied to acquire images.

3.15.2. Confocal microscopy

Confocal scanning was performed with a Leica laser scanning spectral confocal microscope, model DMIRE2 equipped with an HCX PL Apo 40 ×/1.32 numeric aperture oil objective (Leica Microsystems, Wetzlar, Germany). Excitation was obtained with an argon laser which emits at 488 nm, a krypton laser at 568 nm and a helium/neon laser at 633 nm. Images were processed by a TCS SP2 scanner and Leica confocal software (version 2.5) (Leica Microsystems, Wetzlar, Germany).

3.16. Statistical analyses

The association between immunohistochemical staining levels and clinicopathological features was evaluated with kendall-tau rank correlation analysis in SAS version 9.2 (Cary, NC, USA). (done by Dr. Li Li)

Student's *t*-test was used to analyze the result of the migration assay. Error bars were the standard error of the mean. $P<0.05$ was considered statistically significant.

4. Results

(will be partially published in Breitkopf-Heinlein et al., submitted to Hepatology and Li et al., submitted to Oncogene)

Part I

Activation of the BMP-9/Smad1 signaling pathway in acute carbon tetrachloride-induced mouse liver injury *in vivo* and its potential functions in hepatocytes and hepatic stellate cells *in vitro*

4.1. Acute CCl_4-induced liver injury is established in Balb/c mice

Acute carbon tetrachloride (CCl_4) intoxication led to necrosis of pericentral hepatocytes within 24 h which peaked at day 2 when serum ALT, AST and LDH levels were maximally elevated (Fig. 9 A, B) implicating serious liver damage. Subsequently a resolution of the necrotic damage occurred and at day 6 liver histology was almost recovered to the normal appearance. Serum markers for damage returned to low levels already on day 3 (Fig. 9 A). HE stainings demonstrated that within the pericentral area necrosis and inflammation occurred at day 1 and maximally at day 2, which was consistent with the elevation of the plasma enzymes (Fig. 9 B). Albumin is a specific marker for hepatocytes. Its synthesis and excretion is one of the important functions of hepatocytes (Schwarz et al., 1986). In the damaged area, the intensity of the positive signal of albumin mRNA as determined by ISH was largely reduced, especially at day 3 the damaged pericentral area could be clearly determined by its almost negative staining for albumin in hepatocytes (Fig. 9 C).

This canonical acute liver injury model was used to investigate Smad1 activation, α-SMA, desmin, cleaved caspase3, BMP-9 and Id-1 expressions and their localizations within the liver tissue.

A

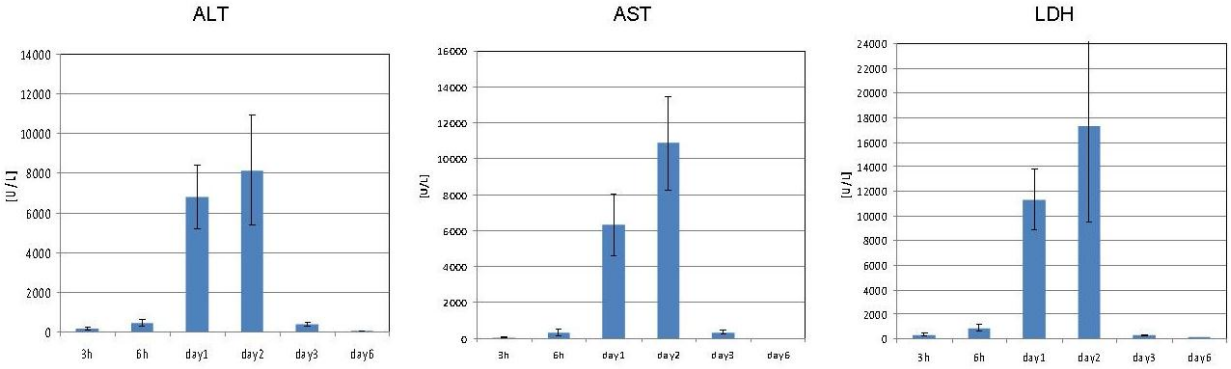
ALT
AST
LDH
[U/L]
3h
6h
day1
day2
day3
day6

B

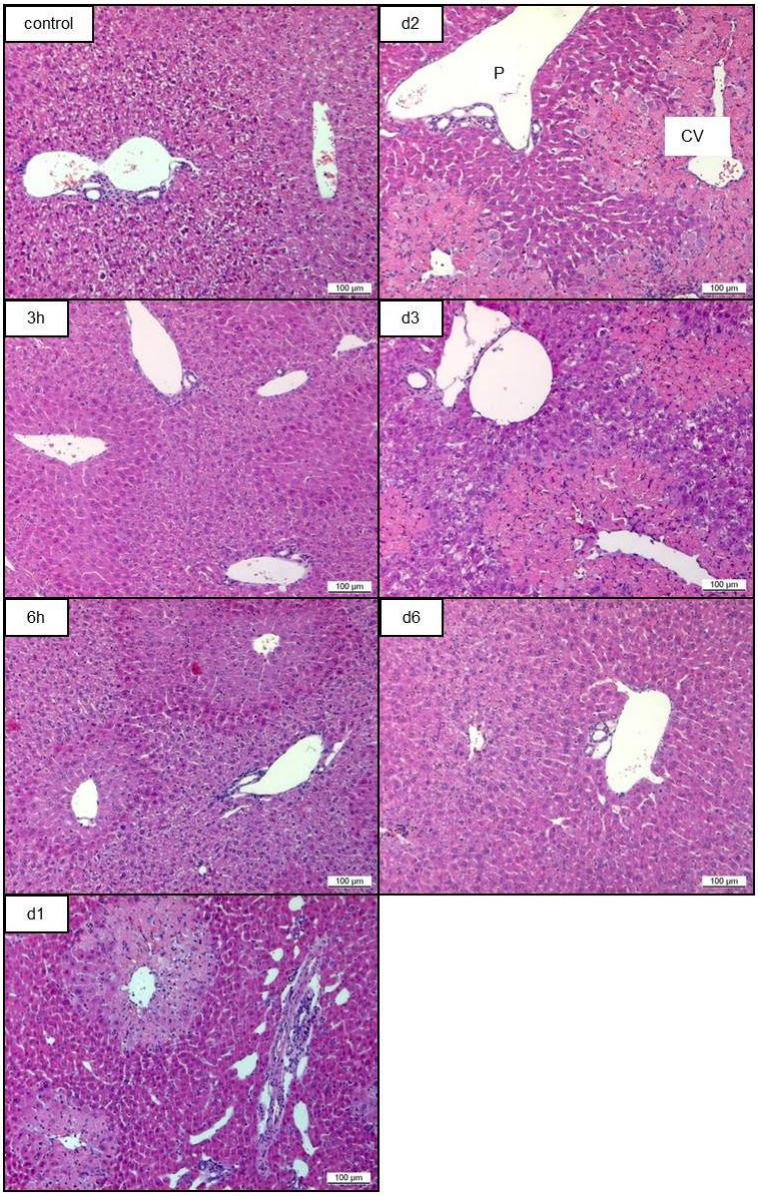
control
d2
P
CV
3h
d3
6h
d6
d1
100 µm

C

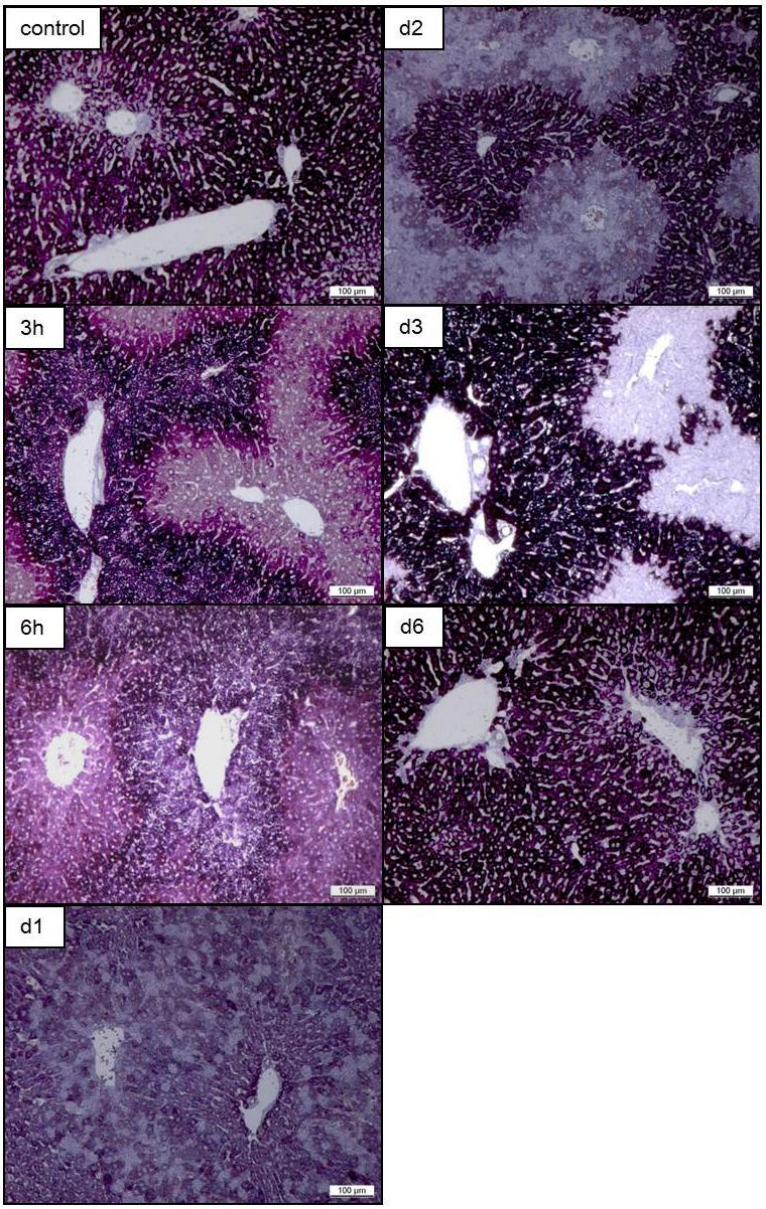

Fig.9. Typical characteristics of the acute CCl_4 mouse model for liver injury. **A,** Serum ALT, AST and LDH levels at the indicated time points after CCl_4 application. **B,** HE staining showed transient necrotic damage. P, portal area; CV, central vein. Magnification, 10×. **C,** *In situ* hybridization of albumin mRNA. Magnification, 10×.

4.1.1 Expressions of BMP-9 and pSmad1 are increased after CCl_4 intoxication

At the protein level, BMP-9 expression was significantly increased at day 3, which went down at day 6 (Fig. 10 A). From ISH, positive signal of BMP-9 mRNA existed in the cholangiocytes of the normal control liver (Fig. 10 D). After liver injury, BMP-9 mRNA expression was increased and positive signal could also be observed in hepatocytes. Especially at day 3, in the pericentral area, BMP-9 positive staining was observed (Fig. 10 D).

Interestingly, with real-time quantitative PCR BMP-9 mRNA increased very rapidly, within 3 h after CCl_4 injection (Fig. 10 B). This first, transient induction was followed by an up-regulation of the BMP-9 target gene Id1 on the mRNA level (Fig. 10 C). At day 3 to 6 BMP-9 mRNA expression increased again, but without a corresponding up-regulation of Id-1, implying that there exists a fine-tuned schedule of BMP-9 expression upon liver damage.

By Western blot analyses, an increase of phosphorylated Smad1 appeared as early as 3 h after CCl_4 application. This level of pSmad1 was reduced at day 1, but was still elevated until at least day 6 compared to normal livers (Fig. 10 A). From 3 h to day 3, within the lobule, intensities of pSmad1 immunostainings decreased gradually from the central vein to the portal area. At 3 h and 6 h, positive staining was mainly localized in hepatocytes and it was negative in sinusoidal cells. But from day 1 to day 3, besides positivity in hepatocytes, there was also positive staining in sinusoidal cells, most likely Kupffer cells, endothelial cells and hepatic stellate cells. In the pericentral area, positive staining was localized to the nucleus as well as cytoplasm of damaged hepatocytes. Furthermore, positivity could be observed in infiltrating cells, probably proliferating, activated HSCs. At day 6, when the liver nearly recovered to the normal status, only very weak pSmad1 expression was observed (Fig. 10 E). These data indicate that BMP-9/Smad1 signaling is activated upon CCl_4-induced liver injury.

A

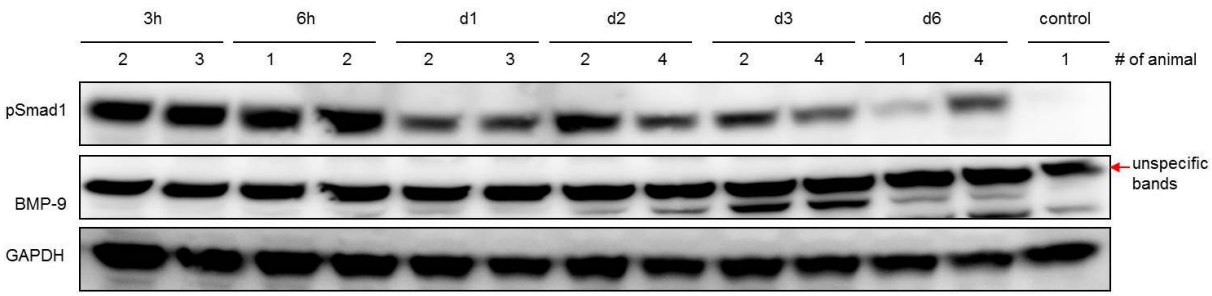

B

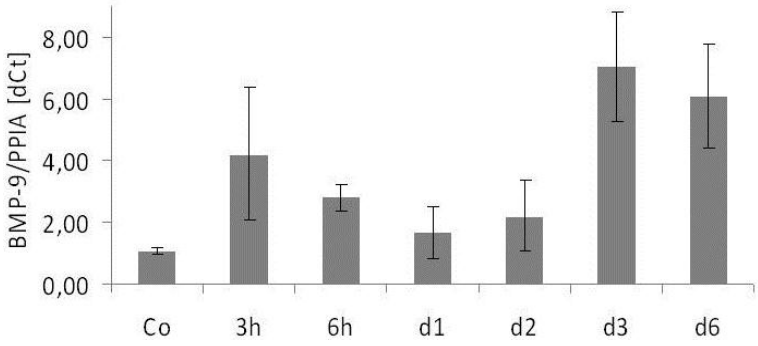

C

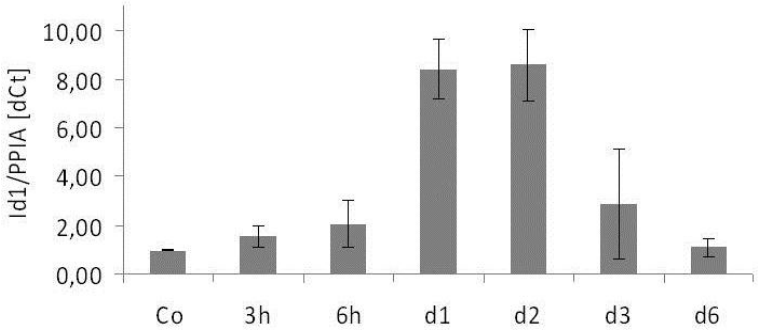
Id1/PPIA [dCt]
10,00
8,00
6,00
4,00
2,00
0,00
Co
3h
6h
d1
d2
d3
d6

D

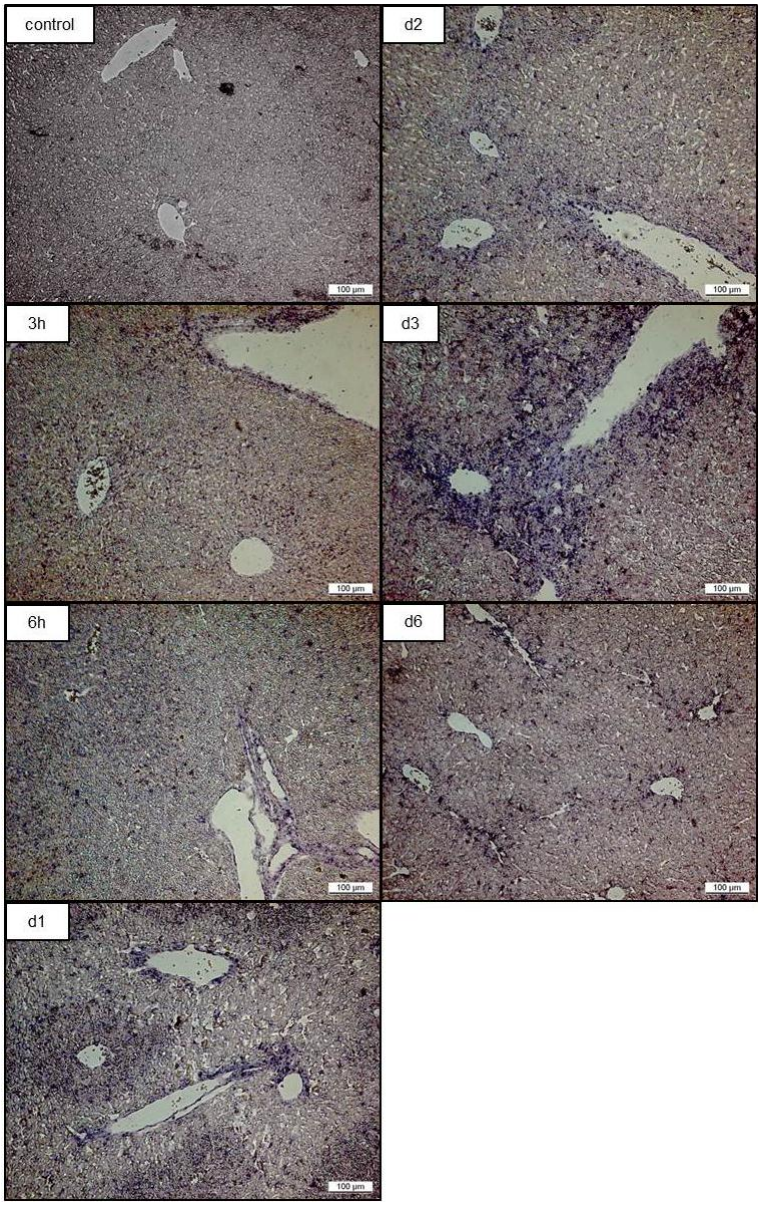
control
d2
3h
d3
6h
d6
d1

E

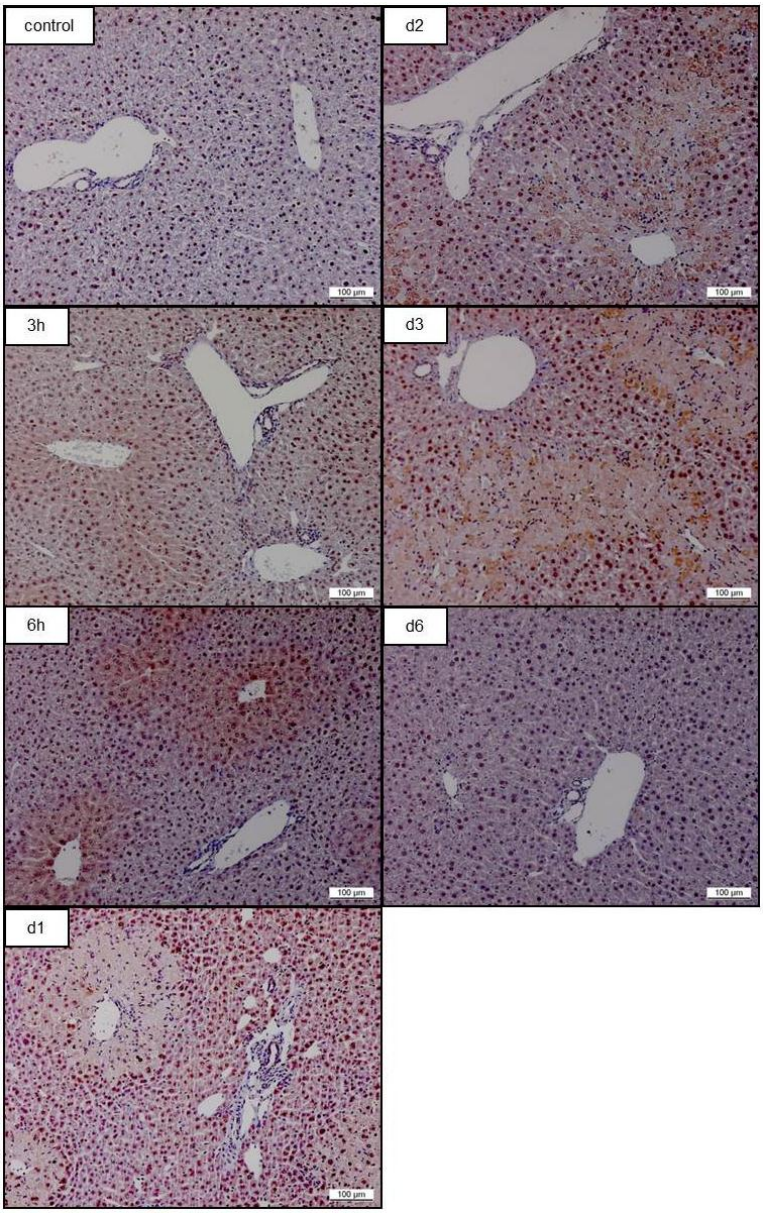

Fig.10. Expression of BMP-9 and pSmad1 in response to CCl_4-mediated liver injury. **A,** Western blots against BMP-9 and pSmad1 with GAPDH as a loading control. **B,** Real-time PCR analysis of BMP-9 expression. PPIA was used as internal control. **C,** Real-time PCR analysis of Id-1 expression. PPIA was used as internal control. **D,** *In situ* hybridization using BMP-9 cRNA as probes (positive staining = dark purple). Magnification, 10×. **E,** Immunohistochemistry (IHC) for pSmad1 using DAB (reddish brown color). Magnification, 10×.

4.1.2 BMP-9 and Id-1 are increased in the pericentral area

At day 3 after CCl_4 intoxication, expression of albumin in hepatocytes within the pericentral area was largely decreased compared to the remaining area (Fig. 11 A), meaning that due to processes of necrosis and/or apoptosis hepatocytes in this area showed reduced functionality.

ISH staining of serial sections showed that at day 3 in the pericentral area BMP-9 as well as its target gene, Id-1 was increased, implying that the BMP-9/Smad1 pathway was activated (Fig. 11 A, B). This could be further proven by the double staining for BMP-9 and Id-1 which demonstrated that BMP-9 and Id-1 co-localized in the pericentral area (Fig. 11 C). Interestingly, TβR-II was highly expressed in hepatocytes outside the pericentral area. However, inside the pericentral area, just like albumin its expression was lower (Fig. 11 A, B). These patterns of expressions imply that activation of BMP-9 and TGF-β1 signalling during wound healing processes in the liver is restricted to non-overlapping regions, pointing to differential functions of these cytokines.

A

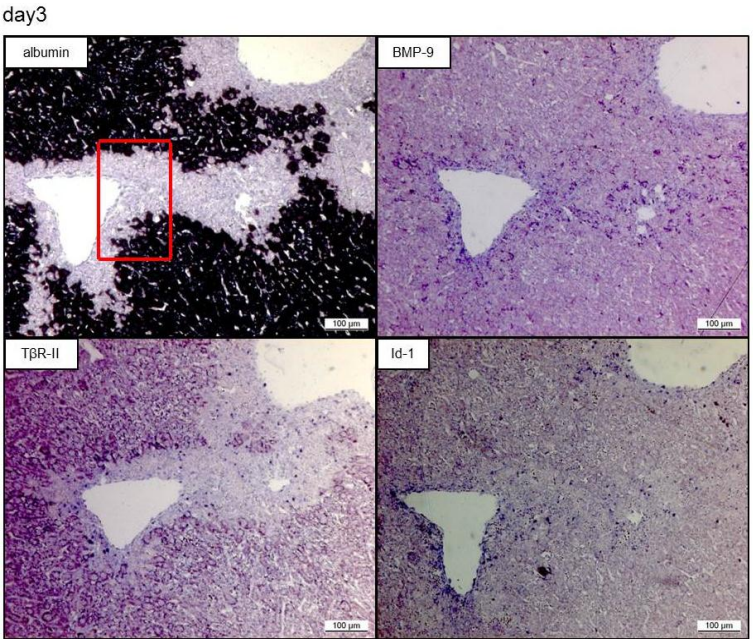

B

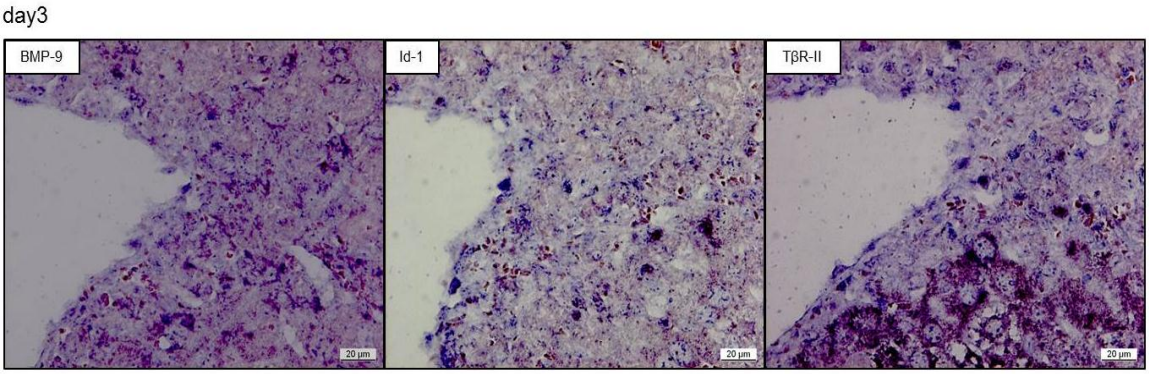

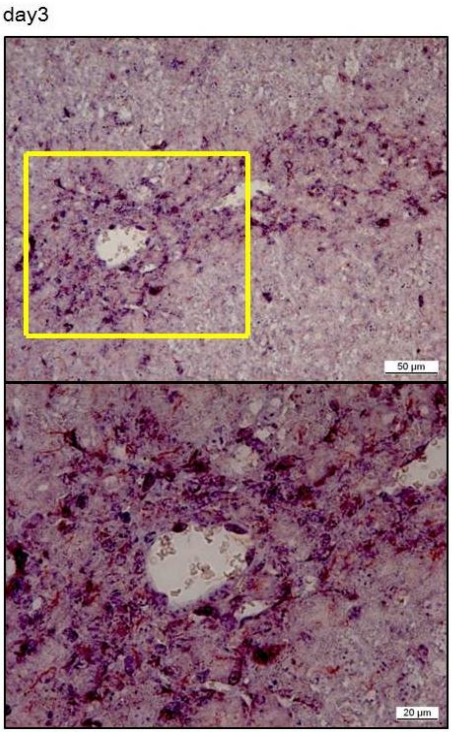

C

Fig.11. Localization of BMP-9, TβR-II and Id-1 in response to CCl_4-medicated liver injury at day 3. **A,** *In situ* hybridization was performed using albumin, TβR-II, Id-1 and BMP-9 cRNA as probes with serial sections. Magnification, 10×. **B,** Higher magnification of the indicated pericentral area in **A** is displayed. Magnification, 40×. **C,** Co-staining of Id-1 and BMP-9 by ISH. The purple color indicated BMP-9 mRNA expression and the red Id-1 mRNA expression. Magnification, 20× and 40×.

4.1.3 Apoptosis of hepatocytes is increased after CCl_4 intoxication in mice

Cell apoptosis is indispensable for tissue self-renewal. In the control normal livers, there was slight positivity of the apoptosis marker, cleaved caspase3, which was detected by IHC as small granules within the cytoplasm of a few hepatocytes. Starting already at 3 h after CCl_4 intoxication its staining intensity was increased, but was limited to the pericentral area, reaching a peak at day 3. Simultaneously, the size of the positive granules reached its maximal at day 3. At day 6, staining almost disappeared and its expression pattern was similar to that in the control liver (Fig. 12 A).

Time-dependent changes of caspase3 activation could not be confirmed using total liver lysates in Western blot analysis but a constant increase compared to the control normal liver was always detected (Fig. 12 B).

Intriguingly, at day 3 in the pericentral area both cleaved caspase3 and pSmad1 were expressed in hepatocytes (Fig. 12 C), suggesting pSmad1 signaling was involved in hepatocyte apoptosis *in vivo*.

A

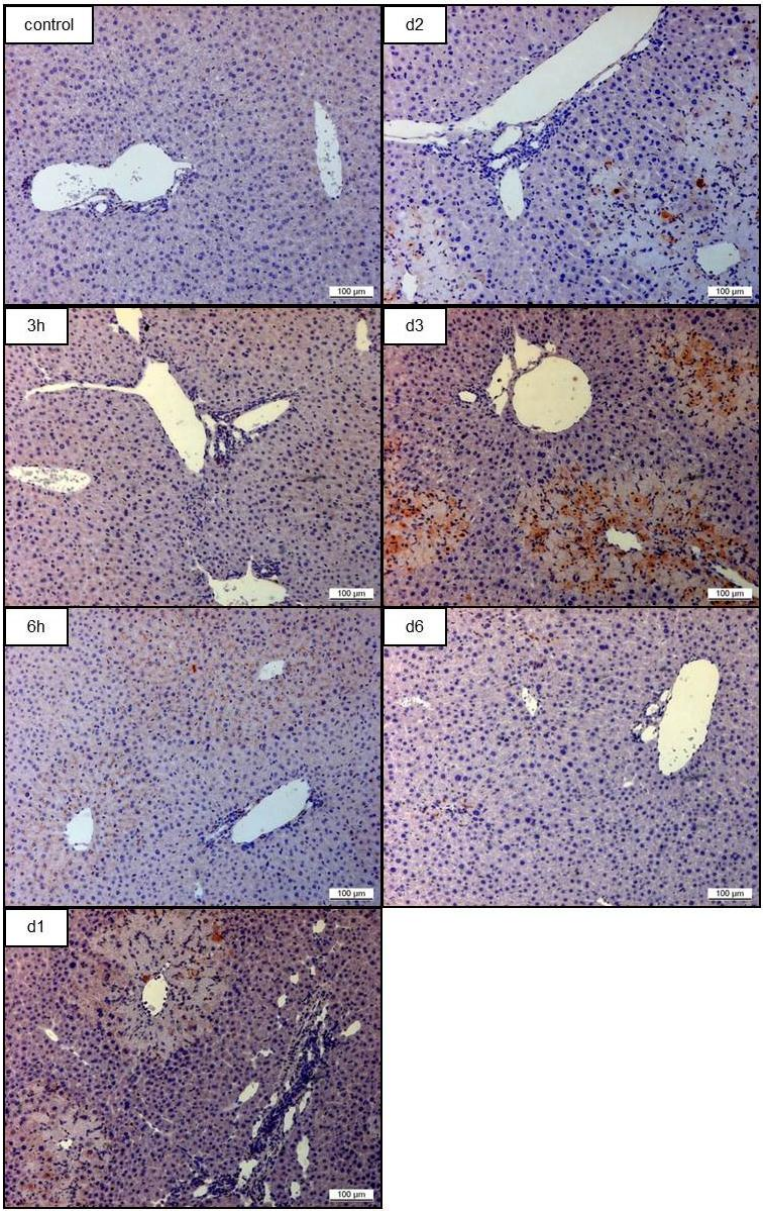
control
d2
3h
d3
6h
d6
d1

B

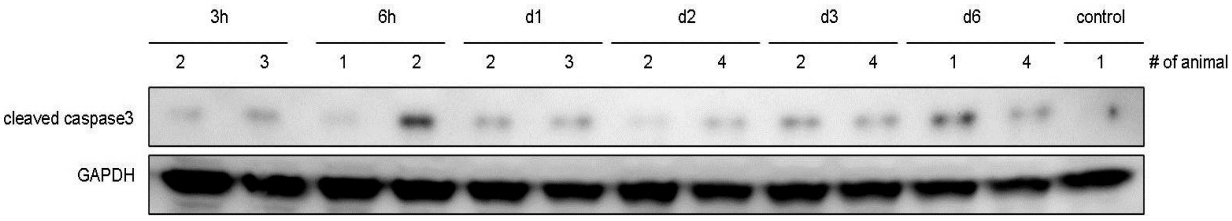
3h
6h
d1
d2
d3
d6
control
2
3
1
2
2
3
2
4
2
4
1
4
1
# of animal
cleaved caspase3
GAPDH

C

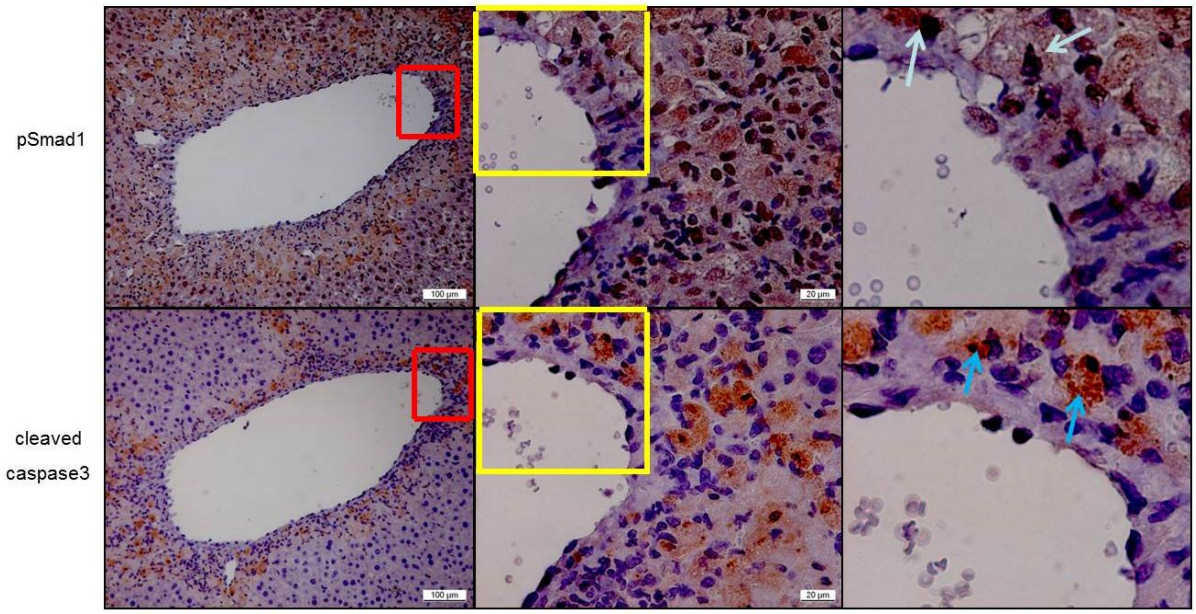

Fig.12. Localization and expression of cleaved caspase3 in the response to CCl_4-mediated liver injury. **A,** IHC was performed for cleaved caspase3. Magnification, 10×. **B,** Western blot for cleaved caspase3 during the time course. **C,** Co-localization of pSmad1 and cleaved caspase3 at day 3 is shown by IHC. Arrow, positive staining. Magnification, 10× and 40×.

4.1.4. CCl_4 intoxication in mice leads to activation and increased proliferation of HSCs

During this pathological process of CCl_4 intoxication, desmin, a widely used marker for HSCs (see also Fig. 21 B), which are located in the Disse space of the liver, was positively stained within the pericentral area at day 1, indicating that HSCs migrated to the area of damage and started to proliferate. Desmin expression in this area kept being increased until day 3 (Fig. 13 A). α-SMA, a marker especially for activated HSCs, was slightly expressed within the pericentral area at day 1, but increased strongly at day 3 and reduced again at day 6 when liver repair after CCl_4 injury was almost achieved. No positive staining against α-SMA could be observed outside the pericentral area (Fig. 13 B). This suggests that at day 3 proliferation and activation of HSCs reached a peak after a single CCl_4 insult.

As mentioned above, at day 3, besides expression of α-SMA and BMP-9 in the pericentral area, pSmad1 expression was also increased (Fig. 13 C). In this area, positive pSmad1 staining was observed not only in damaged hepatocytes with disappeared nucleus and the nuclear of normal hepatocytes, but also in the nuclear of the infiltrating cells, most likely

aHSCs (Fig. 13 C). These results imply that BMP-9/Smad1 signaling might be involved in proliferation and activation of HSCs *in vivo*.

A

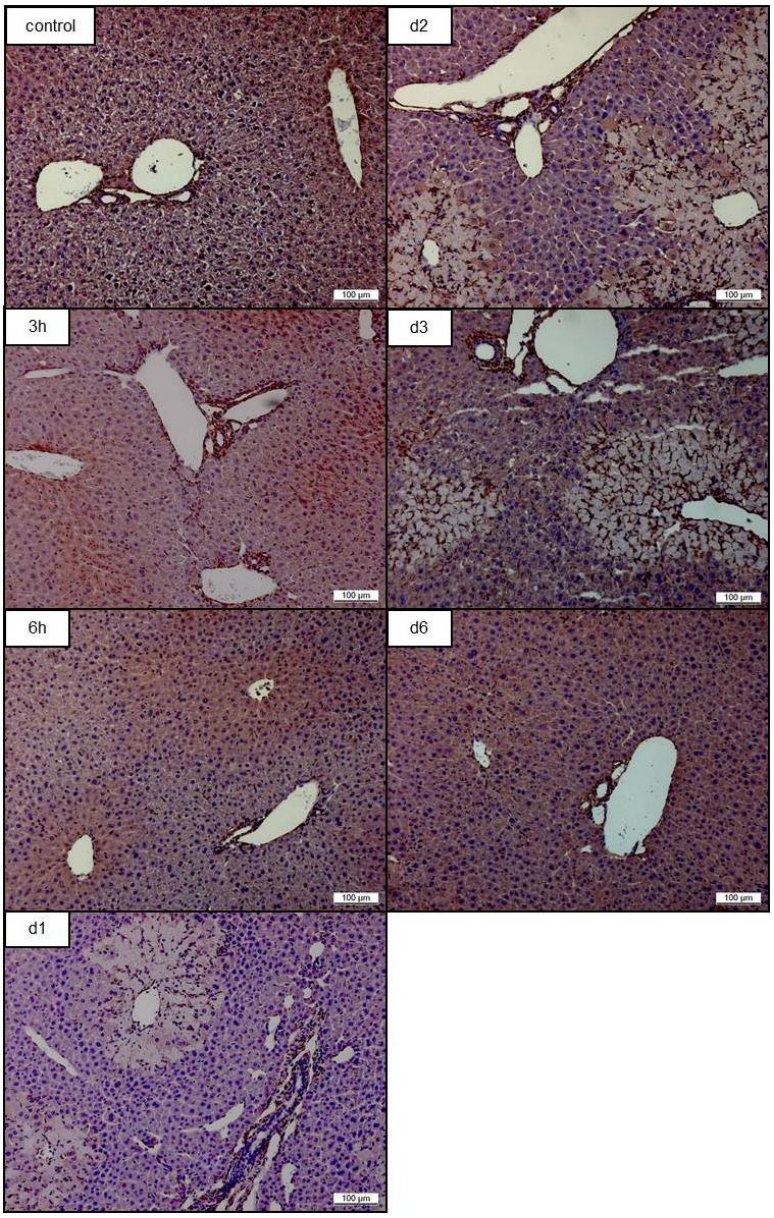

B

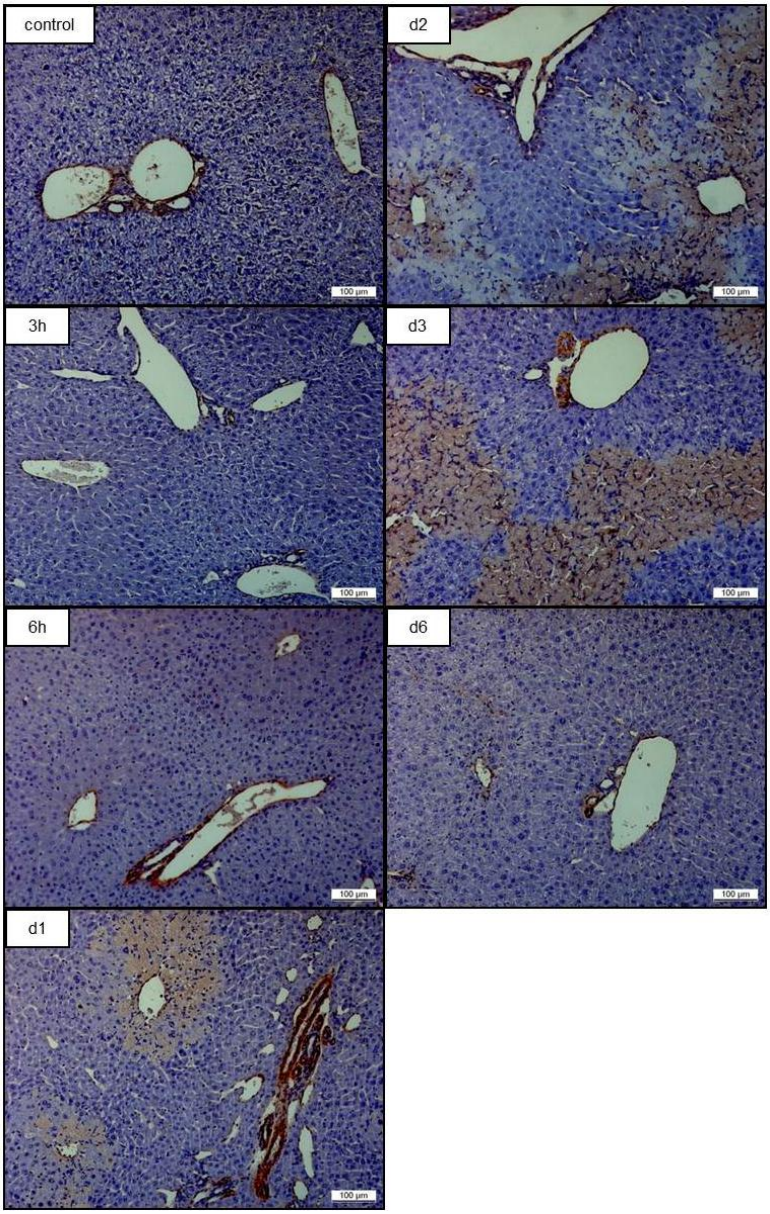

C

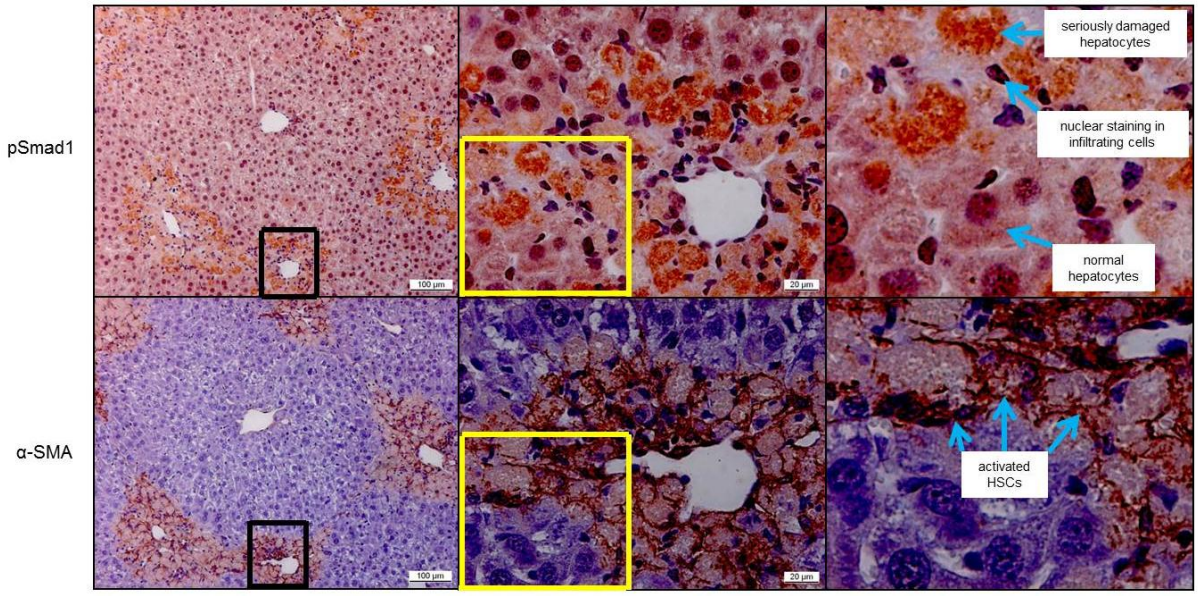

Fig.13. Expression and localization of desmin α-SMA and pSmad1 in response to CCl_4-medicated liver injury. **A,** IHC against desmin. Magnification, 10×. **B,** IHC was performed for α-SMA. Magnification, 10×. **C,** Co-localization of pSmad1 and α-SMA in serial sections at day 3 is shown by IHC. Magnification, 10× and 40×.

4.2. Effects of BMP-9 in primary mouse hepatocytes

4.2.1. BMP-9 reduces expression of PCNA

TGF-β1 itself leads to hepatocyte apoptosis and cell growth arrest (Lee and Bae, 2002). PCNA is a reliable indicator for cell proliferation (Nolte et al., 2005). Like TGF-β1, BMP-9 also reduced PCNA expression in mouse hepatocytes *in vitro* (Fig. 14).

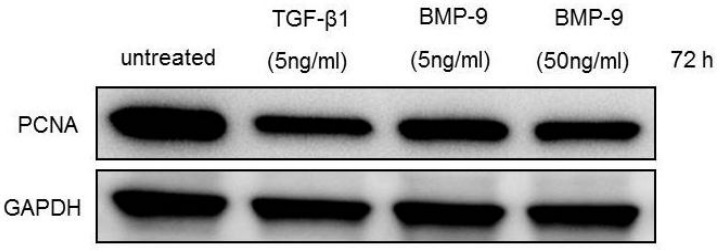

Fig.14. Both BMP-9 and TGF-β1 lead to reduced PCNA expression in mouse hepatocytes. GAPDH was used as a loading control.

4.2.2 BMP-9 alone does not induce strong apoptosis

From the *in vivo* acute CCl_4 model, expression of BMP-9 mRNA was noticeably observed in the pericentral area at day 3 (Fig. 11 B). Furthermore, at the same time point in the same area there was significantly positive staining for the apoptosis marker, cleaved caspase3 (Fig. 12 B). We therefore investigated whether BMP-9 induced hepatocyte apoptosis *in vitro*. From day 1 to day 2, BMP-9 alone did not induce obvious cell apoptosis in cultured mouse hepatocytes although appearance of cleaved caspase3 was slightly induced (Fig. 15 A, B). Compared with TGF-β1, a strong inducer of hepatocyte apoptosis, which promoted caspase3 activity significantly, BMP-9 alone did not lead to strongly enhanced caspase3 activity (Fig. 15 C).

A

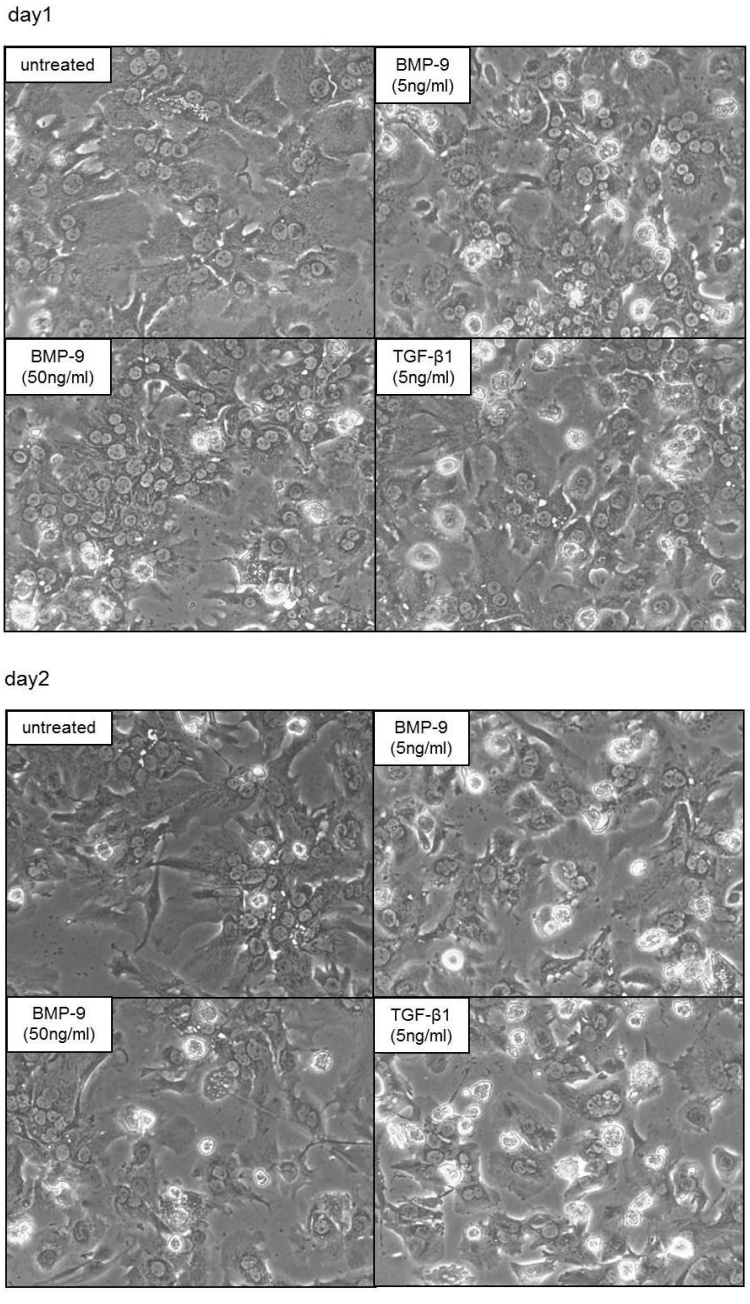

B

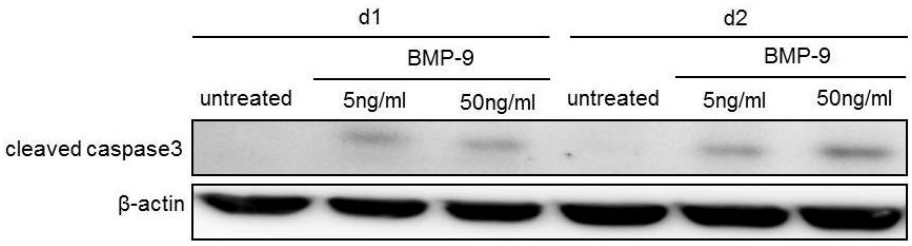

C

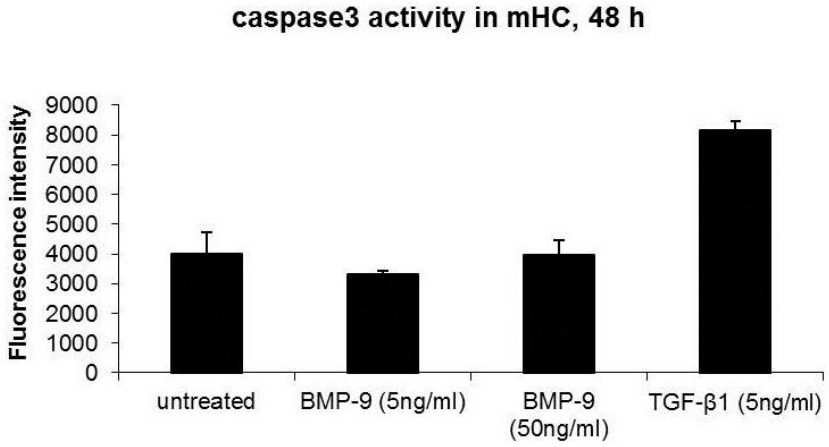

Fig.15. BMP-9 alone does not cause strong cell apoptosis in mouse hepatocytes. **A,** Cell morphology upon stimulation of hepatocytes with either BMP-9 or TGF-β1. Magnification, 10×. **B,** Western blot showing that cleaved caspase3 was slightly up-regulated by BMP-9 stimulation. **C,** Caspase3 assay demonstrating no cell apoptosis by BMP-9 alone compared to TGF-β1 alone. The experiment was performed in duplicates and was repeated 3 times.

4.2.3. Co-stimulation of BMP-9 and TGF-β1 results in enhanced activation of caspase3

As mentioned above, BMP-9 alone did not induce strong hepatocyte apoptosis, which is a well-described function of TGF-β1. However, reduced cell density could be observed after co-stimulation with TGF-β1 and BMP-9 (Fig. 16 A). In addition, cleaved caspase3 was largely up-regulated and Bcl-2, an anti-apoptotic marker was down-regulated when hepatocytes were treated with BMP-9 and TGF-β1 simultaneously (Fig. 16 B). These outcomes were dose-dependent for BMP-9. Furthermore, co-stimulation enhanced caspase3 activity compared to TGF-β1 alone (Fig. 16 C). This indicates that BMP-9 enhances TGF-β1 mediated hepatocyte apoptosis.

A

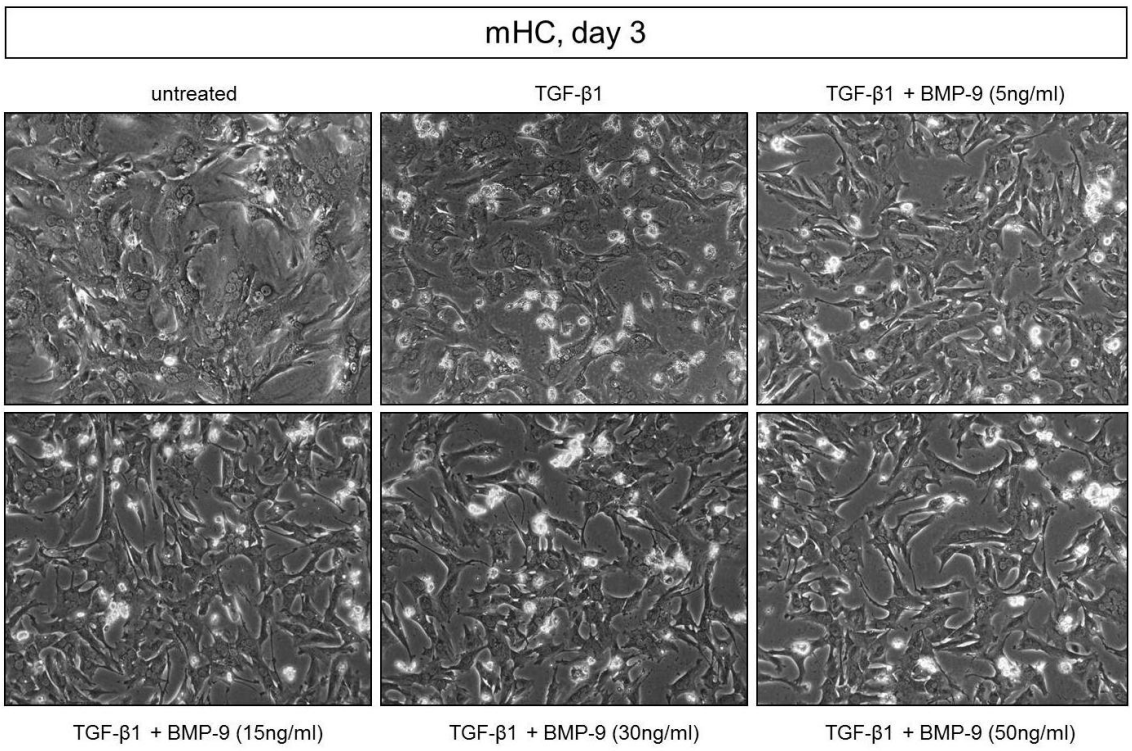
mHC, day 3
untreated
TGF-β1
TGF-β1 + BMP-9 (5ng/ml)
TGF-β1 + BMP-9 (15ng/ml)
TGF-β1 + BMP-9 (30ng/ml)
TGF-β1 + BMP-9 (50ng/ml)

B

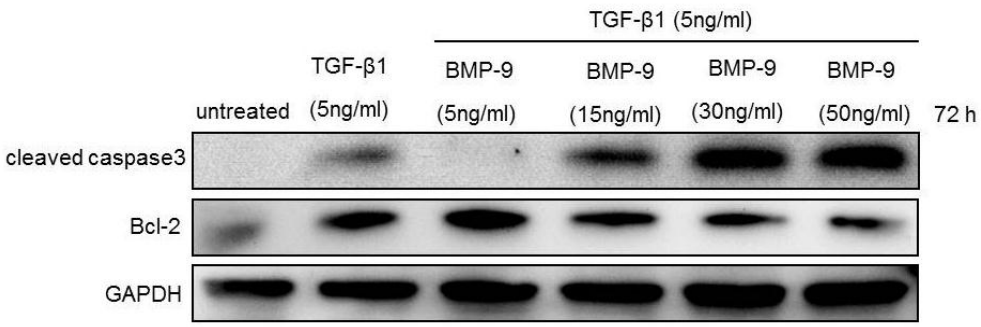
TGF-β1 (5ng/ml)
untreated
TGF-β1 (5ng/ml)
BMP-9 (5ng/ml)
BMP-9 (15ng/ml)
BMP-9 (30ng/ml)
BMP-9 (50ng/ml)
72 h
cleaved caspase3
Bcl-2
GAPDH

C

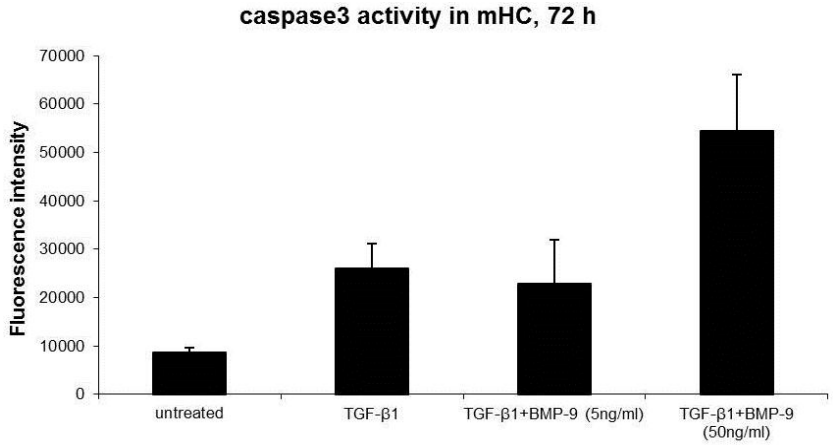
caspase3 activity in mHC, 72 h
Fluorescence intensity
70000
60000
50000
40000
30000
20000
10000
0
untreated
TGF-β1
TGF-β1+BMP-9 (5ng/ml)
TGF-β1+BMP-9 (50ng/ml)

Fig.16. Co-stimulation of mouse hepatocytes with BMP-9 and TGF-β1 leads to enhanced cell death. **A,** Cell morphology on day 3 of culture. Magnification, 10×. **B,** Western blot showing that cleaved caspase3 was enhanced and expression of Bcl-2 was down-regulated by co-stimulation. GAPDH was used as a loading control. **C,** Caspase3 assay demonstrating enhanced cell apoptosis by co-stimulation of TGF-β1 and BMP-9 compared to TGF-β1 alone. The experiment was performed in duplicate and repeated 3 times.

4.2.4. BMP-9 facilitates the maintenance of an epithelial phenotype

Primary hepatocytes de-differentiate when being cultured *in vitro*. Especially, when cells are treated with TGF-β1, the de-differentiation process is significantly enhanced, which is indicated by obvious reduction of E-cadherin (Caja et al., 2011a) and other changes in expression which correlate with EMT (Dooley et al., 2008). From the morphology with co-stimulation (Fig. 16 A), we expected an EMT-enhancing function of BMP-9, but from the expression levels this was not supported: while BMP-9 alone did not influence E-cadherin and albumin expression in hepatocytes, it reduced the expression of N-cadherin, a mesenchymal marker (Fig. 17 A). Furthermore, TGF-β1 induced down-regulation of E-cadherin could be partially rescued by BMP-9 which was not dose-dependent for BMP-9 (Fig. 17 B, C). And N-cadherin still could be largely reduced (Fig. 17 C). Therefore, BMP-9 may function in maintaining the epithelial character of primary mouse hepatocytes.

A

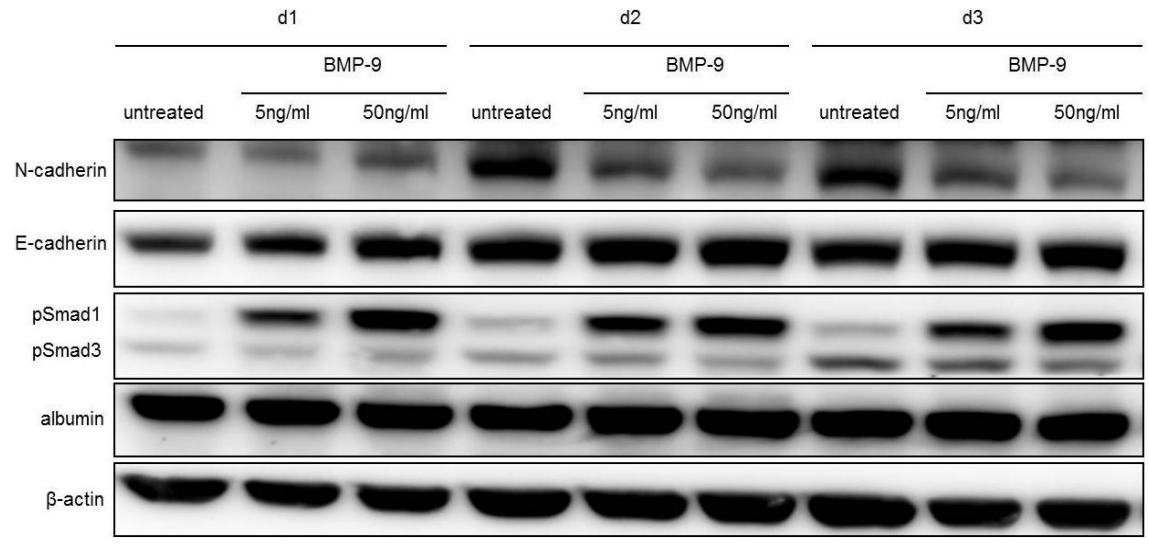

B

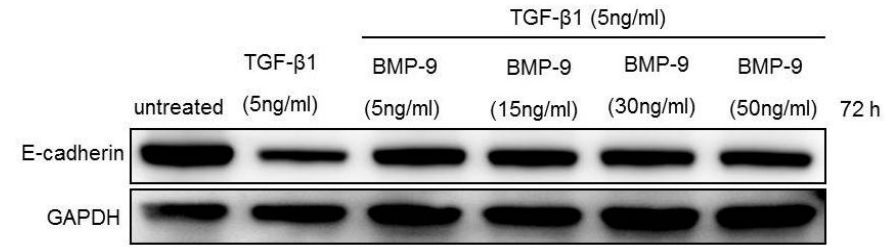

C

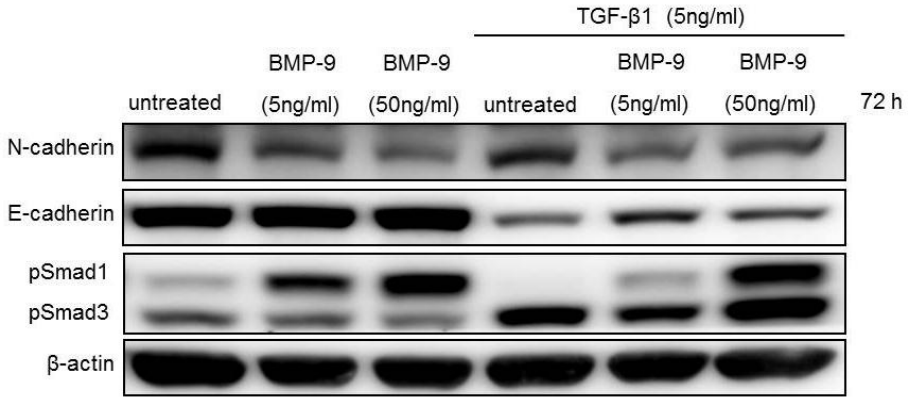

Fig.17. BMP-9 promotes an epithelial expression pattern in mouse hepatocytes with or without co-treatment with TGF-β1. By Western blot analyses it was shown that **A,** BMP-9 alone reduced expression of N-cadherin and induced Smad1 phosphorylation from day 1 to day 3. **B,** TGF-β1 induced down-regulation of E-cadherin was partially rescued by BMP-9. **C,** BMP-9 down-regulated expression of N-cadherin with or without TGF-β1 co-treatment. GAPDH or β-actin served as loading controls.

4.2.5. Microarray analysis of samples from mouse hepatocytes stimulated with BMP-9 for 24 h

To further investigate whether BMP-9 has other potential functions in the liver besides its possible roles in HSC activation and hepatocyte apoptosis, and to know which genes will be up- and down-regulated by BMP-9 in mouse hepatocytes, we performed a microarray analysis. Freshly isolated mouse hepatocytes were incubated with BMP-9 (5 ng/ml) for 24 h. 32 genes were up-regulated and only 4 genes were down-regulated by more than 1.4-fold (Tab. 10). Through classifying these genes, we can speculate that BMP-9 most likely participates in liver metabolism, such as iron metabolism, triglyceride metabolism and sugar metabolism (Tab. 11).

up-regulated genes		down-regulated genes	
Hamp	6.9702	Ms4a4d	-2.1725
Apoa5	5.6998	Ubd	-2.0067
Id1	4.3041	Ms4a6b	-1.7281
Hamp2	3.7273	Ier3	-1.6407
Id3	3.4078		
Atoh8	3.2771		
Id2	2.9294		
Tinag	2.7970		
Fmo1	2.6756		
Smad6	2.5863		
Nrn1	2.5168		
Cyp1a1	2.4086		
Bambi	2.3875		
Sec 14l4	2.3703		
Id4	2.3696		
Arg1	2.2717		
AI132487	2.1110		
Smad7	2.0291		
Cyp8b1	1.8932		
Akr1c14	1.7551		
Zfp259	1.7520		
Aldh8a1	1.6958		
1190002N15Rik	1.5995		
Slc2a2	1.58075		
Smoc1	1.5757		
Apoc2	1.5586		
Hgd	1.4903		
Asgr1	1.4716		
Cyp2b10	1.4688		
Sgk1	1.4579		
Fgg	1.4299		
Nox4	1.4185		

Tab.10. Genes up- or down-regulated by ≥ 1.4-fold at 24 h after addition of BMP-9 (5 ng/ml) to primary cultured mouse hepatocytes.

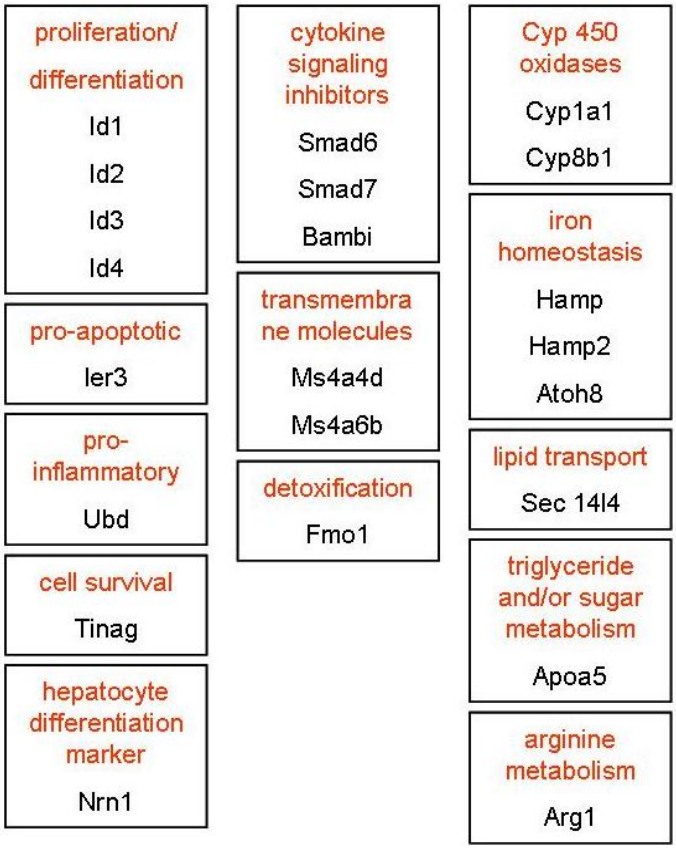

Tab.11. The BMP-9 regulated genes were grouped according to their possible functions as described in the literature.

4.3. Effects of BMP-9 in primary mouse HSCs

4.3.1. BMP-9 is increasingly expressed during *in vitro* transdifferentiation of HSCs together with enhanced Smad1 activation

Since we observed that BMP-9, pSmad1 and α-SMA were all expressed in the pericentral area of the liver at day 3 after acute CCl_4 intoxication, and the main profibrogenic cell type of the liver is HSCs, we further investigated whether the BMP-9/Smad1 pathway was involved in the transdifferentiation of HSCs *in vitro*. During this process, fat droplets disappeared gradually and cells transdifferentiate into myofibroblasts which produced extracellular matrix proteins (Fig. 18 A). In parallel, BMP-9 was increasingly expressed with a peak at day 3 and day 5 at the RNA level (Fig. 18 B, C) and at day 7 on the protein level (Fig. 18 D). As for pSmad1 and total Smad1, their expressions were continuously increased from day 1 to day 7 along with increased α-SMA and PCNA, typical markers for HSC activation and proliferation,

respectively (Fig. 18 D). This expression pattern *in vitro* points to a role of the BMP-9/Smad1 signaling pathway during transdifferentiation and proliferation of mouse HSCs.

A

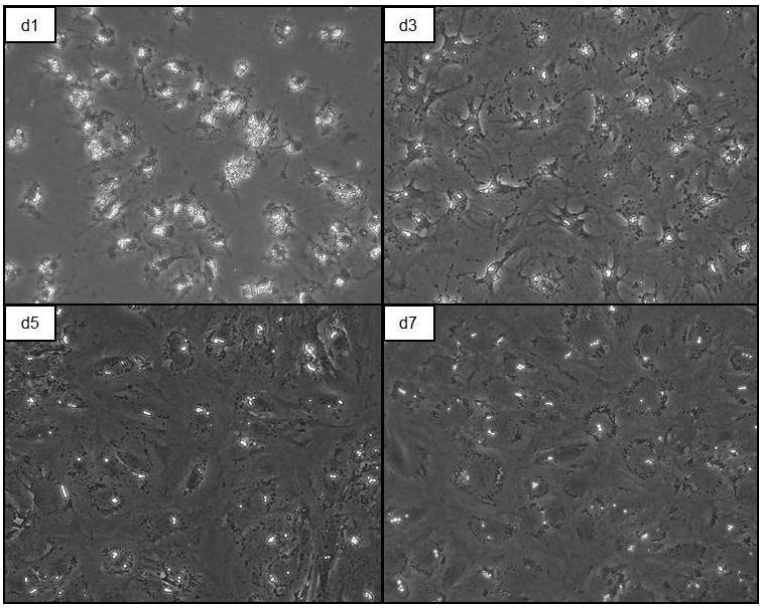

B

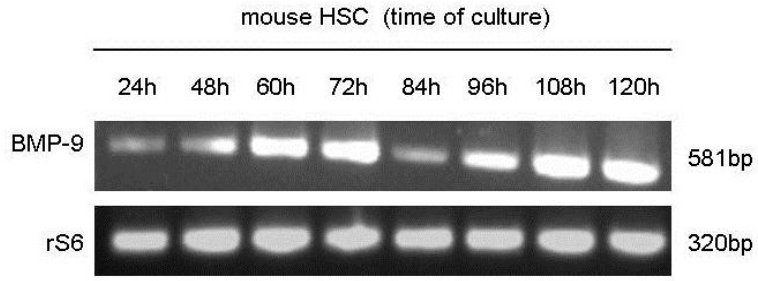

C

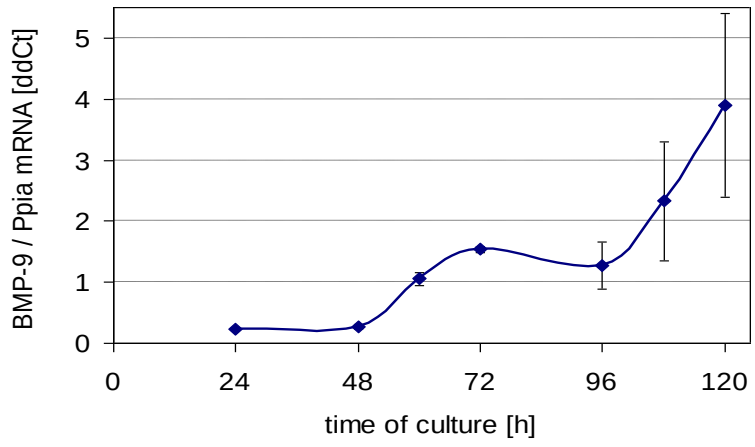

D

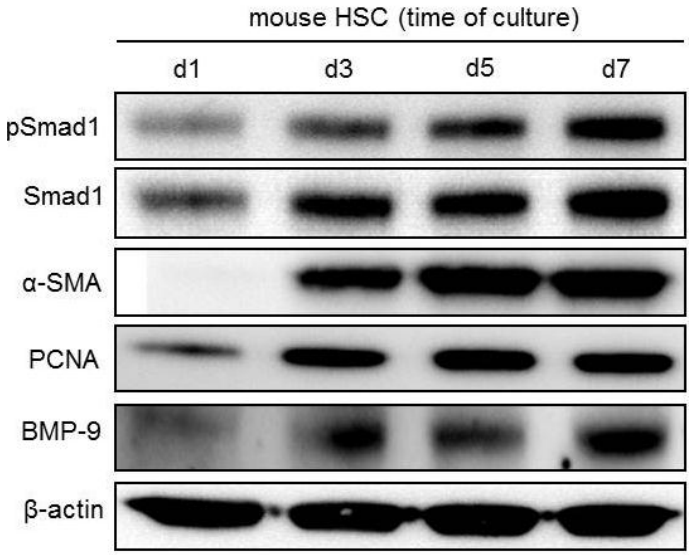

Fig.18. BMP-9 and pSmad1 are increasingly expressed during mouse HSC transdifferentitation *in vitro*. Mouse HSCs were isolated from C57BL/6 mice. Protein and RNA were harvested at the indicated time points. **A,** Morphological changes of mouse HSCs *in vitro* during the time course. Magnification, 20×. **B,** BMP-9 expression was detected with RT-PCR. rS6 served as internal control. **C,** BMP-9 expression was detected with real-time PCR. PPIA served as internal control. **D,** Detection of BMP-9, PCNA, α-SMA, Smad1 and pSmad1 protein expressions by Western blot of samples from days 1 to 7. β-actin was used as loading control.

4.3.2. BMP-9 induces proliferation in a human HSC cell line (LX-2)

To investigate whether BMP-9 can promote cell proliferation in HSCs, LX-2, a human HSC cell line was incubated with BMP-9 (5 ng/ml), with TGF-β1 (5 ng/ml) as a negative control and PDGF (20 ng/ml) as a positive control for 72 h. At the end point, cell number was determined. The result showed that BMP-9 induced proliferation of HSCs (Fig. 19).

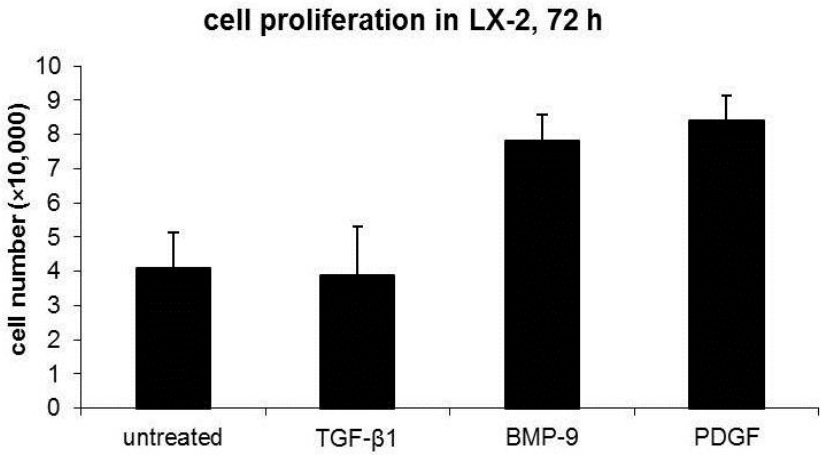

Fig.19. BMP-9 induces cell proliferation in LX-2 cells. LX-2 cells were stimulated with BMP-9, TGF-β1 or PDGF for 72 h and cell numbers were determined. The experiment was performed in triplicates and repeated 3 times.

4.3.3. Dorsomorphin (DM) inhibits BMP-9-induced Smad1 activation in primary HSCs and LX-2 cells

BMPs transduce their signals via activation of a group of so called "type I receptors". These Smad1/5/8 activating receptors include ALKs 1, 2, 3, 6 (Miyazono et al., 2010). DM specifically inhibits this group of receptors (Yu et al., 2008). Both hepatocytes and HSCs responded to rhBMP-9 with activation of Smad1 signaling. Accordingly, in HSCs, pSmad1 induction by BMP-9 could be completely blocked by DM treatment *in vitro* (Fig. 20). Although TGF-β1 induced transient pSmad1 expression was also reduced by DM, its canonical signaling via Smad3 was not influenced. As expected, DM also inhibited phosphorylation of Smad1 by other BMPs (BMP-2 and -6 in this case) in LX-2 cells (Fig. 20 D).

A

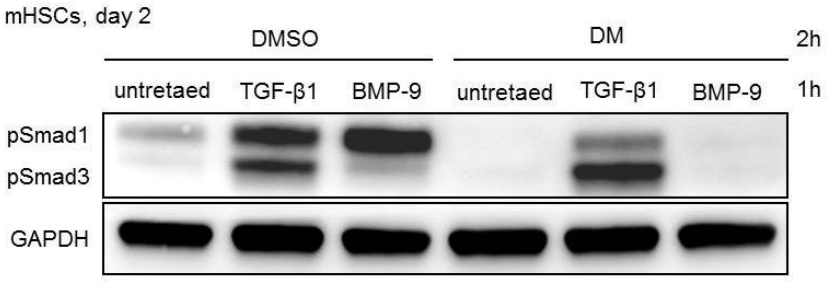

B

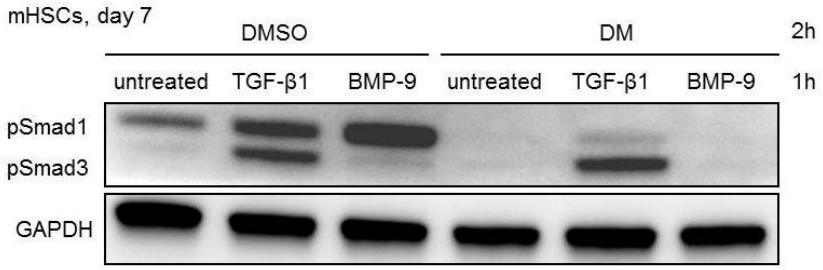

C

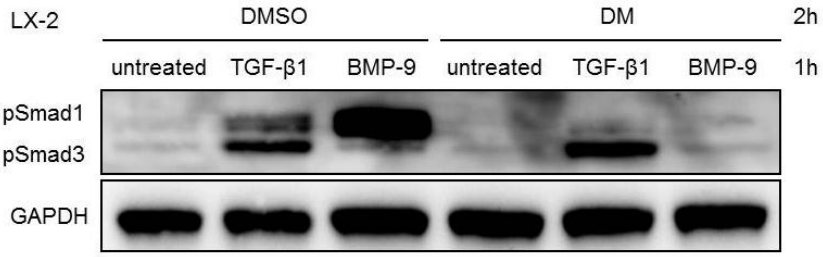

D

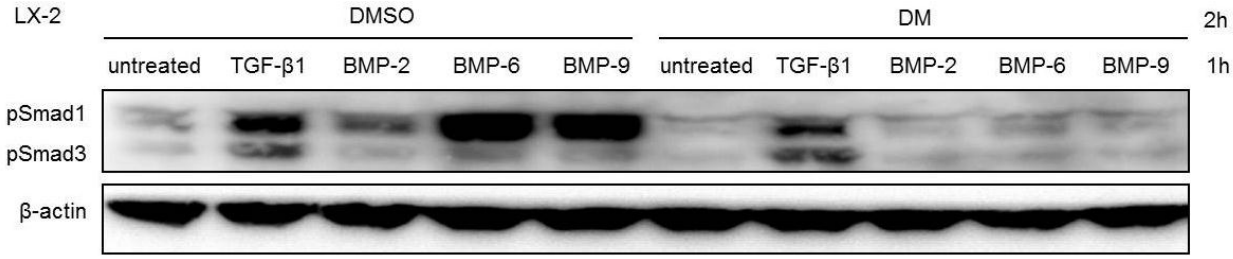

Fig.20. BMP-induced pSmad1 signaling is effectively blocked by DM in HSCs. Western blot analyses were performed and pSmad1 and pSmad3 were detected. Cultured primary "mHSC day 2" (**A**) "mHSC day 7" (**B**) treated with DM or DMSO 1 h before being treated with TGF-β1 or BMP-9 for another 1 h. **C,** A human HSC cell line, LX-2 cells were treated with DM or DMSO 1 h before being treated with TGF-β1 or BMP-9 for another 1 h. **D,** LX-2 cells were treated with DM or DMSO 1 h before being treated with TGF-β1, BMP-2 (20 ng/ml), 6 (20 ng/ml) , 9 (5 ng/ml) for another 1 h. β-actin or GAPDH served as loading controls as indicated.

4.3.4. Smad1 pathway inhibition by DM significantly decreases gene expression of markers for HSC activation *in vitro*

We then investigated whether Smad1 activity is required for transdifferentiation of HSCs *in vitro*. When the cells were plated in the presence of DM they did not activate at all. When DM was added 24 h after initial cell attachment and remained on the cells from day 1 to day 2 this already profoundly affected cell morphology and reduced expression of marker genes like α-SMA, desmin, Id-1, collagen I or fibronectin. Similar results were acquired when the cells

were cultured with DM from day 4 to day 6 (Fig. 21 A, B). These results imply that the Smad-1 pathway is required for transdifferentiation and blocking it seemed to revert the fibrogenic phenotype of HSCs back towards a more quiescent appearance. Since BMP-9 is a strong inducer for Smad1 activation and DM can inhibit BMP-9/Smad1 pathway in HSCs, BMP-9 might act as a profibrogenic factor during HSC transdifferantiation. However, since DM is not specific for BMP-9 it can at this stage not be excluded that any other BMP is also involved in this process.

A

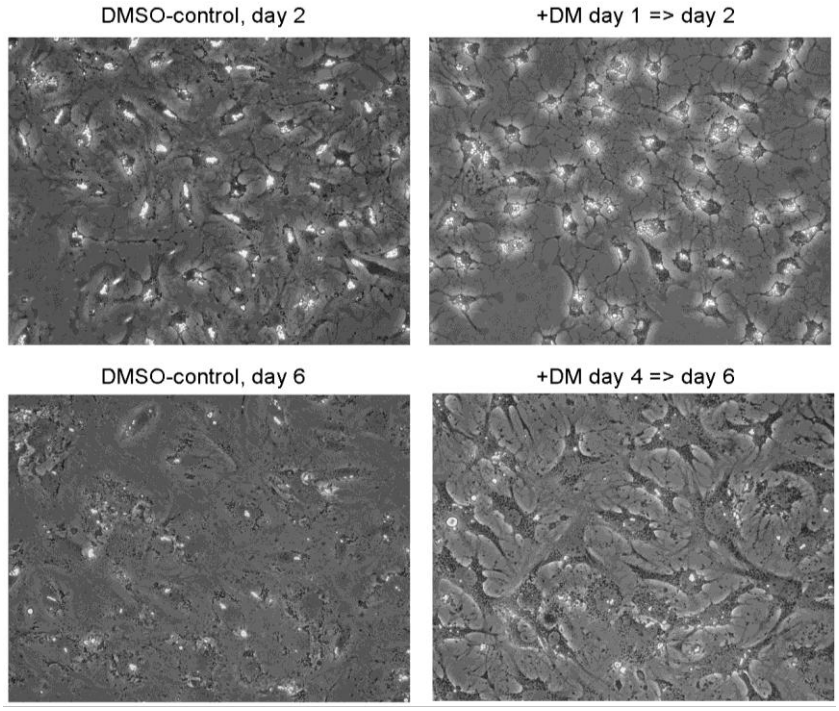

B

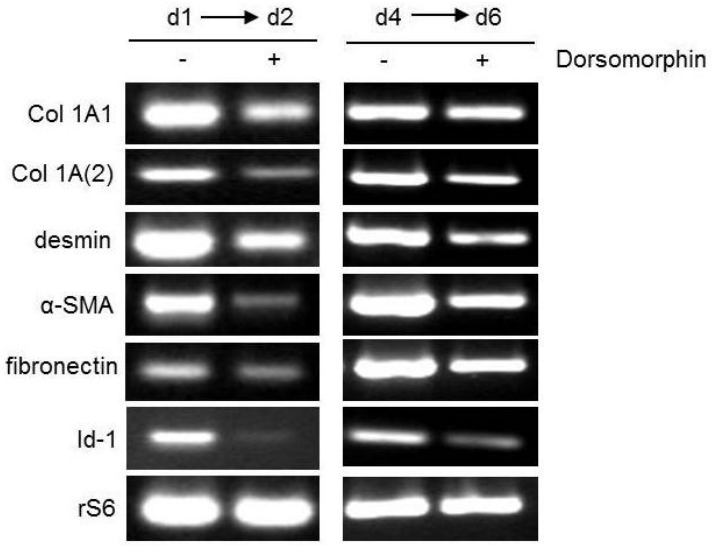

Fig.21. HSC transdifferantiation is inhibited by DM. **A,** Cell morphology was altered by DM during the early stage as well as late stages of HSC transdifferentiation. Magnification, 20×. **B,** RT-PCR demonstrating that DM reduced expression of genes which are otherwise up-regulated during HSC activation (Collagen type I, desmin, α-smooth-muscle-actin, fibronectin and Id-1). rS6 served as loading control.

Part II

BMP-9 induces epithelial-mesenchymal transition (EMT) in hepatocellular carcinoma (HCC) cells

4.4. BMP-9 expression and signaling in liver samples from HCC patients

4.4.1. BMP-9 is expressed in HCC tissue

We analyzed BMP-9 mRNA and protein expression in 41 HCC tissues and 36 paired non-cancer liver tissues from liver cancer patients by IHC and ISH, respectively. We found that BMP-9 protein and mRNA expression existed in all patients, although the expression levels strongly varied (Fig. 22 A, B). BMP-9 protein expression levels were higher in the cancer area as compared to "normal" liver tissue in 9/36 (25%) patients, whereas 21/36 (58.33%) displayed similar expression levels in both areas (Tab. 12). BMP-9 protein staining was found in cancerous regions and due to ISH data we can conclude that BMP-9 did not only bind to the outer surface of HCC cells, but that it was indeed also synthesized by them (Fig. 22 A, B). According to an evaluation system as indicated in materials and methods, mildly positive (1+) BMP-9 staining was observed in 25/41 (61%), and moderately to strongly positive (2+) staining was present in 16/41 (39%) cancer samples of the patients. In 27/41 (65.85%) patients, BMP-9 protein and mRNA expression level were consistent. In 7/41 (17.07%) patients, there were 1+ mRNA levels correlated with 2+ protein levels, whereas in another 7/41 (17.07%) patients, it was the other way around.

A comparison of BMP-9 protein expression with clinicopathological features of the 41 investigated HCC samples demonstrated a significant association of BMP-9 protein expression with T stage ($\tau_B = 0.381$, $P = 0.016$) and Child Pugh score ($\tau_B = -0.328$, $P = 0.04$) (Tab. 13), indicating that high BMP-9 levels correlated with invasion of the tumor, but did not mirror the decrease of liver functionality.

A

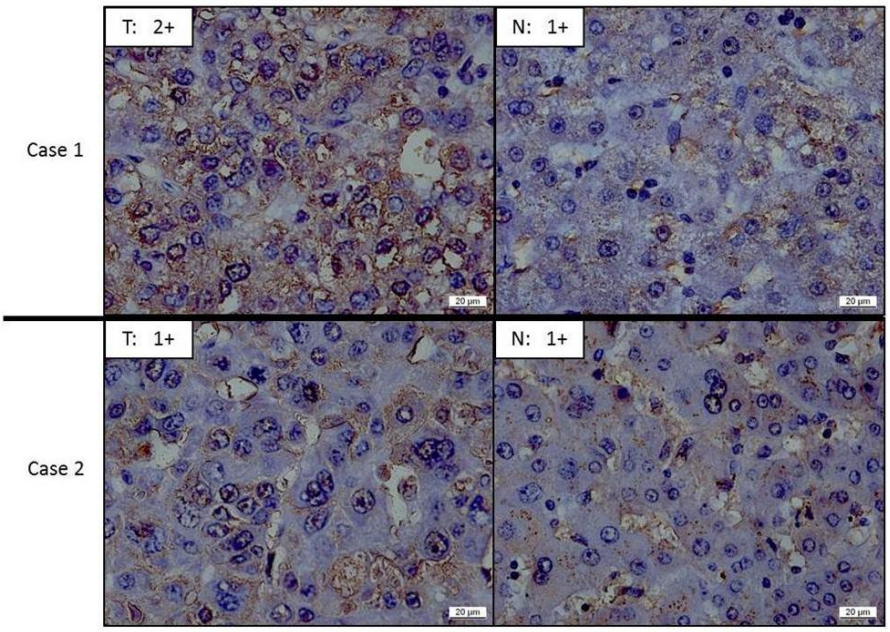

B

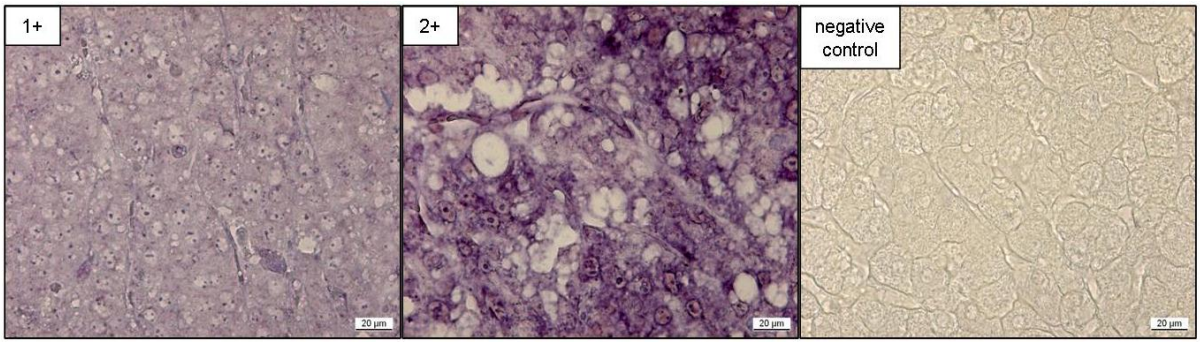

Fig.22. BMP-9 is expressed in HCC. Immunohistochemical analysis of BMP-9 expression was performed in paraffin-embedded HCC tissues from liver cancer patients (n=41 for tumor area and n=36 for non-tumor area). **A,** Immunohistochemical staining for BMP-9 in tumor and paired non-tumor regions of livers from HCC patients (brown color) varied from case to case. The extent was determined as mild (1+) and moderate to strong (2+). T: cancer area; N: paired non-cancer area. Magnification, 40×. **B,** Detection of BMP-9 mRNA expression by ISH. ISH with sense probe for BMP-9 was performed as negative control. Magnification, 40×.

BMP-9 protein expression in cancer area and paired non-cancer area

T	N			
	2+ (%)	1+ (%)	0 (%)	total (%)
2+ (%)	6 (17)	7 (19)	1 (3)	14 (39)
1+ (%)	6 (17)	15 (42)	1 (3)	22 (61)
total (%)	12 (34)	22 (61)	2 (6)	36 (100)

Tab.12. BMP-9 protein expression in cancer area and paired non-cancer area in HCC in 36 patients.

Relationship between immunohistochemical expression of BMP-9 and clinicopathological factors in HCC patients

Clinicopathological factor	n	BMP-9 expression		τ_B	*P* value
		1+ (%)	2+ (%)		
Total	41	25 (61)	16 (39)		
Age					
< 60	32	18 (56)	14 (44)		
≥ 60	9	7 (78)	2 (22)	0.059	0.709
Gender					
Male	37	21 (57)	16 (43)		
Female	4	4 (100)	0 (0)	0.263	0.096
T stage					
T1, 2	20	16 (80)	4 (20)		
T3, 4	21	9 (43)	12 (57)	0.381	0.016
Size (cm)					
≤ 5	18	12 (67)	6 (33)		
> 5	23	13 (57)	10 (43)	0.103	0.514
Tumor grade					
1,2	10	8 (80)	2 (20)		
3,4	31	17 (55)	14 (45)	- 0.036	0.822
Tumor number					
single	32	21 (66)	11 (34)		
multiple	9	4 (44)	5 (56)	0.18	0.256
Child-Pugh class					
A	22	10 (45)	12 (55)		
B,C	19	15 (79)	4 (21)	- 0.328	0.04
TNM stage					
I+II	19	16 (84)	3 (16)		
III+IV	22	9 (41)	13 (59)	0.042	0.793

Tab.13. Relationship between immunohistochemical expression of BMP-9 and clinicopathological factors in HCC in 41 patients.

4.4.2. BMP-9 expression is associated with increased pSmad1 and Snail and decreased E-cadherin levels in HCC

The BMP/Smad1 signaling pathway has been regarded as a significant player participating in the progression of carcinoma (Li, 2008). Snail and E-cadherin, two well-known EMT markers, play crucial roles in carcinogenesis. Therefore we next examined BMP-9 down-stream signaling and features of EMT using antibodies for phosphorylated Smad1 (pSmad1), Snail and E-cadherin and associated their occurrence/expression with BMP-9 protein levels. In HCC patients with 1+ BMP-9 level, E-cadherin signals were stronger, while those of Snail and pSmad1 were weaker, as compared to liver cancer samples with 2+ BMP-9 levels (Fig. 23 A).

A semi-quantitative analysis of the staining results indicates a significant correlation of BMP-9 expression with increased activity of Smad1. Although expression of BMP-9 was positively related to Snail expression and reversely correlated to E-cadherin expression, this did not reach statistical significance (Fig. 23 B).

A

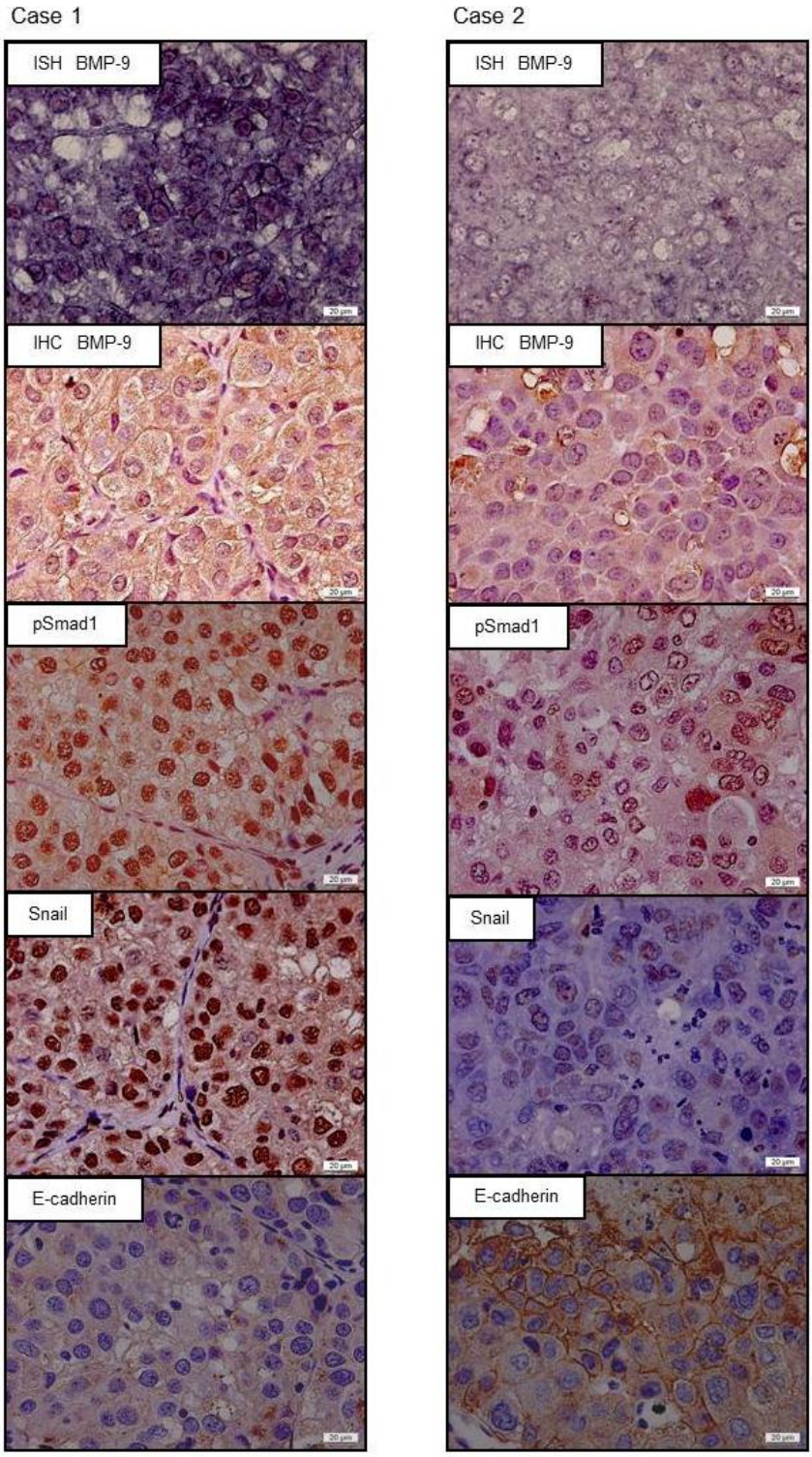

B

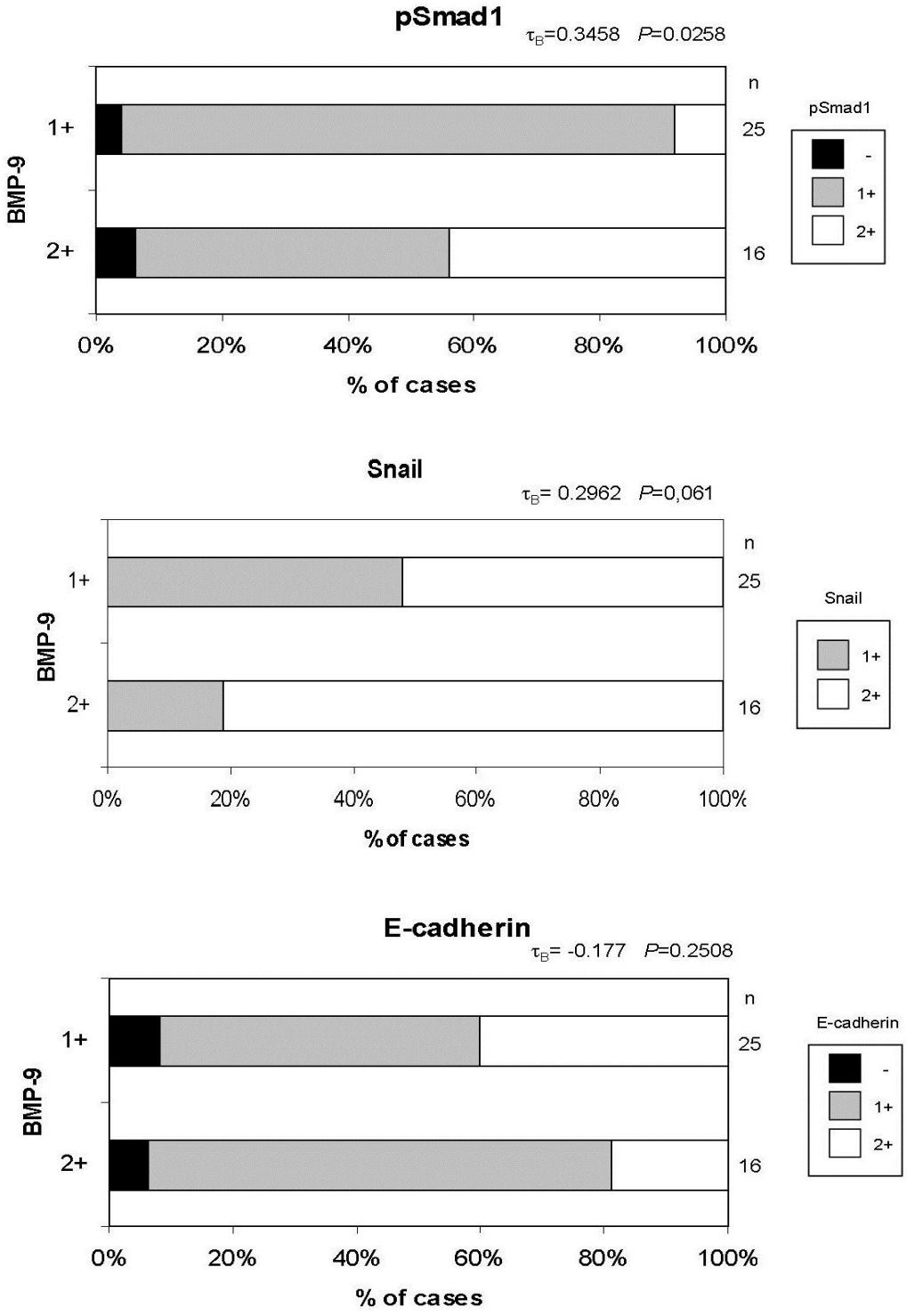

Fig.23. Expression of BMP-9 is associated with Smad1 phosphorylation, Snail and E-cadherin expression in HCC. Immunohistochemical analysis was performed in paraffin-embedded tissues of HCC (n=41). Additionally, BMP-9 mRNA expression was shown with ISH. **A,** At 1+ BMP-9 expression levels, pSmad1 staining was mildly positive, E-cadherin cell surface expression was present and positive Snail nuclear staining was lower compared to those samples having 2+ BMP-9 expression levels. Representative images are shown. Magnification, 40×. **B,** Immunohistochemical staining of pSmad1, Snail and E-cadherin in HCC cells was semi-quantitatively evaluated in 3 grades (-, 1+, 2+) as described in the Materials and Methods, and the association

with BMP-9 expression was calculated, demonstrating that BMP-9 expression is significantly correlated with nuclear pSmad1, positively related to nuclear Snail reversely related to cell surface E-cadherin expression in HCC.

4.5. BMP-9 expression and signaling in HCC cell lines (HepG2 and HLE)

4.5.1. BMP-9 signaling is functional in HCC cell lines

In order to learn more about BMP-9 signaling in HCC cells, we assessed whether BMP-9/Smad1 signaling components are expressed in the well-established HCC cell lines, HepG2 and HLE. These cells were originally derived from primary tumors (Aden et al., 1979; Dor et al., 1975). Histologically HepG2 are classified as a well-differentiated liver cancer cell line and HLE as an invasive HCC cell line, but commonly representing epithelial phenotype.

BMP-type I and II receptors ALK1, ALK2, BMPRII, ACVR2A as well as Smads-1 and -4 were expressed in both cell lines at different levels as determined by PCR (Fig. 24 A).

To investigate whether expression of the receptors correlated with BMP-9 responsiveness of the cells, we treated them with rhBMP-9 (50 ng/ml) and examined Smad1 C-terminal phosphorylation. Both HCC cell lines were responsive to rhBMP-9 even at concentration as low as 5 ng/ml. Smad1 phosphorylation occurred as early as 10 min after stimulation, lasting at least 72 h (Fig. 24 B, C).

Taken together, these data indicate that the BMP-9/Smad1 pathway is functional in HCC cells *in vitro* with a prolonged instead of a transient response, which is in line with previous descriptions of Smad1 signaling participating in EMT (Xu et al., 2011).

A

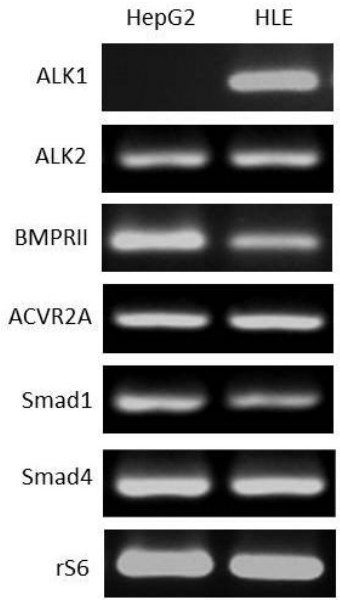
HepG2
HLE
ALK1
ALK2
BMPRII
ACVR2A
Smad1
Smad4
rS6

B

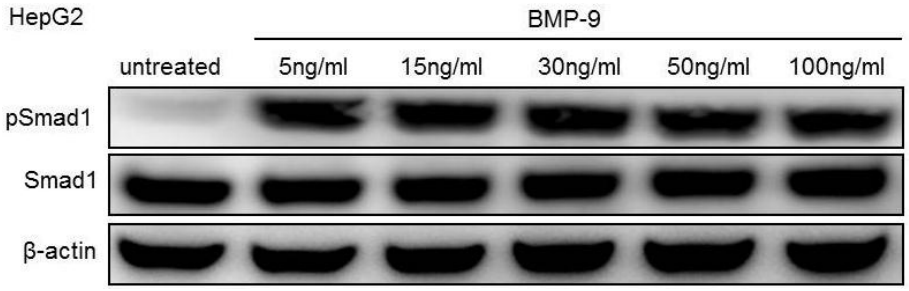
HepG2
BMP-9
untreated
5ng/ml
15ng/ml
30ng/ml
50ng/ml
100ng/ml
pSmad1
Smad1
β-actin

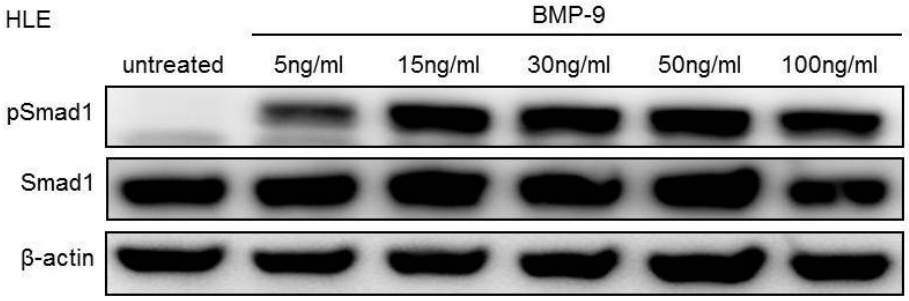
HLE
BMP-9
untreated
5ng/ml
15ng/ml
30ng/ml
50ng/ml
100ng/ml
pSmad1
Smad1
β-actin

C

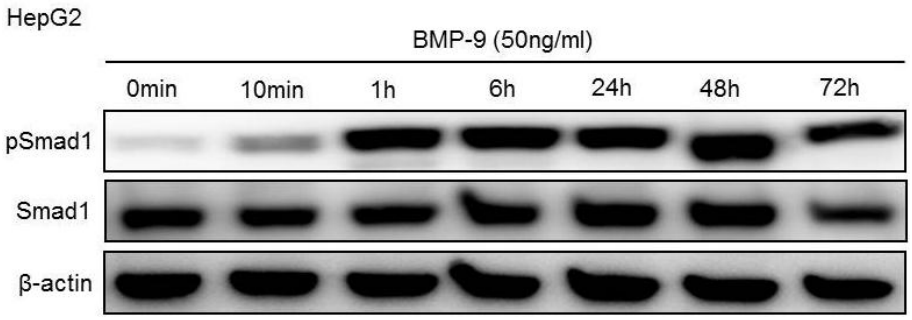
HepG2
BMP-9 (50ng/ml)
0min
10min
1h
6h
24h
48h
72h
pSmad1
Smad1
β-actin

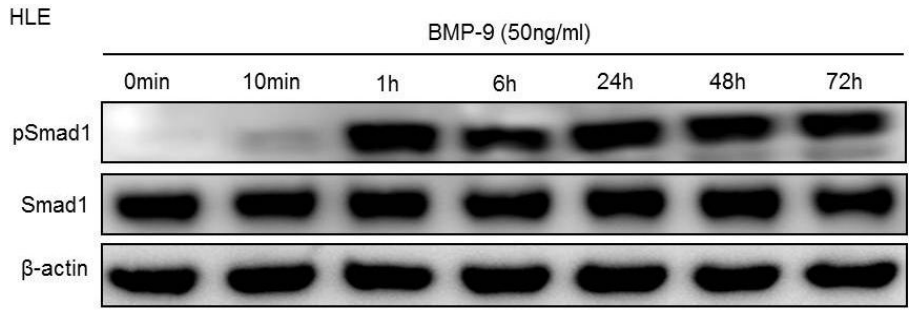

Fig.24. BMP-9 induces Smad1 phosphorylation in HCC cells. **A,** Components of the Smad1 pathway were slightly or strongly expressed in HepG2 and HLE cells. **B,** Cells were untreated or treated with different concentrations of BMP-9 as indicated for 1 h. pSmad1 and total Smad1 were analyzed by Western blot. **C,** Cells were treated with 50 ng/ml BMP-9 for the indicated time points. β-actin was used as loading control.

4.5.2 BMP-9 promotes migration

The immunohistochemical analysis of the patient samples shown above point to a correlation between BMP-9 and EMT in HCC. Since increased migration is a typical feature of EMT we performed Transwell assays using the two cell lines. Treatment with BMP-9 (50 ng/ml) increased cell migration in HLE and HepG2 cells by 2.38 and 3.72 fold, respectively (Fig. 25).

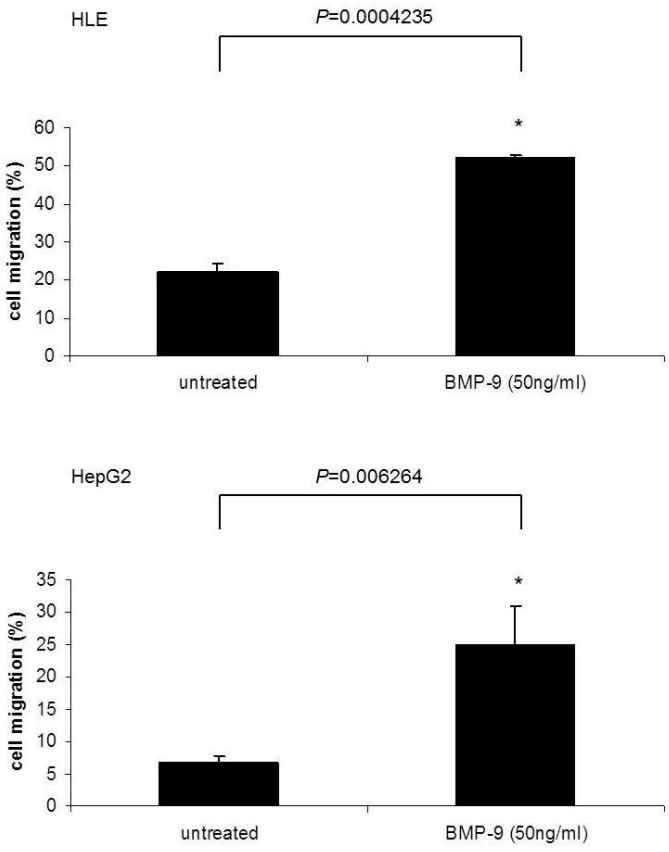

Fig.25. BMP-9 enhances cell motility in HLE and HepG2. HCC cell lines were plated into the Transwell chambers and treated or not with BMP-9 (50 ng/ml). At the end point of the migration assay, cells in the upper and lower chambers were trypsinized and transferred to a fresh 96-well flat bottom plate. ATP content, which correlates to cell number, was evaluated for migrated and non-migrated cells. **P*<0.05, Student's *t*-test was done to analyze statistical difference. Experiments were performed in triplicates and repeated three times. The average ±SEM of all experiments is shown.

4.5.3. BMP-9 induces morphological changes typical for EMT

We then investigated cell morphology and expression levels of EMT markers upon stimulation of the cells with BMP-9 for 72 h. Cell morphology displayed that BMP-9 led to some conversion of the cells from an epithelial to a fibroblastic cell morphology (Fig. 26 A). Although both the cell lines are considered to be of epithelial phenotype, stainings of fixed cells showed that basal E-cadherin expression was rather diffuse and not strictly localized to the cell membranes and the cell-cell contacts (Fig. 26 B, C). However, BMP-9 treatment reduced E-cadherin and increased Vimentin immunofluorescence (Fig. 26 B, C).

A

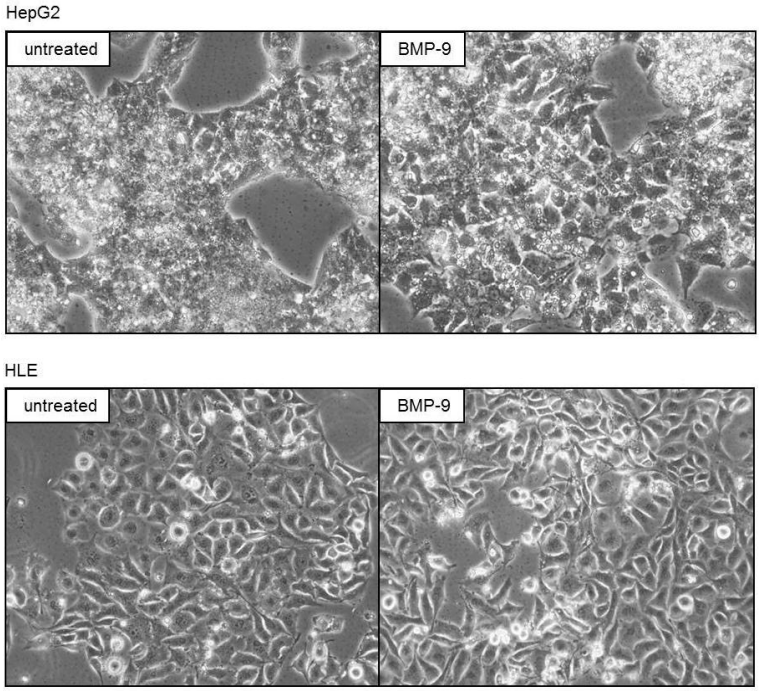

B

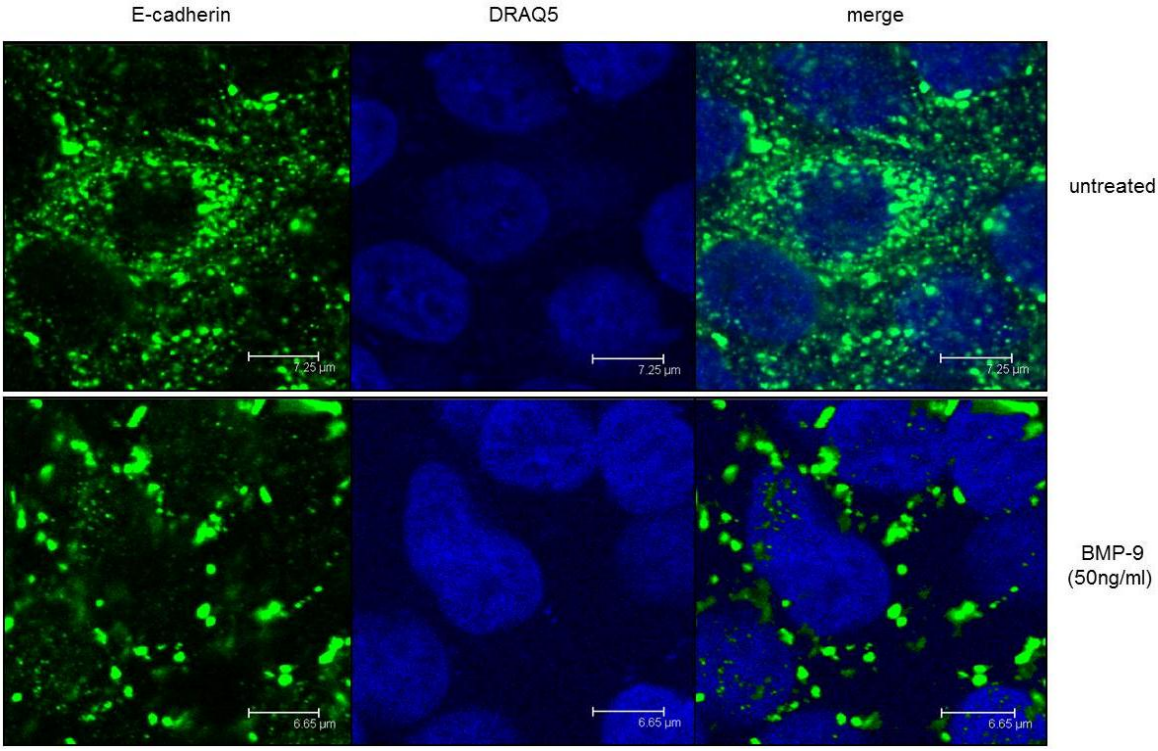
E-cadherin
DRAQ5
merge
untreated
BMP-9
(50ng/ml)
7.25 µm
6.65 µm

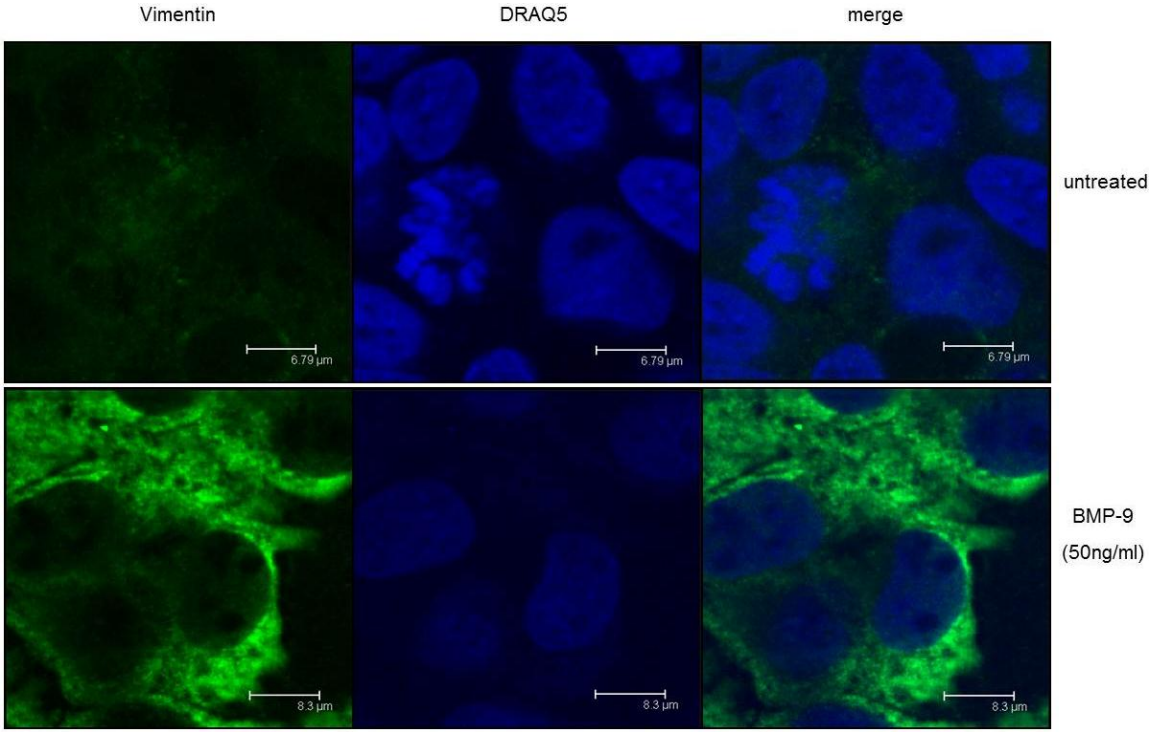
Vimentin
DRAQ5
merge
untreated
BMP-9
(50ng/ml)
6.79 µm
8.3 µm

C

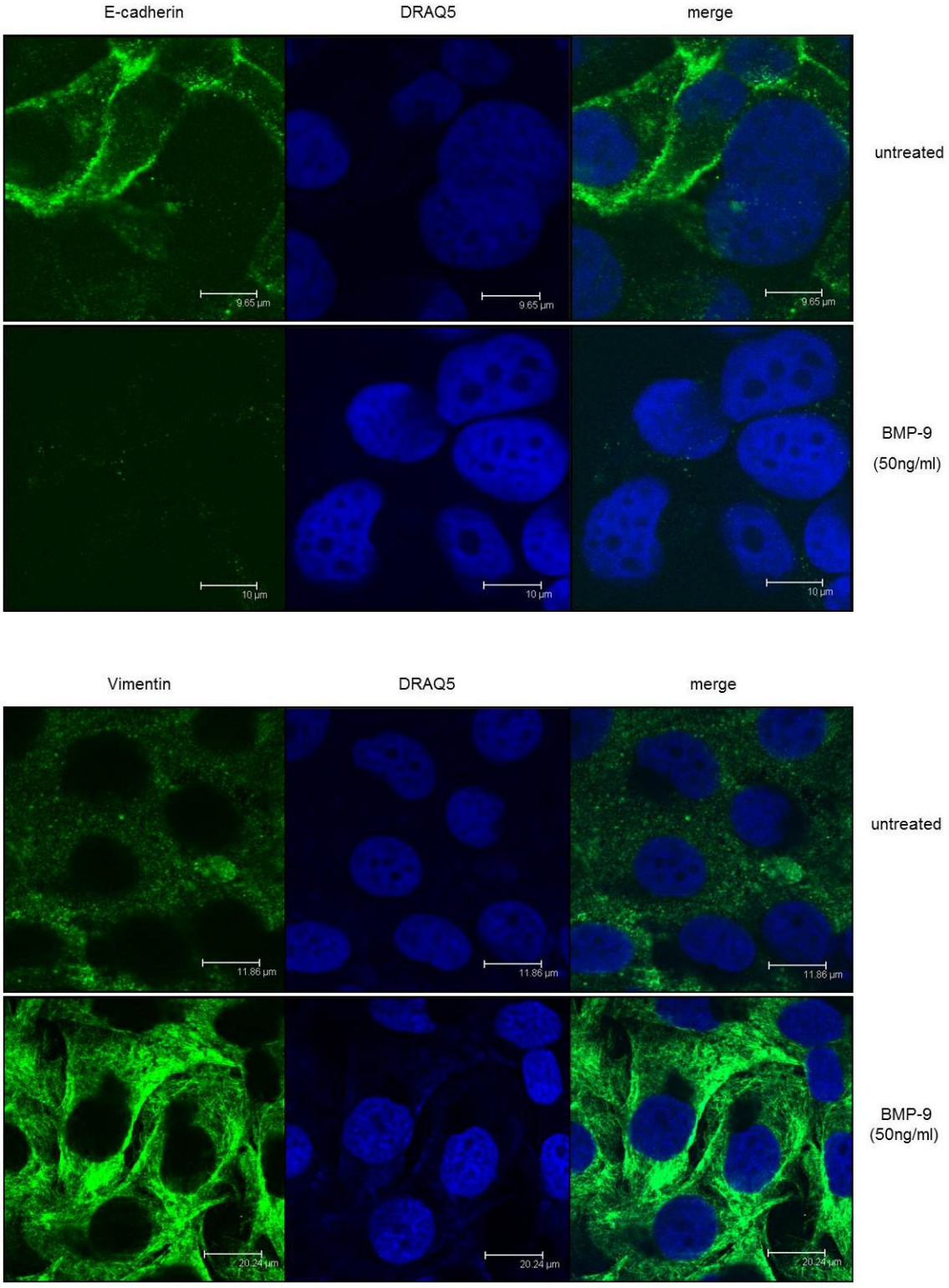

Fig.26. BMP-9 induces morphological changes of EMT in HCC cells. HLE and HepG2 cell lines were untreated or treated with BMP-9 50 ng/ml for 72 h after serum-starvation overnight. **A,** Mophological changes induced by BMP-9. Magnification, 20×. **B,** HepG2 cells and **C,** HLE cells were immunostained with anti-E-cadherin and anti-Vimentin antibodies. DRAQ5 was used to show nuclei (Scale was indicated in the image).

4.5.4. BMP-9 induces expression of EMT makers

In accordance with the fibroblastoid morphological changes, BMP-9 down-regulated E-cadherin and induced Vimentin expression (Fig. 27 A). Snail, a key transcription factor responsible for the down-regulation of E-cadherin was significantly induced by BMP-9 at the RNA level (Fig. 27 B).

Collectively, these results support the hypothesis that BMP-9 facilitates EMT and migration, and therefore eventually also metastasis of HCC cells.

A

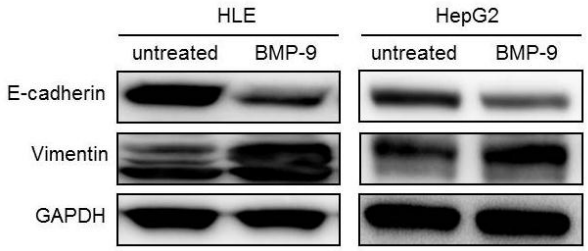

B

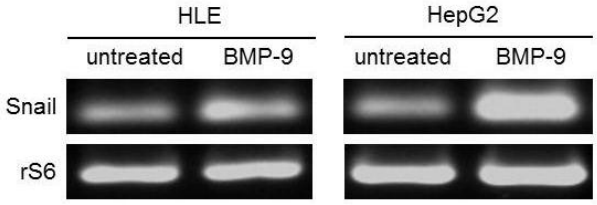

Fig.27. BMP-9 induces expression of EMT markers in HCC cells. HLE and HepG2 cells were untreated or treated with BMP-9 50 ng/ml for 72 h after serum-starvation overnight. **A,** Western blots against E-cadherin and Vimentin. GAPDH served as a loading control. **B,** RT-PCR showing that BMP-9 induced Snail mRNA expression in both HCC cell lines.

4.5.5. BMP-9-induced down-regulation of E-cadherin is rescued by overexpression of dominant negative ALK1/2 (AddnALK1/2)

Some studies using other cell types have demonstrated that ALK1 and ALK2 are BMP-9 specific type I receptors (Luo et al., 2010). We used adenoviral infection to functionally link BMP-9 mediated signal transduction to down-regulation of E-cadherin in HCC cell lines. With overexpression of dominant negative forms of these receptors (AddnALK1/2), phosphorylation of Smad1 was blocked along with down-regulation of E-cadherin upon stimulation with BMP-9 (Fig. 28).

A

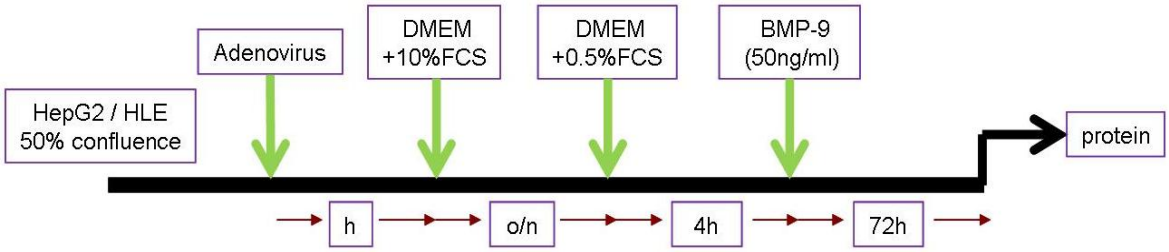

B

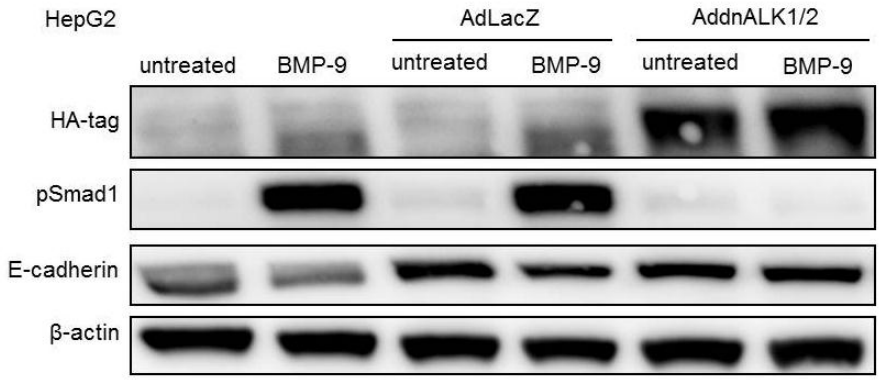

C

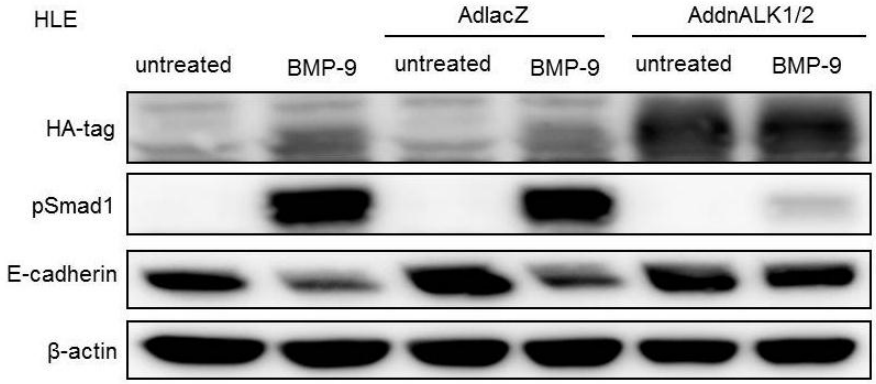

Fig.28. ALK1/2 is required for BMP-9 mediated E-cadherin expression. **A,** Scheme of the experimental setup for adenovirus infection. **B,** HepG2 cells were infected with either AdLacZ (infection control) or AddnALK1/2. Anti-pSmad1 immunoblots showing that Smad1 phosphorylation was blocked by AddnALK1/2 and down-regulated E-cadherin induced by BMP-9 was rescued by AddnALK1/2. **C,** The same effects of AddnALK1/2 on HLE cells are shown.

4.5.6. Overexpression of constitutively active ALK1 down-regulates E-cadherin

Furthermore, overexpression of constitutive active ALK1 (AdcaALK1) could mimic the function of BMP-9, leading to phosphorylation of Smad1 and down-regulation of E-cadherin (Fig. 29).

A

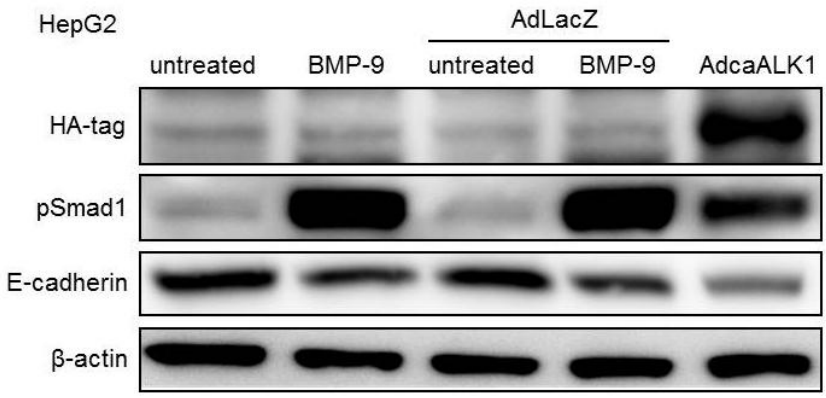

B

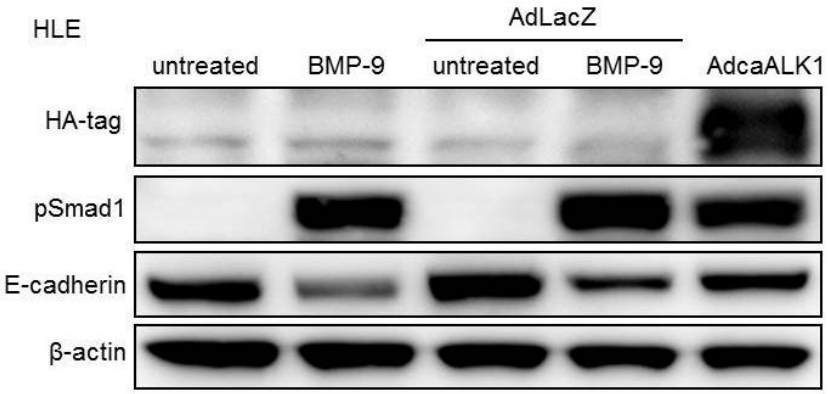

Fig.29. caALK1mimices BMP-9 mediated E-cadherin down-regulation in HCC cells. HCC cell lines were seeded in 6-well plates and infected with either AdLacZ or AdcaALK1 overnight followed by medium change. Cells were untreated or treated with BMP-9 (50 ng/ml) for 72 h after serum starvation for 4 hs. A, HepG2 cells were infected with AdcaALK1. Anti-pSmad1 immunoblots showing that Smad1 phosphorylation was induced and E-cadherin was down-regulated by AdcaALK1. B, The same effects of AdcaALK1 on HLE cells are shown.

4.5.7. Overexpression of constitutively activate ALK2 down-regulates E-cadherin

Since BMP-9 has also been described to signal via ALK2 in some cell types (Luo et al., 2010), constitutive active ALK2 (AdcaALK2) was used in our study. AdcaALK2 could also mimic the function of BMP-9, leading to phosphorylation of Smad1 and down-regulation of E-cadherin (Fig. 30 A, B).

These results imply that BMP-9 induces an EMT response in HCC via signaling through the type I receptors ALK1 and/or ALK2.

A

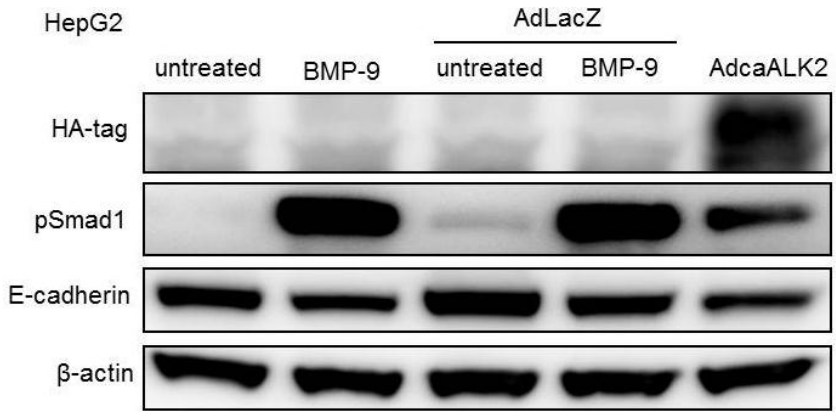

B

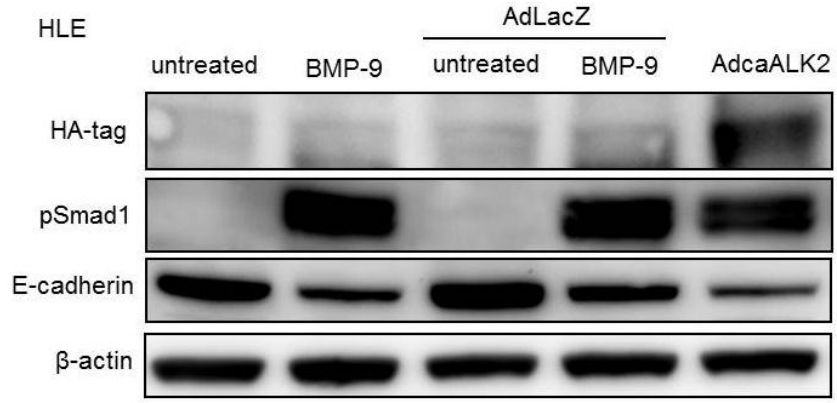

Fig.30. caALK2 mimics BMP-9 mediated E-cadherin expression in HCC cells. HCC cell lines were seeded in 6-well plates and infected with either AdLacZ or AdcaALK2 overnight followed by medium change. Cells were untreated or treated with BMP-9 (50 ng/ml) for 72 h after serum starvation for 4 hs. A, HepG2 cells were infected with AdcaALK2. Anti-pSmad1 immunoblots showing Smad1 phosphorylation was induced and E-cadherin was down-regulated by AdcaALK2. B, The same effects of AdcaALK2 on HLE cells are shown.

4.5.8. Smad1 overexpression does not further enhance BMP-9 induced down-regulation of E-cadherin

Since BMP-9 signals via Smad1, we further studied whether over-expression of Smad1 could enhance the down-regulation of E-cadherin upon BMP-9 treatment in HepG2 and HLE cells. Though overexpression of Smad1 successfully increased Smad1 levels in HCC cells, without

additional application of BMP-9 this failed to activate Smad1 signaling and especially in HepG2 cells reduction of expression of E-cadherin was not massively enhanced by Smad1 over-expression (Fig. 31 A, B).

These results imply that availability of Smad1 protein is not the limiting factor in this context and that endogenous Smad1 levels seem to suffice for maximal BMP-9 responses. The results further demonstrate that there do not seem to be any Smad1 activating cytokines endogenously expressed in these cells because increased total Smad1 did not lead to any basal phosphorylation. The cell lines differ in this regard from the primary HCC cells *in vivo* which express BMP-9 by themselves as shown above.

A

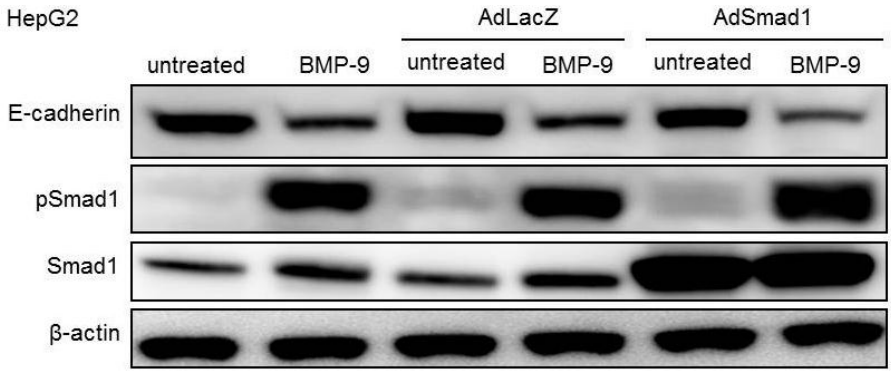

B

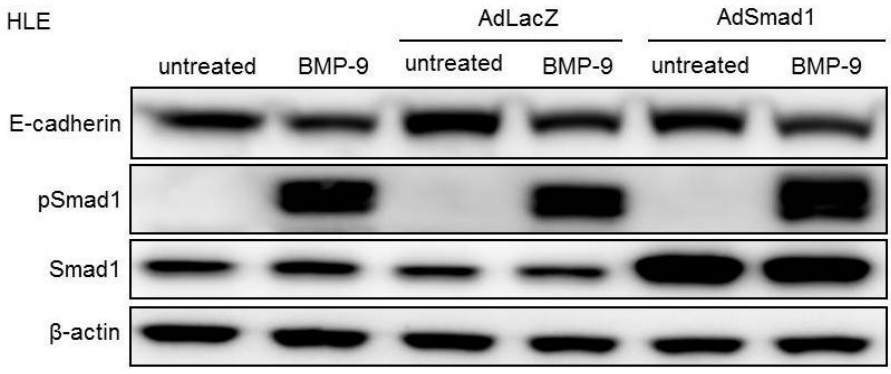

Fig.31. Smad1 overexpression does not strongly enhance BMP-9 mediated E-cadherin down-regulation. HCC cell lines were seeded in 6-well plates and infected with either AdLacZ or AdSmad1 overnight followed by medium change. Cells were untreated or treated with BMP-9 (50 ng/ml) for 72 h after serum starvation for 4 hs. **A,** Western blot of lysates from HepG2 cells infected with AdSmad1. **B,** Western blot of lysates from HLE cells infected with AdSmad1. B-actin was used as loading control.

5. Discussion

BMPs are a subfamily of the TGF-β superfamily and its first member, TGF-β1, was originally described in 1983 (Assoian et al., 1983). TGF-β family members have been discovered to play important roles in various physiological and pathological conditions such as embryonic development, angiogenesis, fibrogenesis and carcinogenesis (David et al., 2009; Rahimi and Leof, 2007). BMP-9 was first described in the mouse liver by Celeste AJ, et al (Celeste, 1994). In healthy rat liver, only non-parenchymal cells, like HSCs and Kupffer cells are the main source of BMP-9, whereas hepatocytes were initially reported to be negative for BMP-9 (Miller et al., 2000). In this study, the researchers used ribonuclease protection assay and Western blot to detect BMP-9 mRNA and protein expression in different liver cell types and whole liver lysates. At the RNA level they found BMP-9 expression in the whole liver lysates and in non-parenchymal cells. In contrast to this, at the protein level, BMP-9 expression was detected in non-parenchymal cells, but not in the whole liver lysates. In another study investigating mouse and human liver, cholangiocytes and hepatocytes were identified as major producers of BMP-9 (Bidart et al., 2012). These authors also detected BMP-9 expression in whole liver lysates as well as different liver cell types including cholangiocytes, hepatocytes, hepatic stellate cells and hepatic sinusoidal endothelial cells at the RNA and protein levels, but here these were measured with real-time PCR and IHC. Their data are consistent at both levels and indicate that basal expression of BMP-9 exists in healthy liver. Furthermore, BMP-9 mRNA level in cholangiocytes is 6 times higher than in hepatocytes and nearly 100 times higher than in HSCs and hepatic sinusoidal endothelial cells (Bidart et al., 2012). These results are mainly consistent with ours. With ISH we found a positive signal for BMP-9 mRNA in normal mouse liver which was located mainly in cholangiocytes, whereas in hepatocytes and other cell types, it was rather low or negative. Most likely, ISH is not sensitive enough to detect basal BMP-9 levels in these other cell types under healthy conditions. Bidart et al have recently reported that under physiological conditions, BMP-9 circulates in inactive (40%) as well as active (60%) forms in plasma and the active form functions in endothelial cells to keep them in a resting state (Bidart et al., 2012). BMP-9 is one of the most potent BMPs inducing bone formation. Furthermore, it has been reported to function in hematopoiesis, glucose homeostasis, iron balance, angiogenesis, neuronal differentiation and carcinogenesis (Bessa et al., 2009; Chen et al., 2003; Suzuki et al., 2010; Truksa et al., 2006). Although liver has been identified as the dominant source of active BMP-9 and Song et al reported that BMP-9 induces cell proliferation in primary rat hepatocytes

(Song et al., 1995), possible roles of this cytokine in various liver diseases have not been fully clarified. Therefore, in the present study potential functions of BMP-9 in the liver were investigated *in vitro* and *in vivo*.

As canonical model for liver injury, acute intoxication with CCl_4 was established in Balb/c mice. HE staining, ISH of albumin and serum levels of ALT, AST and LDH showed that in this model liver damage occurred rapidly in the pericentral areas with increased serum levels of liver enzymes at day 1 after CCl_4 injection, reaching a peak at day 2. This result is consistent with previous reports (Taniguchi et al., 2004; Tsuchiya et al., 2007), and this model was therefore used for further experiments.

During the process of acute liver damage and recovery, a special pattern for BMP-9 expression appeared. In total liver lysates BMP-9 RNA was rapidly increased within 3 h after CCl_4 injection followed by a transient reduction until day 3. At day 3, its expression reached another peak at both protein and RNA levels, implying that BMP-9 might be involved in the wound-healing process that is initiated upon acute liver damage *in vivo*. Interestingly, in the pericentral area where hepatocytes were seriously damaged, positive signal was observed in hepatocytes when BMP-9 expression increased after CCl_4-mediated liver injury. Furthermore, at day 3 BMP-9 and its main target gene, Id-1 were co-localized. To our knowledge, we show for the first time that during liver recovery, BMP-9 expression is induced which implies that this cytokine is involved in liver damage and/or liver regeneration processes. Because BMP-9 improves glycemia in diabetic mice, Sosa I et al hypothesized that BMP-9 has a certain potential regenerative role in the liver and they also describe expression of BMP-9 in the Space of Disse (Sosa et al., 2011). However, nothing was reported yet about BMP-9's possible role in liver regeneration.

After CCl_4 insult, the BMP-signal transducer, Smad1 was also increasingly activated. Phosphorylated Smad1 appeared mainly in hepatocytes already at 3 h after CCl_4 application with a transient reduction at day 1, but remaining still higher than that in normal mouse liver. This result is in line with data from Ryusuke Nakastsuka et al, who also found rapid pSmad1 expression at 3 h post CCl_4-mediated injury in rats. They show that induction of pSmad1 precedes an increase of BMP-2, another Smad1 inducer and conclude that this first increase of pSmad1 must be induced by proteins other than BMP-2 (Nakatsuka et al., 2007). In our study, the pSmad1 expression pattern, including very early time-points, matched well with BMP-9

mRNA up-regulation. Therefore, it seems reasonable to conclude that BMP-9 is one of the candidates responsible for early activation of the Smad1 pathway after liver injury. Of course participation of other BMPs like BMP-2 can, especially at later time-points, not be excluded. From day 1 to day 3, positive staining against pSmad1 was seen not only in hepatocytes, but also in sinusoidal cells. In damaged hepatocytes of the pericentral area positivity was located in both the cytoplasm and nucleus. At day 3, positivity was additionally observed in infiltrating cells, probably proliferating activated HSCs. At the same time, Id-1 expression reached a peak. Id-1 up-regulation is reported to be directly mediated by the Smad1 pathway in HSCs, and Id-1 is involved in transdifferentiation of HSCs. Furthermore, in the chronic CCl_4 model, phosphorylation of Smad1 correlates with up-regulation of Id-1 *in vivo* (Wiercinska et al., 2006). According to these expression patterns and localizations of BMP-9, pSmad1 and Id-1, and the importance of activated HSCs to liver regeneration and recovery (Iredale, 2001), we speculate that in the acute CCl_4 model Id-1 is at least to some extent up-regulated by the BMP-9/Smad1 pathway and that this pathway takes part in acute liver regeneration/wound-healing processes.

When BMP-9 expression was significantly increased at day 3, within the pericentral area some hepatocyte apoptosis occurred. Apoptosis is an important type of cell death to terminate excessive or dangerous cell growth during organ evolution, remodeling of tissues and so on (Lockshin and Zakeri, 1990). On the other hand cell apoptosis is indispensable for tissue self-renewal. Jialan Shi et al have found that large numbers of hepatocytes perform apoptosis induced by CCl_4 intoxication and apoptosis of hepatocytes is increased at 3 h and peaked at 6 h after CCl_4 intoxication in rats. Furthermore, the percentage of apoptotic ballooned cells is increased until day 3 (Shi et al., 1998). Similar results could be achieved in our mouse model. Compared to the normal liver, the expression pattern of the apoptosis marker, cleaved caspase3 experienced significant change after CCl_4 intoxication, and especially at day 3, the quantity of cleaved caspase3 was maximal as determined by IHC. Because BMP-9, pSmad1 as well as cleaved caspase3 localized in the pericentral area at day 3, we investigated if BMP-9 might induce hepatocyte death via apoptosis. When isolated primary mouse hepatocytes were stimulated with BMP-9 alone, we did not observe strong BMP-9-induced apoptosis. We therefore looked at a possible cross-talk of BMP-9 with known apoptosis-inducing factors like TGF-β1.

TGF-β1 has been proven to trigger hepatocyte apoptosis in the liver *in vitro* as well as *in vivo*

(Oberhammer et al., 1992). In the CCl_4-mediated liver injury mouse model, TGF-β1 mRNA is increased, arriving at a peak on day 1 and remaining at this high level at least until day 3 (Hellerbrand et al., 1999). The mRNA levels of TGF-β1 receptors are decreased in rat hepatocytes from 12 h to 48 h, but recover at 72 h after CCl_4 treatment and in HSCs their levels do not change (Date et al., 1998). In our stainings with serial sections, at day 3 BMP-9 and Id-1 were highly expressed in the pericentral area whereas TβRII and albumin were comparably low here and higher outside the pericentral area. However, TβRII expression was still present within the pericentral area. Hence we expect that although there seem to be diverse patterns of activity of the BMP- vs. the TGF-β pathway in the different areas *in vivo*, the BMP-9/Smad1 pathway might still synergize with the TGF-β1 pathway in the pericentral area or at the borders of these areas mediating for example apoptosis of selected hepatocytes. Furthermore, expression of cleaved caspase3 was also increased in the pericentral area at day 3. Interestingly, we found that combined stimulation of cultured hepatocytes with TGF-β1 and BMP-9 led to enhanced presence of cleaved caspase3 along with down-regulation of Bcl-2 expression, the latter one being an anti-apoptotic factor and involved in TGF-β-triggered apoptosis (Motyl et al., 1998; Teramoto et al., 1998). This TGF-β1 enhancing effect of BMP-9 on apoptosis was dose-dependent. These observations suggest that even though BMP-9 alone does not induce apoptosis, it synergizes with TGF-β1 in this regard. TGF-β1, activin A, TNF and CD95 ligand have as well been demonstrated to induce apoptosis in the liver (Schulte-Hermann et al., 1997), it still requires further investigation to clarify whether BMP-9 also has synergistic effects with these factors to facilitate apoptosis in hepatocytes. In some liver cancer cells, like Hep3B, Huh7, SNU449 and PLC/PRF/5, TGF-β1 has also been shown to induce apoptosis (Caja et al., 2011b). If BMP-9 synergizes with TGF-β1 in these cells too, this might provide a new option for BMP-9 as an enhancer of TGF-β1-induced apoptosis in liver cancer cells which could contribute to possible cancer treatment options.

We further investigated the molecular mechanism underlying BMP-9's enhancing effect on TGF-β1-induced hepatocyte apoptosis. Irena CC et al have demonstrated that in hepatocytes, TGF-β1-induced expression of the NADPH oxidase NOX4 is necessary for induction of apoptosis (Carmona-Cuenca et al., 2008) and in endothelial cells BMP-4 induces apoptosis via NOX4 dependent ROS production and ROS-dependent p38 and JNK activation leading to caspase3 activation (Tian et al., 2012). From our microarray data, we can see that NOX4 was also up-regulated by BMP-9 in hepatocytes. This may be a possible explanation for the enhanced caspase3 activity and cell death by co-stimulation of BMP-9 and TGF-β1. Another

reason may be that BMP-9 facilitates to keep the epithelial phenotype of hepatocytes and epithelial cells are known to be more sensitive to TGF-β1-induced apoptosis than mesenchymal cells. During *in vitro* hepatocyte culture, hepatocytes undergo dedifferentiation and loose there epithelial phenotype (Dooley et al., 2008; Elaut et al., 2006). Liver cells undergoing EMT acquired enhanced resistance to apoptosis, most likely owing to the increased expression of Snail (Vega et al., 2004). On the other hand, down-regulation of Snail promotes the apoptotic effects of TGF-β1 on liver cells (Franco et al., 2010). We found in the present study that BMP-9 enhanced expression of epithelial marker proteins like E-cadherin in primary hepatocytes while down-regulating the mesenchymal marker N-cadherin. BMP-9 even partially reverted TGF-β1-mediated down-regulation of E-cadherin implying that it antagonizes TGF-β1-mediated EMT to some degree. Whether this indeed represents the apoptosis-enhancing mechanism described above deserves further exploration.

In our study, we did not see cell proliferation induced by BMP-9 in primary mouse hepatocytes. In addition, PCNA, a cell proliferation marker was reduced by BMP-9 implying that BMP-9 acts anti-proliferative on primary hepatocytes. This differs from the data by Song et al. who reported that BMP-9 leads to increased cell proliferation in primary rat hepatocytes and HepG2 cells (Song et al., 1995). However, this study also showed that only sub-confluent primary rat hepatocytes exhibit some proliferative response to rhBMP-9, confluent primary rat hepatocytes do not. Furthermore, they did not find a dose-dependent response meaning that after 36 h the maximal increase in proliferation (= 0.5-fold increase in thymidine incorporation) was reached with 8 ng/ml BMP-9. This effect started to decrease again with 10 ng/ml and was insignificant with 80 ng/ml. Therefore, our different results might originate from differing cell culture conditions, species difference, and/or using different detection techniques. Future studies will also aim at investigating if BMP-9 might decrease the pro-proliferative effects of known mediators like e.g. HGF.

After CCl_4 intoxication, we observed a transient activation of HSCs. This result fits well to those from Hong et al who found that after a single injection of CCl_4 in rats, the α-SMA protein level was greatly elevated at day 3 (Shen et al., 2007). TGF-β1 has been regarded as the key promoter for HSC activation (Breitkopf et al., 2005) and Claus et al reported that in wild type mice expression of TGF-β1 peaked at day 1 after a single CCl_4 treatment. The peak of TGF-β1 preceded that of α-SMA expression, implying that TGF-β1 is involved in HSC activation. But interestingly, in TGFβ1 knock-out mice which had no TGF-β1 and low TGF-

β2 and TGF-β3, CCl_4 injection still resulted in relatively small but significant expression of Collagen α1(I) and α-SMA, and HSC activation *in vivo* still occurred (Hellerbrand et al., 1999). So TGF-β1 seems not indispensable for HSC activation even though it most likely enhances it leading to the maximal fibrotic effect *in vivo*. Other cytokines and/or pathways may also participate in the process of early HSC activation. In our mouse model, increased pSmad1 was observed as early as 3 h after CCl_4 injection, but only in hepatocytes. At day 1, in the damaged area, few activated HSCs were detected, but at day 3, the number of α-SMA positive cells was significantly increased. At the same time, pSmad1 was also detected in this area. Our observation is consistent with the report that increase of Smad1 protein expression is seen at day 2 with a peak at day 3 in isolated HSCs from the acute CCl_4 model (Shen et al., 2007). This group further reported that Smad1 expression and transcriptional activity are also increased when HSCs activate in the acute CCl_4 animal model (Shen et al., 2007). These observations and the facts that BMP-9 and pSmad1 expressions increased with *in vitro* activation of HSCs and that BMP-9-induced proliferation of the HSC cell line LX-2, imply that the Smad1 pathway participates in HSC activation *in vivo*. Hong et al have demonstrated that in rat HSCs, Smad1 expression and its phosphorylation are increased along with HSC activation. Adenoviruses overexpressing Smad1 or Smad1 short hairpin RNA (shRNA) increase or decrease α-SMA expression, respectively, in CSFC-8B, an HSC cell line (Shen et al., 2003). These *in vitro* data further support the conclusion that the Smad1 pathway plays an important role in activation of HSCs. Therefore, besides TGF-β induced Smad2/3 signaling which has been regarded as the most important pathway in HSC activation and fibrogenesis (Gressner and Weiskirchen, 2006), BMP/Smad1 signaling may be another critical player in this process.

Although Smad1 signaling can be activated by both TGF-β1 and BMPs (Kretzschmar et al., 1997b), BMPs are its dominant triggers in hepatocytes and HSCs. TGF-β1-induced Smad1 phosphorylation is only transient, returning to basal levels within hours and at least *in vitro* this response requires higher amounts of TGF-β1 than needed for maximal activation of Smads 2 and 3 (data not shown). Therefore it is reasonable to hypothesize that *in vivo* mainly BMPs are the inducers of Smad1 signaling in the liver and TGF-β mainly activates the Smad2/3 pathway. In the bile duct ligation (BDL) model, another liver fibrosis model, expression of BMP-4 is markedly elevated in the fibrotic liver and presence of activated HSCs along with significantly increased down-stream signaling via Smad1, but also via ERK1/2 and p38 was described. BMP-4 directly stimulated pSmad1 and pERK1/2 expression

in an HSC cell line. Moreover, BMP-4 promoted transdifferentiation of HSCs, though without affecting their proliferation (Fan et al., 2006). Since BMP-9 is another strong inducer of Smad1 signaling, we investigated if BMP-9/Smad1 signal transduction played a role in early activation of HSCs. *In vitro* culture of primary mouse HSCs led to transdifferentiation, during which both BMP-9 and pSmad1 expression were elevated along with the increase of α-SMA and PCNA expression. In collaboration with P. ten Dijke's group at the University of Leiden, the Netherlands, we used injection of AdALK1-Fc, an adenovirus expressing a secreted mutant of the BMP-9 receptor to capture BMP-9 *in vivo* in the chronic CCl_4-induced mouse model of liver fibrosis. Here we found that inhibition of BMP-9 by AdALK1-Fc reduced collagen deposition and α-SMA expression in the liver (manuscript in preparation). Together with our results presented in this thesis we draw the conclusion that BMP-9 is indeed a pro-fibrotic cytokine *in vivo*. Based on the fact that BMP-9, pSmad1, desmin and α-SMA expression were localized within the pericentral area at day 3 after CCl_4 injection *in vivo*, it is speculated that the BMP-9/Smad1 pathway might play a role in the transdifferentiation of HSCs *in vivo*. It still needs to be established if overexpressed BMP-9 directly promotes liver fibrogenesis, but our data strongly imply that it is involved in HSC activation and TGF-β1 mediated apoptosis of hepatocytes, both representing events that trigger fibrogenesis *in vivo*.

Dorsomorphin, also named compound C, has been described as a potent inhibitor of AMPK (AMP-activated protein kinase) (Gao et al., 2008). Later, it has been discovered to also have high selectivity for inhibition of the BMP/Smad1 pathway (Anderson and Darshan, 2008) and it has been used to inhibit BMP signaling in iron homeostasis (Yu et al., 2008), osteogenesis (Seib et al., 2009), T cell activation and differentiation (Yoshioka et al., 2012). Interestingly, activation of AMPK inhibits transdifferentiation of HSCs and liver fibrosis (Adachi and Brenner, 2008; Lim et al., 2012). But AMPK-deficiency was not responsible for enhanced CCl_4-induced fibrosis *in vivo* (da Silva Morais et al., 2010). Therefore, if inhibition of AMPK by Dorsomorphin happens in HSCs, it can be expected to have no influence or even act as a promoter on HSC activation. In our study, the presence of Dorsomorphin significantly inhibited HSC transdifferentiation *in vitro* as monitored by reduced expressions of fibrotic markers including α-SMA, collagen, Id-1, desmin and fibronectin. Together with the above discussed involvement of the BMP-9/Smad1 signaling in HSC activation, we conclude that the inhibitory effects of Dorsomorphin on HSC activation were dominantly related to its inhibitory effect on the BMPs/Smad1 pathway.

It has been generally accepted that liver fibrosis is a reversible dynamic process. Therefore anti-fibrotic treatment was often considered as tool for reducing the occurrence of liver cirrhosis, even liver cancer. Several candidates to be targeted in such antifibrotic therapies have been tested in preclinical or clinical studies and they include Interferon-γ, Angiotension receptor blockers, PPAR ligands, Endothelin-1 receptor antagonists and TGF-β neutralizing agents (Thompson and Patel, 2010). According to others' and our study, the Smad1 pathway plays an important role in HSC activation and its inhibitor, Dorsomorphin can reverse this process. Therefore neutralization of this pathway or even of BMP-9 alone might provide another practical anti-fibrotic strategy in the near future which needs to be evaluated further.

Besides acute and chronic liver diseases, TGF-β members have also been described to play important roles in various types of cancers such as gastric, liver and pancreatic cancer (Achyut and Yang, 2011). In premalignant cells TGF-β1 serves as a tumor suppressor, while in later stages of cancer, it functions as a tumor promoter. It has not been clearly clarified how and when TGF-β1 is converted from a tumor suppressor to a tumor promoter during carcinogenesis (Achyut and Yang, 2011). As for the roles of TGF-β in HCC, one explanation proposed by Yamazaki et al indicates that TGF-β inhibits proliferation in premalignant hepatocytes and early HCC cells, along with promotion of stroma formation, whereas in late stages of HCC, TGF-β induces cancer invasion via tumor-stromal interaction (Yamazaki et al., 2011). During the past decades, although BMPs as well have been demonstrated to participate in the formation and progression of human cancer, compared to the dual roles of TGF-β1 in cancer development, BMPs perform quite different or may even exert completely opposite functions depending on the cancer cell type, the tumor microenvironment and other cell functions. For example, BMP-2 inhibits growth of gastric cancer cells through increasing the levels of p21/WAF1/CIP1, leading to cell cycle arrest in the G1-phase (Wen et al., 2004), but it facilitates proliferation of lung cancer cells through Smad1/5 signaling and induction of Id-1 expression (Langenfeld et al., 2006).

Nine different BMPs are up-regulated in HCC cells and their described functions in disease progression include cell proliferation, migration and angiogenesis (Lu et al., 2012; Maegdefrau and Bosserhoff, 2012; Qiu et al., 2010). BMP-4 and BMP-7 are up-regulated in HBx-induced HCC mouse models and in human HBV-related HCC patients and are therefore included to what they have defined the "most common regulators" during the transition from normal liver to HCC. Furthermore, their ectopic overexpression increases cell viability and

promotes migration in Hep3B (Lu et al., 2012). Overexpression of BMP-4 is significantly associated with the number of tumor nodules, TNM stage and vascular invasion, and is proposed as a new marker to predict the recurrence and prognosis of HCC patients (Guo et al., 2012). Further, BMP-4 induces cell proliferation and migration in HepG2 and Hep3B (Chiu et al., 2012). BMP-2 induces angiogenesis in Bel7402 and SMMC7721 tumor xenografted nude mice, and WSS25, an antagonist of BMP-2 inhibits angiogenesis via blocking BMP/Smad1/Id-1 signaling in these mouse models (Qiu et al., 2010).

In human cancer, variant functions for BMP-9 have been described depending on the cancer types. In prostate and breast cancer, BMP-9 provides tumor suppressor activity, since it inhibits growth, migration and invasion (Wang et al., 2011; Ye et al., 2008), whereas in ovarian cancer, it acts as a proliferation promoter via activation of ALK2/Smad1 signaling (Herrera et al., 2009). Although BMP-9 has been found to be up-regulated in HCC cell lines (Maegdefrau and Bosserhoff, 2012), so far, its contribution to HCC development and progression has not been explored.

In the present study, we demonstrated that BMP-9 mRNA and protein were expressed at different degrees in liver tissues from HCC patients. Slightly positive (1+) staining of BMP-9 protein was observed in 61%, and moderately to strongly positive staining (2+) in 39% of HCC tissue. BMP-9 protein expression levels were higher in the cancer area than that in its adjacent “normal” liver tissue in 25% of the patients and were similar in both areas in 58.33% patients. In the remaining 16%, expression levels were even lower in the cancer area than in its adjacent “normal” liver tissue. Based on the finding that liver is the main organ producing BMP-9 (Song et al., 1995), we can expect that low levels of BMP-9 expression should always be detectable. Furthermore, the “normal” liver tissues investigated in the present study still came from HCC patients and should therefore be considered as rather damaged. Comparing this with our in situ hybridizations of healthy mouse livers which showed strong positivity only in cholangiocytes, together with the 25% of patients showing increased presence of BMP-9 in HCC compared to adjacent tissue, we conclude that there is a tendency of increase in BMP-9 in diseased liver, especially in HCC. We want to mention also that 95.12% of the investigated HCC patients were HBV-infected and it will be an interesting task to investigate in the future if HBV infection as such impacts BMP-9 expression and if there are differences in regard to disease etiology.

Expression of BMP-9 in HCC, as resolved with immunohistochemical staining, was significantly associated with the T stage showing stronger expression in patients with T3, 4 than in T1, 2 patients, indicating that high levels of BMP-9 correlate with the degree of tumor invasion into the surrounding tissue. The Child-Pugh classification is well accepted as robust predictor of death in HCC (Tandon and Garcia-Tsao, 2009) and represents a measure for the level of liver damage: Child-Pugh B/C corresponds to reduced liver function (Mandli et al., 2008). When comparing BMP-9 expression with the Child-Pugh class of the patients we found that Child-Pugh class B/C was stronger associated with the group with lower BMP-9 levels (1+; 79%) while in patients with Child-Pugh class A the distribution was almost 50% (1+) and 50% (2+). This inverse correlation shows that although BMP-9 protein expression correlates with invasiveness of the tumor (T stage), it does not seem to increase along with loss of liver function as determined by Child-Pugh classification.

Studying HCC cells *in vitro*, we found that BMP-9 promoted cell migration, a typical feature of mesenchymal cells. Together with the known pro-proliferative effect of BMP-9 in liver cells (Song et al., 1995), this observation prompted us to investigate if BMP-9 induces EMT in HCC cells. EMT is required for epithelial cancer cell migration and metastasis and down-regulated epithelial (E)-cadherin and up-regulated Snail are well described features of EMT. E-cadherin is a Ca^{2+}-dependent cell adhesion transmembrane glycoprotein, which links adjacent cells by homophilic interactions (Kemler, 1993), thus representing a typical marker for epithelial polarity. Membranous E-cadherin is down-regulated during loss of the epithelial phenotype and is a classical molecular hall mark of EMT. The expression of E-cadherin is negatively regulated by Snail at the transcriptional level. Appearance of mesenchymal markers like Vimentin or N-cadherin is other features typical for EMT. Indeed, besides promoting migration, BMP-9 down-regulated E-cadherin expression and induced Snail and Vimentin expression, indicating that in full contrast to its effects on primary hepatocytes, BMP-9 leads to EMT in HCC cells. In accordance with these *in vitro* findings, in HCC patient samples, BMP-9 expression was positively correlated with Snail expression and reversely correlated with E-cadherin expression, although these correlations did not reach statistical significance, which may be due to the relatively small number of samples. Hence, our results are supportive for the hypothesis that BMP-9 can promote migration and metastasis of HCC cells via induction of EMT.

We further investigated the BMP-9 down-stream signaling pathway involved in EMT, and

especially in BMP-9 induced down-regulation of E-cadherin. In mesenchymal stem cells, BMP-9 was reported to signal via the BMP type I receptors ALK1 and ALK2 which both activate Smad1 signaling to mediate osteogenesis (Luo et al., 2010). We here show that ALK2 is expressed in both HCC cell lines tested and by using adenovirally overexpressed constructs, we could confirm that dominant negative or constitutive active mutants of ALKs 1 and 2 impact E-cadherin expression levels and EMT in HLE and HepG2 cells.

Downstream of ALK1/2 activation, Smad1 is activated and mediates the signal to the nucleus. BMP/Smad1 signaling was described to participate in different tumor types with diverse outcomes, either as tumor promoter or as tumor suppressor. Activation of Smad1/5 is correlated with TGF-β-induced growth inhibition in B-cell lymphoma (Bakkebo et al., 2010). In human breast cancer cells, activation of BMP-2/Smad1 signaling inhibits cancer cell proliferation via up-regulation of p21 (Pouliot and Labrie, 2002). In breast cancer patients and a corresponding xenograft mouse model, enhanced phospho-Smad1 staining was found in bone metastasis as compared to the primary tumor or lymph node metastases, which suggests that Smad1 signaling contributes to bone metastasis of breast cancer (Katsuno et al., 2008). In pancreatic cancer, BMP-2, 4 and 7 induce EMT and increase cancer cell invasiveness, and their common canonical down-stream signaling component, Smad1 is indispensable for BMP-mediated invasiveness (Gordon et al., 2009). In line with the presence of BMP-9, Smad1 phosphorylation was increased in HCC cells of liver samples from patients. These results further support the conclusion that the BMP-9/Smad1 pathway might be involved in the pathogenesis of HCC. However, we can at this stage not exclude that besides BMP-9, other members of the TGF-β superfamily (e.g. other BMPs or TGF-β itself) take part in inducing Smad1 phosphorylation.

On the basis of the findings in HCC, it is implicated that the BMP-9/Smad1 pathway may function as a potential promoter in HCC via inducing EMT. Further studies with larger human patient sample numbers and animal models with a disturbed BMP-9 signaling pathway are planned to elucidate the functional implication of BMP-9 and its downstream signaling in liver cancer progression and to estimate its potential as new marker for HCC progression and prognosis as well as testing BMP-9 as novel therapeutic target to treat HCC.

To discover more potential functions of BMP-9 in the liver, we performed microarray analysis with samples from hepatocytes treated with BMP-9 for 24 h. 32 genes were up-regulated and

only 4 genes were down-regulated by more than 1.4 fold. After grouping these genes, we found that BMP-9 might participate in detoxification, proliferation/differentiation, iron homeostasis, lipid transport, triglyceride metabolism and sugar metabolism. Several functions have been also reported by other groups. For instance, Luciana Chagas Caperuto et al reported that in normal rats BMP-9 may serve as HISS (hepatic insulin-sensitizing substance) to mediate glucose homeostasis and in the insulin-resistant rats, BMP-9 expression and processing is severely decreased (Caperuto et al., 2008). In line with our results, Jaroslav Truksa et al demonstrated that BMP-9 is the most potent inducer of murine hepcidin expression, which is a peptide playing key role in iron homeostasis (Truksa et al., 2006). Therefore, besides liver regeneration and HCC, BMP-9 might additionally function in liver diseases related to metabolism like NASH (non-alcoholic steatohepatitis) and haemochromatosis.

In summary, our data indicate that BMP-9 may directly or indirectly play a role in hepatocyte apoptosis, HSC transdifferentioation and HCC progression. Therefore, our data may lead to novel therapeutic options based on interference with the BMP-9/Smad1 pathway in various liver diseases.

6. Abbreviations

ALT, Alanine aminotransferase

AST, Aspartate aminotransferase

APAF1, Apoptotic protease-activator factor-1

AIF, Apoptosis-inducing factor

aHSC, Activated HSCs

ACVR2A, Activin receptor Type 2

ActRIIA, Activin A receptor type IIA

ActRIIB, Activin A receptor type IIB

ALK-1, Activin receptor-like kinase-1

AMH, Anti-Mülerian hormone

Ad, Adenovirus

AMPK, AMP-activated protein kinase

BMP-9, Bone morphogenetic protein-9

BMPRII, BMP receptor type II

BMPR-IA, BMP receptor type IA

BDL, Bile duct ligation

cDNA, Complementary DNA

cRNA, Copy RNA

caALK1, Constitutive active ALK1

caALK2, Constitutive active ALK2

COX-2, Cyclooxygenase-2

CCl_4, Carbon tetrachloride

Cyp2E1, Cytochrome P-450 IIE1

dnALK1/2, Dominant negative ALK1/2

DMSO, Dimethylsulfoxide

DM, Dorsomorphin

DEPC, Diethylpyrocarbonate

DIG, Digoxigenin

DAB, 3,3'-diaminobenzidine tetrahydrochloride

ERK, Extracellular signal-regulated kinase

ECM, Extracellular matrix

EMT, Epithelial-mesenchymal transition

FOXO3A, O forkhead box transcription factor-3A

GSK3β, Glycogen synthase kinase3β

GDF, Growth and differentiation factor

GAPDH, Glyceraldehyde-3-phosphate dehydrogenase

HNF-4, Hepatocyte nuclear factore-4

HISS, Hepatic insulin-sensitizing substance

HHT, Hereditary hemorrhagic telangiectasia

HGF, Hepatocyte growth factor

HCC, Hepatocellular carcinoma

HE, Hematoxylin and eosin

HBV, Hepatitis B virus

HCV, Hepatitis C virus

HSC, Hepatic stellate cell

Id, Inhibitor of differentiation

IHC, Immunohistochemistry

IF, Immunofluorescence

ISH, *In situ* hybridization

I-Smads, Inhibitory-Smads

JNK, C-Jun N-terminal kinases

LacZ, β-galactosidase

LDH, Lactate dehydrogenase

MIS, Mülerian inhibiting substance

MH1, N-terminal Mad Homology 1

MEK, Mitogen-activated protein kinase/extracellular signal-regulated kinase kinase

mHC, Mouse hepatocyte

MAPK, Mitogen activated protein kinase

NBT/BCIP, Nitro blue tetrazolium chloride/5-Bromo-4-chloro-3-indolyl phosphate

NOX4, NADPH oxidase-4

NASH, Non-alcoholic steatohepatitis

NKT, Natural killer T cells

PCNA, Proliferating Cell Nuclear Antigen

PFA, Paraformaldehyde

PDGF, Platelet derived growth factor

PPIA, Peptidylprolyl isomerase A

R-Smads, Receptor-Smads

RT-PCR, Reverse transcription-polymerase chain reaction

ROS, Reactive oxygen species

SSC, Saline-sodium citrate

SSXS C-terminal, Phosphorylation site of R-Smads

shRNA, Short hairpin RNA

α-SMA, α-smooth muscle actin

TGF-β, Transforming growth factor-β

TNFR, Tumor necrosis factor receptor

TIMP-1, Tissue inhibitor of metalloproteinase-1

TNF-α, Tumor necrosis factor-α

7. References

Achyut, B.R., and L. Yang. 2011. Transforming growth factor-beta in the gastrointestinal and hepatic tumor microenvironment. *Gastroenterology*. 141:1167-1178.

Adachi, M., and D.A. Brenner. 2008. High molecular weight adiponectin inhibits proliferation of hepatic stellate cells via activation of adenosine monophosphate-activated protein kinase. *Hepatology*. 47:677-685.

Aden, D.P., A. Fogel, S. Plotkin, I. Damjanov, and B.B. Knowles. 1979. Controlled synthesis of HBsAg in a differentiated human liver carcinoma-derived cell line. *Nature*. 282:615-616.

Anderson, G.J., and D. Darshan. 2008. Small-molecule dissection of BMP signaling. *Nature chemical biology*. 4:15-16.

Assoian, R.K., A. Komoriya, C.A. Meyers, D.M. Miller, and M.B. Sporn. 1983. Transforming growth factor-beta in human platelets. Identification of a major storage site, purification, and characterization. *The Journal of biological chemistry*. 258:7155-7160.

Bakkebo, M., K. Huse, V.I. Hilden, E.B. Smeland, and M.P. Oksvold. 2010. TGF-beta-induced growth inhibition in B-cell lymphoma correlates with Smad1/5 signalling and constitutively active p38 MAPK. *BMC immunology*. 11:57.

Battaglia, S., N. Benzoubir, S. Nobilet, P. Charneau, D. Samuel, A.L. Zignego, A. Atfi, C. Brechot, and M.F. Bourgeade. 2009. Liver cancer-derived hepatitis C virus core proteins shift TGF-beta responses from tumor suppression to epithelial-mesenchymal transition. *PloS one*. 4:e4355.

Bedossa, P., and V. Paradis. 1995. Transforming growth factor-beta (TGF-beta): a key-role in liver fibrogenesis. *Journal of hepatology*. 22:37-42.

Benyon, R.C., and M.J. Arthur. 2001. Extracellular matrix degradation and the role of hepatic stellate cells. *Seminars in liver disease*. 21:373-384.

Bessa, P.C., M.T. Cerqueira, T. Rada, M.E. Gomes, N.M. Neves, A. Nobre, R.L. Reis, and M. Casal. 2009. Expression, purification and osteogenic bioactivity of recombinant human BMP-4, -9, -10, -11 and -14. *Protein expression and purification*. 63:89-94.

Bidart, M., N. Ricard, S. Levet, M. Samson, C. Mallet, L. David, M. Subileau, E. Tillet, J.J. Feige, and S. Bailly. 2012. BMP9 is produced by hepatocytes and circulates mainly in an active mature form complexed to its prodomain. *Cellular and molecular life sciences : CMLS*. 69:313-324.

Bissell, D.M., S.S. Wang, W.R. Jarnagin, and F.J. Roll. 1995. Cell-specific expression of transforming growth factor-beta in rat liver. Evidence for autocrine regulation of hepatocyte proliferation. *The Journal of clinical investigation*. 96:447-455.

Bissell, M.J., and D. Radisky. 2001. Putting tumours in context. *Nature reviews. Cancer*. 1:46-54.

Bolos, V., H. Peinado, M.A. Perez-Moreno, M.F. Fraga, M. Esteller, and A. Cano. 2003. The transcription factor Slug represses E-cadherin expression and induces epithelial to mesenchymal transitions: a comparison with Snail and E47 repressors. *Journal of cell science*. 116:499-511.

Breitkopf, K., S. Haas, E. Wiercinska, M.V. Singer, and S. Dooley. 2005. Anti-TGF-beta strategies for the treatment of chronic liver disease. *Alcoholism, clinical and experimental research*. 29:121S-131S.

Breuhahn, K., T. Longerich, and P. Schirmacher. 2006. Dysregulation of growth factor signaling in human hepatocellular carcinoma. *Oncogene*. 25:3787-3800.

Brown, M.A., Q. Zhao, K.A. Baker, C. Naik, C. Chen, L. Pukac, M. Singh, T. Tsareva, Y. Parice, A. Mahoney, V. Roschke, I. Sanyal, and S. Choe. 2005. Crystal structure of BMP-9 and functional interactions with pro-region and receptors. *The Journal of biological chemistry*. 280:25111-25118.

Burlacu, A. 2003. Regulation of apoptosis by Bcl-2 family proteins. *Journal of cellular and molecular medicine*. 7:249-257.

Caja, L., E. Bertran, J. Campbell, N. Fausto, and I. Fabregat. 2011a. The transforming growth factor-beta (TGF-beta) mediates acquisition of a mesenchymal stem cell-like phenotype in human liver cells. *Journal of cellular physiology*. 226:1214-1223.

Caja, L., P. Sancho, E. Bertran, and I. Fabregat. 2011b. Dissecting the effect of targeting the epidermal growth factor receptor on TGF-beta-induced-apoptosis in human hepatocellular carcinoma cells. *Journal of hepatology*. 55:351-358.

Calle, E.E., L.R. Teras, and M.J. Thun. 2005. Obesity and mortality. *The New England journal of medicine*. 353:2197-2199.

Caperuto, L.C., G.F. Anhe, T.D. Cambiaghi, E.H. Akamine, D. do Carmo Buonfiglio, J. Cipolla-Neto, R. Curi, and S. Bordin. 2008. Modulation of bone morphogenetic protein-9 expression and processing by insulin, glucose, and glucocorticoids: possible candidate for hepatic insulin-sensitizing substance. *Endocrinology*. 149:6326-6335.

Carmona-Cuenca, I., C. Roncero, P. Sancho, L. Caja, N. Fausto, M. Fernandez, and I. Fabregat. 2008. Upregulation of the NADPH oxidase NOX4 by TGF-beta in

hepatocytes is required for its pro-apoptotic activity. *Journal of hepatology*. 49:965-976.

Celeste, A.J.S., J. J.; Cox, K.; Rosen, V.; and Wozney, J. M. 1994. Bone morphogenetic protein-9, a new member of the TGF-β superfamily. *J Bone Min Res* 136.

Chang, H., C.W. Brown, and M.M. Matzuk. 2002. Genetic analysis of the mammalian transforming growth factor-beta superfamily. *Endocrine reviews*. 23:787-823.

Chen, C., K.J. Grzegorzewski, S. Barash, Q. Zhao, H. Schneider, Q. Wang, M. Singh, L. Pukac, A.C. Bell, R. Duan, T. Coleman, A. Duttaroy, S. Cheng, J. Hirsch, L. Zhang, Y. Lazard, C. Fischer, M.C. Barber, Z.D. Ma, Y.Q. Zhang, P. Reavey, L. Zhong, B. Teng, I. Sanyal, S.M. Ruben, O. Blondel, and C.E. Birse. 2003. An integrated functional genomics screening program reveals a role for BMP-9 in glucose homeostasis. *Nature biotechnology*. 21:294-301.

Chiu, C.Y., K.K. Kuo, T.L. Kuo, K.T. Lee, and K.H. Cheng. 2012. The activation of MEK/ERK signaling pathway by bone morphogenetic protein 4 to increase hepatocellular carcinoma cell proliferation and migration. *Molecular cancer research : MCR*. 10:415-427.

Cory, S., and J.M. Adams. 2002. The Bcl2 family: regulators of the cellular life-or-death switch. *Nature reviews. Cancer*. 2:647-656.

da Silva Morais, A., J. Abarca-Quinones, B. Guigas, B. Viollet, P. Starkel, Y. Horsmans, and I.A. Leclercq. 2010. Development of hepatic fibrosis occurs normally in AMPK-deficient mice. *Clinical science*. 118:411-420.

Danial, N.N., and S.J. Korsmeyer. 2004. Cell death: critical control points. *Cell*. 116:205-219.

Date, M., K. Matsuzaki, M. Matsushita, K. Sakitani, K. Shibano, A. Okajima, C. Yamamoto, N. Ogata, T. Okumura, T. Seki, Y. Kubota, M. Kan, W.L. McKeehan, and K. Inoue. 1998. Differential expression of transforming growth factor-beta and its receptors in hepatocytes and nonparenchymal cells of rat liver after CCl4 administration. *Journal of hepatology*. 28:572-581.

David, L., J.J. Feige, and S. Bailly. 2009. Emerging role of bone morphogenetic proteins in angiogenesis. *Cytokine & growth factor reviews*. 20:203-212.

David, L., C. Mallet, S. Mazerbourg, J.J. Feige, and S. Bailly. 2007. Identification of BMP9 and BMP10 as functional activators of the orphan activin receptor-like kinase 1 (ALK1) in endothelial cells. *Blood*. 109:1953-1961.

De Bleser, P.J., T. Niki, V. Rogiers, and A. Geerts. 1997. Transforming growth factor-beta gene expression in normal and fibrotic rat liver. *Journal of hepatology*. 26:886-893.

Derynck, R. 1998. SMAD proteins and mammalian anatomy. *Nature*. 393:737-739.

Derynck, R., and Y.E. Zhang. 2003. Smad-dependent and Smad-independent pathways in TGF-beta family signalling. *Nature*. 425:577-584.

Doh, K.O., H.K. Jung, I.J. Moon, H.G. Kang, J.H. Park, and J.G. Park. 2008. Prevention of CCl4-induced liver cirrhosis by ribbon antisense to transforming growth factor-beta1. *International journal of molecular medicine*. 21:33-39.

Dooley, S., B. Delvoux, B. Lahme, K. Mangasser-Stephan, and A.M. Gressner. 2000. Modulation of transforming growth factor beta response and signaling during transdifferentiation of rat hepatic stellate cells to myofibroblasts. *Hepatology*. 31:1094-1106.

Dooley, S., J. Hamzavi, L. Ciuclan, P. Godoy, I. Ilkavets, S. Ehnert, E. Ueberham, R. Gebhardt, S. Kanzler, A. Geier, K. Breitkopf, H. Weng, and P.R. Mertens. 2008. Hepatocyte-specific Smad7 expression attenuates TGF-beta-mediated fibrogenesis and protects against liver damage. *Gastroenterology*. 135:642-659.

Dooley, S., H. Weng, and P.R. Mertens. 2009. Hypotheses on the role of transforming growth factor-beta in the onset and progression of hepatocellular carcinoma. *Digestive diseases*. 27:93-101.

Dor, I., M. Namba, and J. Sato. 1975. Establishment and some biological characteristics of human hepatoma cell lines. *Gann = Gan*. 66:385-392.

Elaut, G., T. Henkens, P. Papeleu, S. Snykers, M. Vinken, T. Vanhaecke, and V. Rogiers. 2006. Molecular mechanisms underlying the dedifferentiation process of isolated hepatocytes and their cultures. *Current drug metabolism*. 7:629-660.

Elsharkawy, A.M., F. Oakley, and D.A. Mann. 2005. The role and regulation of hepatic stellate cell apoptosis in reversal of liver fibrosis. *Apoptosis : an international journal on programmed cell death*. 10:927-939.

Fan, J., H. Shen, Y. Sun, P. Li, F. Burczynski, M. Namaka, and Y. Gong. 2006. Bone morphogenetic protein 4 mediates bile duct ligation induced liver fibrosis through activation of Smad1 and ERK1/2 in rat hepatic stellate cells. *Journal of cellular physiology*. 207:499-505.

Farazi, P.A., and R.A. DePinho. 2006. Hepatocellular carcinoma pathogenesis: from genes to environment. *Nature reviews. Cancer*. 6:674-687.

Franco, D.L., J. Mainez, S. Vega, P. Sancho, M.M. Murillo, C.A. de Frutos, G. Del Castillo, C. Lopez-Blau, I. Fabregat, and M.A. Nieto. 2010. Snail1 suppresses TGF-beta-

induced apoptosis and is sufficient to trigger EMT in hepatocytes. *Journal of cell science*. 123:3467-3477.

Friedman, S.L. 2003. Liver fibrosis -- from bench to bedside. *Journal of hepatology*. 38 Suppl 1:S38-53.

Friedman, S.L. 2004. Stellate cells: a moving target in hepatic fibrogenesis. *Hepatology*. 40:1041-1043.

Fuentealba, L.C., E. Eivers, A. Ikeda, C. Hurtado, H. Kuroda, E.M. Pera, and E.M. De Robertis. 2007. Integrating patterning signals: Wnt/GSK3 regulates the duration of the BMP/Smad1 signal. *Cell*. 131:980-993.

Galonek, H.L., and J.M. Hardwick. 2006. Upgrading the BCL-2 network. *Nature cell biology*. 8:1317-1319.

Gao, Y., Y. Zhou, A. Xu, and D. Wu. 2008. Effects of an AMP-activated protein kinase inhibitor, compound C, on adipogenic differentiation of 3T3-L1 cells. *Biological & pharmaceutical bulletin*. 31:1716-1722.

Geerts, A. 2001. History, heterogeneity, developmental biology, and functions of quiescent hepatic stellate cells. *Seminars in liver disease*. 21:311-335.

Gordon, K.J., K.C. Kirkbride, T. How, and G.C. Blobe. 2009. Bone morphogenetic proteins induce pancreatic cancer cell invasiveness through a Smad1-dependent mechanism that involves matrix metalloproteinase-2. *Carcinogenesis*. 30:238-248.

Gotzmann, J., H. Huber, C. Thallinger, M. Wolschek, B. Jansen, R. Schulte-Hermann, H. Beug, and W. Mikulits. 2002. Hepatocytes convert to a fibroblastoid phenotype through the cooperation of TGF-beta1 and Ha-Ras: steps towards invasiveness. *Journal of cell science*. 115:1189-1202.

Gressner, A.M., and R. Weiskirchen. 2006. Modern pathogenetic concepts of liver fibrosis suggest stellate cells and TGF-beta as major players and therapeutic targets. *Journal of cellular and molecular medicine*. 10:76-99.

Guo, X., L. Xiong, L. Zou, and J. Zhao. 2012. Upregulation of Bone Morphogenetic Protein 4 is Associated with Poor Prognosis in Patients with Hepatocellular Carcinoma. *Pathology oncology research : POR*.

Hamzavi, J., S. Ehnert, P. Godoy, L. Ciuclan, H. Weng, P.R. Mertens, R. Heuchel, and S. Dooley. 2008. Disruption of the Smad7 gene enhances CCI4-dependent liver damage and fibrogenesis in mice. *Journal of cellular and molecular medicine*. 12:2130-2144.

Hellerbrand, C., B. Stefanovic, F. Giordano, E.R. Burchardt, and D.A. Brenner. 1999. The role of TGFbeta1 in initiating hepatic stellate cell activation in vivo. *Journal of hepatology*. 30:77-87.

Herrera, B., and G.J. Inman. 2009. A rapid and sensitive bioassay for the simultaneous measurement of multiple bone morphogenetic proteins. Identification and quantification of BMP4, BMP6 and BMP9 in bovine and human serum. *BMC cell biology*. 10:20.

Herrera, B., M. van Dinther, P. Ten Dijke, and G.J. Inman. 2009. Autocrine bone morphogenetic protein-9 signals through activin receptor-like kinase-2/Smad1/Smad4 to promote ovarian cancer cell proliferation. *Cancer research*. 69:9254-9262.

Huang, S., K.C. Flanders, and A.B. Roberts. 2000. Characterization of the mouse Smad1 gene and its expression pattern in adult mouse tissues. *Gene*. 258:43-53.

Iredale, J.P. 2001. Hepatic stellate cell behavior during resolution of liver injury. *Seminars in liver disease*. 21:427-436.

Itoh, S., F. Itoh, M.J. Goumans, and P. Ten Dijke. 2000. Signaling of transforming growth factor-beta family members through Smad proteins. *European journal of biochemistry / FEBS*. 267:6954-6967.

Jeong, W.I., O. Park, S. Radaeva, and B. Gao. 2006. STAT1 inhibits liver fibrosis in mice by inhibiting stellate cell proliferation and stimulating NK cell cytotoxicity. *Hepatology*. 44:1441-1451.

Johansson, I., and M. Ingelman-Sundberg. 1985. Carbon tetrachloride-induced lipid peroxidation dependent on an ethanol-inducible form of rabbit liver microsomal cytochrome P-450. *FEBS letters*. 183:265-269.

Johnson, D.W., J.N. Berg, M.A. Baldwin, C.J. Gallione, I. Marondel, S.J. Yoon, T.T. Stenzel, M. Speer, M.A. Pericak-Vance, A. Diamond, A.E. Guttmacher, C.E. Jackson, L. Attisano, R. Kucherlapati, M.E. Porteous, and D.A. Marchuk. 1996. Mutations in the activin receptor-like kinase 1 gene in hereditary haemorrhagic telangiectasia type 2. *Nature genetics*. 13:189-195.

Josephs, D.H., and P.J. Ross. 2010. Sorafenib in hepatocellular carcinoma. *British journal of hospital medicine*. 71:451-456.

Katsuno, Y., A. Hanyu, H. Kanda, Y. Ishikawa, F. Akiyama, T. Iwase, E. Ogata, S. Ehata, K. Miyazono, and T. Imamura. 2008. Bone morphogenetic protein signaling enhances invasion and bone metastasis of breast cancer cells through Smad pathway. *Oncogene*. 27:6322-6333.

Kemler, R. 1993. From cadherins to catenins: cytoplasmic protein interactions and regulation of cell adhesion. *Trends in genetics : TIG*. 9:317-321.

Kretzschmar, M., J. Doody, and J. Massague. 1997a. Opposing BMP and EGF signalling pathways converge on the TGF-beta family mediator Smad1. *Nature*. 389:618-622.

Kretzschmar, M., F. Liu, A. Hata, J. Doody, and J. Massague. 1997b. The TGF-beta family mediator Smad1 is phosphorylated directly and activated functionally by the BMP receptor kinase. *Genes & development*. 11:984-995.

Lafdil, F., M.N. Chobert, D. Couchie, A. Brouillet, E.S. Zafrani, P. Mavier, and Y. Laperche. 2006. Induction of Gas6 protein in CCl4-induced rat liver injury and anti-apoptotic effect on hepatic stellate cells. *Hepatology*. 44:228-239.

Lamouille, S., C. Mallet, J.J. Feige, and S. Bailly. 2002. Activin receptor-like kinase 1 is implicated in the maturation phase of angiogenesis. *Blood*. 100:4495-4501.

Langenfeld, E.M., Y. Kong, and J. Langenfeld. 2006. Bone morphogenetic protein 2 stimulation of tumor growth involves the activation of Smad-1/5. *Oncogene*. 25:685-692.

Lau, W.Y., and E.C. Lai. 2008. Hepatocellular carcinoma: current management and recent advances. *Hepatobiliary & pancreatic diseases international : HBPD INT*. 7:237-257.

Lazarevich, N.L., O.A. Cheremnova, E.V. Varga, D.A. Ovchinnikov, E.I. Kudrjavtseva, O.V. Morozova, D.I. Fleishman, N.V. Engelhardt, and S.A. Duncan. 2004. Progression of HCC in mice is associated with a downregulation in the expression of hepatocyte nuclear factors. *Hepatology*. 39:1038-1047.

Lee, K.Y., and S.C. Bae. 2002. TGF-beta-dependent cell growth arrest and apoptosis. *Journal of biochemistry and molecular biology*. 35:47-53.

Lee, T.K., K. Man, R.T. Poon, C.M. Lo, A.P. Yuen, I.O. Ng, K.T. Ng, W. Leonard, and S.T. Fan. 2006. Signal transducers and activators of transcription 5b activation enhances hepatocellular carcinoma aggressiveness through induction of epithelial-mesenchymal transition. *Cancer research*. 66:9948-9956.

Lei, W., K. Zhang, X. Pan, Y. Hu, D. Wang, X. Yuan, G. Shu, and J. Song. 2010. Histone deacetylase 1 is required for transforming growth factor-beta1-induced epithelial-mesenchymal transition. *The international journal of biochemistry & cell biology*. 42:1489-1497.

Li, B. 2008. Bone morphogenetic protein-Smad pathway as drug targets for osteoporosis and cancer therapy. *Endocrine, metabolic & immune disorders drug targets*. 8:208-219.

Li, H., H. Zhu, C.J. Xu, and J. Yuan. 1998. Cleavage of BID by caspase 8 mediates the mitochondrial damage in the Fas pathway of apoptosis. *Cell*. 94:491-501.

Lim, J.Y., M.A. Oh, W.H. Kim, H.Y. Sohn, and S.I. Park. 2012. AMP-activated protein kinase inhibits TGF-beta-induced fibrogenic responses of hepatic stellate cells by targeting transcriptional coactivator p300. *Journal of cellular physiology*. 227:1081-1089.

Lindroos, P.M., R. Zarnegar, and G.K. Michalopoulos. 1991. Hepatocyte growth factor (hepatopoietin A) rapidly increases in plasma before DNA synthesis and liver regeneration stimulated by partial hepatectomy and carbon tetrachloride administration. *Hepatology*. 13:743-750.

Lockshin, R.A., and Z.F. Zakeri. 1990. Programmed cell death: new thoughts and relevance to aging. *Journal of gerontology*. 45:B135-140.

Lopez-Coviella, I., T.M. Mellott, V.P. Kovacheva, B. Berse, B.E. Slack, V. Zemelko, A. Schnitzler, and J.K. Blusztajn. 2006. Developmental pattern of expression of BMP receptors and Smads and activation of Smad1 and Smad5 by BMP9 in mouse basal forebrain. *Brain research*. 1088:49-56.

Louis, H., J.L. Van Laethem, W. Wu, E. Quertinmont, C. Degraef, K. Van den Berg, A. Demols, M. Goldman, O. Le Moine, A. Geerts, and J. Deviere. 1998. Interleukin-10 controls neutrophilic infiltration, hepatocyte proliferation, and liver fibrosis induced by carbon tetrachloride in mice. *Hepatology*. 28:1607-1615.

Lu, J.W., Y. Hsia, W.Y. Yang, Y.I. Lin, C.C. Li, T.F. Tsai, K.W. Chang, G.S. Shieh, S.F. Tsai, H.D. Wang, and C.H. Yuh. 2012. Identification of the common regulators for hepatocellular carcinoma induced by hepatitis B virus X antigen in a mouse model. *Carcinogenesis*. 33:209-219.

Luo, J., M. Tang, J. Huang, B.C. He, J.L. Gao, L. Chen, G.W. Zuo, W. Zhang, Q. Luo, Q. Shi, B.Q. Zhang, Y. Bi, X. Luo, W. Jiang, Y. Su, J. Shen, S.H. Kim, E. Huang, Y. Gao, J.Z. Zhou, K. Yang, H.H. Luu, X. Pan, R.C. Haydon, Z.L. Deng, and T.C. He. 2010. TGFbeta/BMP type I receptors ALK1 and ALK2 are essential for BMP9-induced osteogenic signaling in mesenchymal stem cells. *The Journal of biological chemistry*. 285:29588-29598.

Lux, A., L. Attisano, and D.A. Marchuk. 1999. Assignment of transforming growth factor beta1 and beta3 and a third new ligand to the type I receptor ALK-1. *The Journal of biological chemistry*. 274:9984-9992.

Maegdefrau, U., T. Amann, A. Winklmeier, S. Braig, T. Schubert, T.S. Weiss, K. Schardt, C. Warnecke, C. Hellerbrand, and A.K. Bosserhoff. 2009. Bone morphogenetic protein 4 is induced in hepatocellular carcinoma by hypoxia and promotes tumour progression. *The Journal of pathology*. 218:520-529.

Maegdefrau, U., and A.K. Bosserhoff. 2012. BMP activated Smad signaling strongly promotes migration and invasion of hepatocellular carcinoma cells. *Experimental and molecular pathology*. 92:74-81.

Mandli, T., J. Fazakas, G. Ther, M. Arkosy, B. Fule, E. Nemeth, J. Fazakas, M. Hidvegi, and S. Toth. 2008. [Evaluation of liver function before living donor liver transplantation and liver resection]. *Orvosi hetilap*. 149:779-786.

Mann, J., and D.A. Mann. 2009. Transcriptional regulation of hepatic stellate cells. *Advanced drug delivery reviews*. 61:497-512.

Massague, J. 1990. The transforming growth factor-beta family. *Annual review of cell biology*. 6:597-641.

Michalopoulos, G.K., and M.C. DeFrances. 1997. Liver regeneration. *Science*. 276:60-66.

Miller, A.F., S.A. Harvey, R.S. Thies, and M.S. Olson. 2000. Bone morphogenetic protein-9. An autocrine/paracrine cytokine in the liver. *The Journal of biological chemistry*. 275:17937-17945.

Minguez, B., V. Tovar, D. Chiang, A. Villanueva, and J.M. Llovet. 2009. Pathogenesis of hepatocellular carcinoma and molecular therapies. *Current opinion in gastroenterology*. 25:186-194.

Miyazono, K., Y. Kamiya, and M. Morikawa. 2010. Bone morphogenetic protein receptors and signal transduction. *Journal of biochemistry*. 147:35-51.

Miyazono, K., S. Maeda, and T. Imamura. 2005. BMP receptor signaling: transcriptional targets, regulation of signals, and signaling cross-talk. *Cytokine & growth factor reviews*. 16:251-263.

Mizuno, S., and T. Nakamura. 2007. Hepatocyte growth factor: a regenerative drug for acute hepatitis and liver cirrhosis. *Regenerative medicine*. 2:161-170.

Motyl, T., K. Grzelkowska, W. Zimowska, J. Skierski, P. Wareski, T. Ploszaj, and L. Trzeciak. 1998. Expression of bcl-2 and bax in TGF-beta 1-induced apoptosis of L1210 leukemic cells. *European journal of cell biology*. 75:367-374.

Moustakas, A., and C.H. Heldin. 2003. Ecsit-ement on the crossroads of Toll and BMP signal transduction. *Genes & development*. 17:2855-2859.

Moustakas, A., and C.H. Heldin. 2005. Non-Smad TGF-beta signals. *Journal of cell science*. 118:3573-3584.

Nakatsuka, R., M. Taniguchi, M. Hirata, G. Shiota, and K. Sato. 2007. Transient expression of bone morphogenic protein-2 in acute liver injury by carbon tetrachloride. *Journal of biochemistry*. 141:113-119.

Nitta, T., J.S. Kim, D. Mohuczy, and K.E. Behrns. 2008. Murine cirrhosis induces hepatocyte epithelial mesenchymal transition and alterations in survival signaling pathways. *Hepatology*. 48:909-919.

Nolte, T., W. Kaufmann, F. Schorsch, T. Soames, and E. Weber. 2005. Standardized assessment of cell proliferation: the approach of the RITA-CEPA working group. *Experimental and toxicologic pathology : official journal of the Gesellschaft fur Toxikologische Pathologie*. 57:91-103.

Oberhammer, F.A., M. Pavelka, S. Sharma, R. Tiefenbacher, A.F. Purchio, W. Bursch, and R. Schulte-Hermann. 1992. Induction of apoptosis in cultured hepatocytes and in regressing liver by transforming growth factor beta 1. *Proceedings of the National Academy of Sciences of the United States of America*. 89:5408-5412.

Ogunwobi, O.O., and C. Liu. 2011. Hepatocyte growth factor upregulation promotes carcinogenesis and epithelial-mesenchymal transition in hepatocellular carcinoma via Akt and COX-2 pathways. *Clinical & experimental metastasis*. 28:721-731.

Ogunwobi, O.O., T. Wang, L. Zhang, and C. Liu. 2012. Cyclooxygenase-2 and Akt mediate multiple growth-factor-induced epithelial-mesenchymal transition in human hepatocellular carcinoma. *Journal of gastroenterology and hepatology*. 27:566-578.

Park, S.H. 2005. Fine tuning and cross-talking of TGF-beta signal by inhibitory Smads. *Journal of biochemistry and molecular biology*. 38:9-16.

Park, S.O., Y.J. Lee, T. Seki, K.H. Hong, N. Fliess, Z. Jiang, A. Park, X. Wu, V. Kaartinen, B.L. Roman, and S.P. Oh. 2008. ALK5- and TGFBR2-independent role of ALK1 in the pathogenesis of hereditary hemorrhagic telangiectasia type 2. *Blood*. 111:633-642.

Peinado, H., D. Olmeda, and A. Cano. 2007. Snail, Zeb and bHLH factors in tumour progression: an alliance against the epithelial phenotype? *Nature reviews. Cancer*. 7:415-428.

Piek, E., C.H. Heldin, and P. Ten Dijke. 1999. Specificity, diversity, and regulation in TGF-beta superfamily signaling. *FASEB journal : official publication of the Federation of American Societies for Experimental Biology*. 13:2105-2124.

Polyak, K., and R.A. Weinberg. 2009. Transitions between epithelial and mesenchymal states: acquisition of malignant and stem cell traits. *Nature reviews. Cancer*. 9:265-273.

Pouliot, F., and C. Labrie. 2002. Role of Smad1 and Smad4 proteins in the induction of p21WAF1,Cip1 during bone morphogenetic protein-induced growth arrest in human breast cancer cells. *The Journal of endocrinology*. 172:187-198.

Qiu, H., B. Yang, Z.C. Pei, Z. Zhang, and K. Ding. 2010. WSS25 inhibits growth of xenografted hepatocellular cancer cells in nude mice by disrupting angiogenesis via blocking bone morphogenetic protein (BMP)/Smad/Id1 signaling. *The Journal of biological chemistry*. 285:32638-32646.

Queva, C., G.A. McArthur, L.S. Ramos, and R.N. Eisenman. 1999. Dwarfism and dysregulated proliferation in mice overexpressing the MYC antagonist MAD1. *Cell growth & differentiation : the molecular biology journal of the American Association for Cancer Research*. 10:785-796.

Rahimi, R.A., and E.B. Leof. 2007. TGF-beta signaling: a tale of two responses. *Journal of cellular biochemistry*. 102:593-608.

Rao, P.S., R.S. Mangipudy, and H.M. Mehendale. 1997. Tissue injury and repair as parallel and opposing responses to CCl4 hepatotoxicity: a novel dose-response. *Toxicology*. 118:181-193.

Riehle, K.J., Y.Y. Dan, J.S. Campbell, and N. Fausto. 2011. New concepts in liver regeneration. *Journal of gastroenterology and hepatology*. 26 Suppl 1:203-212.

Roelen, B.A., M.A. van Rooijen, and C.L. Mummery. 1997. Expression of ALK-1, a type 1 serine/threonine kinase receptor, coincides with sites of vasculogenesis and angiogenesis in early mouse development. *Developmental dynamics : an official publication of the American Association of Anatomists*. 209:418-430.

Sabbah, M., S. Emami, G. Redeuilh, S. Julien, G. Prevost, A. Zimber, R. Ouelaa, M. Bracke, O. De Wever, and C. Gespach. 2008. Molecular signature and therapeutic perspective of the epithelial-to-mesenchymal transitions in epithelial cancers. *Drug resistance updates : reviews and commentaries in antimicrobial and anticancer chemotherapy*. 11:123-151.

Schulte-Hermann, R., W. Bursch, A. Low-Baselli, A. Wagner, and B. Grasl-Kraupp. 1997. Apoptosis in the liver and its role in hepatocarcinogenesis. *Cell biology and toxicology*. 13:339-348.

Schumann, J., and G. Tiegs. 1999. Pathophysiological mechanisms of TNF during intoxication with natural or man-made toxins. *Toxicology*. 138:103-126.

Schwarz, M., G. Peres, D.G. Beer, M. Maor, A. Buchmann, W. Kunz, and H.C. Pitot. 1986. Expression of albumin messenger RNA detected by in situ hybridization in preneoplastic and neoplastic lesions in rat liver. *Cancer research*. 46:5903-5912.

Seib, F.P., M. Franke, D. Jing, C. Werner, and M. Bornhauser. 2009. Endogenous bone morphogenetic proteins in human bone marrow-derived multipotent mesenchymal stromal cells. *European journal of cell biology*. 88:257-271.

Sell, S. 2002. Cellular origin of hepatocellular carcinomas. *Seminars in cell & developmental biology*. 13:419-424.

Shen, H., J. Fan, F. Burczynski, G.Y. Minuk, P. Cattini, and Y. Gong. 2007. Increased Smad1 expression and transcriptional activity enhances trans-differentiation of hepatic stellate cells. *Journal of cellular physiology*. 212:764-770.

Shen, H., G. Huang, M. Hadi, P. Choy, M. Zhang, G.Y. Minuk, Y. Chen, and Y. Gong. 2003. Transforming growth factor-beta1 downregulation of Smad1 gene expression in rat hepatic stellate cells. *American journal of physiology. Gastrointestinal and liver physiology*. 285:G539-546.

Shi, J., K. Aisaki, Y. Ikawa, and K. Wake. 1998. Evidence of hepatocyte apoptosis in rat liver after the administration of carbon tetrachloride. *The American journal of pathology*. 153:515-525.

Shi, Y., and J. Massague. 2003. Mechanisms of TGF-beta signaling from cell membrane to the nucleus. *Cell*. 113:685-700.

Shimizu, S., T. Ide, T. Yanagida, and Y. Tsujimoto. 2000. Electrophysiological study of a novel large pore formed by Bax and the voltage-dependent anion channel that is permeable to cytochrome c. *The Journal of biological chemistry*. 275:12321-12325.

Sigala, F., S. Theocharis, K. Sigalas, S. Markantonis-Kyroudis, E. Papalabros, A. Triantafyllou, G. Kostopanagiotou, and I. Andreadou. 2006. Therapeutic value of melatonin in an experimental model of liver injury and regeneration. *Journal of pineal research*. 40:270-279.

Slater, T.F. 1987. Free radicals and tissue injury: fact and fiction. *The British journal of cancer. Supplement*. 8:5-10.

Sobin, L.H., Wittekind C. 2002. TNM classification of malignant tumors. John Wiley & Sons, Hoboken, New Jersey.

Song, J.J., A.J. Celeste, F.M. Kong, R.L. Jirtle, V. Rosen, and R.S. Thies. 1995. Bone morphogenetic protein-9 binds to liver cells and stimulates proliferation. *Endocrinology*. 136:4293-4297.

Sosa, I., O. Cvijanovic, T. Celic, D. Cuculic, Z. Crncevic-Orlic, L. Vukelic, S. Zoricic Cvek, L. Dudaric, A. Bosnar, and D. Bobinac. 2011. Hepatoregenerative role of bone morphogenetic protein-9. *Medical science monitor : international medical journal of experimental and clinical research*. 17:HY33-35.

Suzuki, Y., N. Ohga, Y. Morishita, K. Hida, K. Miyazono, and T. Watabe. 2010. BMP-9 induces proliferation of multiple types of endothelial cells in vitro and in vivo. *Journal of cell science*. 123:1684-1692.

Tandon, P., and G. Garcia-Tsao. 2009. Prognostic indicators in hepatocellular carcinoma: a systematic review of 72 studies. *Liver international : official journal of the International Association for the Study of the Liver*. 29:502-510.

Taniguchi, M., T. Takeuchi, R. Nakatsuka, T. Watanabe, and K. Sato. 2004. Molecular process in acute liver injury and regeneration induced by carbon tetrachloride. *Life sciences*. 75:1539-1549.

ten Dijke, P., and C.S. Hill. 2004. New insights into TGF-beta-Smad signalling. *Trends in biochemical sciences*. 29:265-273.

Teramoto, T., A. Kiss, and S.S. Thorgeirsson. 1998. Induction of p53 and Bax during TGF-beta 1 initiated apoptosis in rat liver epithelial cells. *Biochemical and biophysical research communications*. 251:56-60.

Theocharis, S.E., H. Kanelli, A.P. Margeli, C.A. Spiliopoulou, and A.S. Koutselinis. 2000. Metallothionein and heat shock protein expression during acute liver injury and regeneration in rats. *Clinical chemistry and laboratory medicine : CCLM / FESCC*. 38:1137-1140.

Thiery, J.P. 2002. Epithelial-mesenchymal transitions in tumour progression. *Nature reviews. Cancer*. 2:442-454.

Thiery, J.P., and J.P. Sleeman. 2006. Complex networks orchestrate epithelial-mesenchymal transitions. *Nature reviews. Molecular cell biology*. 7:131-142.

Thompson, A.J., and K. Patel. 2010. Antifibrotic therapies: will we ever get there? *Current gastroenterology reports*. 12:23-29.

Thornberry, N.A., and Y. Lazebnik. 1998. Caspases: enemies within. *Science*. 281:1312-1316.

Tian, X.Y., L.H. Yung, W.T. Wong, J. Liu, F.P. Leung, L. Liu, Y. Chen, S.K. Kong, K.M. Kwan, S.M. Ng, P.B. Lai, L.M. Yung, X. Yao, and Y. Huang. 2012. Bone morphogenic protein-4 induces endothelial cell apoptosis through oxidative stress-dependent p38MAPK and JNK pathway. *Journal of molecular and cellular cardiology*. 52:237-244.

Truksa, J., H. Peng, P. Lee, and E. Beutler. 2006. Bone morphogenetic proteins 2, 4, and 9 stimulate murine hepcidin 1 expression independently of Hfe, transferrin receptor 2 (Tfr2), and IL-6. *Proceedings of the National Academy of Sciences of the United States of America*. 103:10289-10293.

Tsuchiya, S., Y. Tsukamoto, E. Taira, and J. LaMarre. 2007. Involvement of transforming growth factor-beta in the expression of gicerin, a cell adhesion molecule, in the regeneration of hepatocytes. *International journal of molecular medicine*. 19:381-386.

Urness, L.D., L.K. Sorensen, and D.Y. Li. 2000. Arteriovenous malformations in mice lacking activin receptor-like kinase-1. *Nature genetics*. 26:328-331.

van Delft, M.F., and D.C. Huang. 2006. How the Bcl-2 family of proteins interact to regulate apoptosis. *Cell research*. 16:203-213.

van Zijl, F., G. Zulehner, M. Petz, D. Schneller, C. Kornauth, M. Hau, G. Machat, M. Grubinger, H. Huber, and W. Mikulits. 2009. Epithelial-mesenchymal transition in hepatocellular carcinoma. *Future oncology*. 5:1169-1179.

Vega, S., A.V. Morales, O.H. Ocana, F. Valdes, I. Fabregat, and M.A. Nieto. 2004. Snail blocks the cell cycle and confers resistance to cell death. *Genes & development*. 18:1131-1143.

Villanueva, A., P. Newell, D.Y. Chiang, S.L. Friedman, and J.M. Llovet. 2007. Genomics and signaling pathways in hepatocellular carcinoma. *Seminars in liver disease*. 27:55-76.

Wang, K., H. Feng, W. Ren, X. Sun, J. Luo, M. Tang, L. Zhou, Y. Weng, T.C. He, and Y. Zhang. 2011. BMP9 inhibits the proliferation and invasiveness of breast cancer cells MDA-MB-231. *Journal of cancer research and clinical oncology*. 137:1687-1696.

Weber, L.W., M. Boll, and A. Stampfl. 2003. Hepatotoxicity and mechanism of action of haloalkanes: carbon tetrachloride as a toxicological model. *Critical reviews in toxicology*. 33:105-136.

Wen, X.Z., S. Miyake, Y. Akiyama, and Y. Yuasa. 2004. BMP-2 modulates the proliferation and differentiation of normal and cancerous gastric cells. *Biochemical and biophysical research communications*. 316:100-106.

Weng, H., P.R. Mertens, A.M. Gressner, and S. Dooley. 2007. IFN-gamma abrogates profibrogenic TGF-beta signaling in liver by targeting expression of inhibitory and receptor Smads. *Journal of hepatology*. 46:295-303.

Whittaker, S., R. Marais, and A.X. Zhu. 2010. The role of signaling pathways in the development and treatment of hepatocellular carcinoma. *Oncogene*. 29:4989-5005.

Wiercinska, E., L. Wickert, B. Denecke, H.M. Said, J. Hamzavi, A.M. Gressner, M. Thorikay, P. ten Dijke, P.R. Mertens, K. Breitkopf, and S. Dooley. 2006. Id1 is a critical mediator in TGF-beta-induced transdifferentiation of rat hepatic stellate cells. *Hepatology*. 43:1032-1041.

Winau, F., G. Hegasy, R. Weiskirchen, S. Weber, C. Cassan, P.A. Sieling, R.L. Modlin, R.S. Liblau, A.M. Gressner, and S.H. Kaufmann. 2007. Ito cells are liver-resident antigen-presenting cells for activating T cell responses. *Immunity*. 26:117-129.

Xu, L., A.Y. Hui, E. Albanis, M.J. Arthur, S.M. O'Byrne, W.S. Blaner, P. Mukherjee, S.L. Friedman, and F.J. Eng. 2005. Human hepatic stellate cell lines, LX-1 and LX-2: new tools for analysis of hepatic fibrosis. *Gut*. 54:142-151.

Xu, T., C.Y. Yu, J.J. Sun, Y. Liu, X.W. Wang, L.M. Pi, Y.Q. Tian, and X. Zhang. 2011. Bone morphogenetic protein-4-induced epithelial-mesenchymal transition and invasiveness through Smad1-mediated signal pathway in squamous cell carcinoma of the head and neck. *Archives of medical research*. 42:128-137.

Yamazaki, K., Y. Masugi, and M. Sakamoto. 2011. Molecular pathogenesis of hepatocellular carcinoma: altering transforming growth factor-beta signaling in hepatocarcinogenesis. *Digestive diseases*. 29:284-288.

Yang, J., S.A. Mani, J.L. Donaher, S. Ramaswamy, R.A. Itzykson, C. Come, P. Savagner, I. Gitelman, A. Richardson, and R.A. Weinberg. 2004. Twist, a master regulator of morphogenesis, plays an essential role in tumor metastasis. *Cell*. 117:927-939.

Yang, J., and R.A. Weinberg. 2008. Epithelial-mesenchymal transition: at the crossroads of development and tumor metastasis. *Developmental cell*. 14:818-829.

Yang, J.D., and L.R. Roberts. 2010. Hepatocellular carcinoma: A global view. *Nature reviews. Gastroenterology & hepatology*. 7:448-458.

Ye, L., H. Kynaston, and W.G. Jiang. 2008. Bone morphogenetic protein-9 induces apoptosis in prostate cancer cells, the role of prostate apoptosis response-4. *Molecular cancer research : MCR*. 6:1594-1606.

Yoshioka, Y., M. Ono, M. Osaki, I. Konishi, and S. Sakaguchi. 2012. Differential effects of inhibition of bone morphogenic protein (BMP) signalling on T-cell activation and differentiation. *European journal of immunology*. 42:749-759.

You, H., W. Ding, H. Dang, Y. Jiang, and C.B. Rountree. 2011. c-Met represents a potential therapeutic target for personalized treatment in hepatocellular carcinoma. *Hepatology*. 54:879-889.

Youle, R.J., and A. Strasser. 2008. The BCL-2 protein family: opposing activities that mediate cell death. *Nature reviews. Molecular cell biology*. 9:47-59.

Yu, P.B., C.C. Hong, C. Sachidanandan, J.L. Babitt, D.Y. Deng, S.A. Hoyng, H.Y. Lin, K.D. Bloch, and R.T. Peterson. 2008. Dorsomorphin inhibits BMP signals required for embryogenesis and iron metabolism. *Nature chemical biology*. 4:33-41.

Yue, J., and K.M. Mulder. 2000. Requirement of Ras/MAPK pathway activation by transforming growth factor beta for transforming growth factor beta 1 production in a smad-dependent pathway. *The Journal of biological chemistry*. 275:35656.